

CHALMERS

ABSTRACT BOOK

GIGAHERTZ SYMPOSIUM 2008

5-6 MARCH 2008
CHALMERS UNIVERSITY OF TECHNOLOGY
GÖTEBORG
SWEDEN



GHR CENTRE

MC2
Microtechnology and Nanoscience

microwave
road

VINNOVA

IEEE

SNRV
Svenska Nationalkommittén
för RadioVetenskap

GigaHertz Symposium 2008

**5-6 March 2008
Chalmers University of Technology
Göteborg
Sweden**

www.ghz2008.se

**Chalmers University of Technology
Department of Microtechnology and Nanoscience - MC2
GigaHertz Centre
Microwave Electronics Laboratory
SE 412 96 Göteborg, Sweden**

Editor: Jan Grahn, Chalmers University of Technology

**Technical Report MC2-125
ISSN 1652-0769**

This Abstract Book is reported in Chalmers Publication Library:

<http://publications.lib.chalmers.se/cpl/>

This Abstract Bok is possible to download in pdf format at www.chalmers.se/ghz



www.chalmers.se/ghz



www.chalmers.se/mc2



www.microwaveroad.se



www.ieee.com



www.radiovetenskap.kva.se

Exhibitors & Sponsors GHz Symposium 2008

Platinum sponsor:

**Swedish Governmental Agency
for Innovation Systems
(VINNOVA)**

www.vinnova.se



Gold sponsor:

Agilent technologies

www.agilent.com



Agilent Technologies

Silver sponsors:

Ageto MTT

www.agetomtt.se

AGETO MTT

AMSKA

www.amska.se



Amtele

www.amtele.se



Anritsu

www.anritsu.se



Applied Wave Research

<http://web.appwave.com>



MicroComp Nordic AB

www.mcnab.se

µComp Nordic AB

National Instruments

www.ni.com



Ranatec Instruments

www.ranatec.se

RANATEC

Rohde Schwarz

www.rohde-schwarz.se



Wasa Millimeter Wave

www.wmmw.se



GigaHertz Symposium 5-6 March 2008 at Chalmers

www.ghz2008.se

Chalmers Conference Center, Chalmers University of Technology

Wednesday 5 March 2008

0830-1000 Registration Coffee + Sandwich

SILVER SPONSORS: Wasa Millimeter Wave AB Applied Wave Research Inc.

1000-1200 SESSION I Runan Chairman: Jan Grahn, Chalmers

1000 Welcome

Jan Grahn, Chalmers; General Chairman GHZ Symposium 2008

Stefan Bengtsson, Vice President, Chalmers

1010 Plenary invited speaker

Intelligent Transmitter Technology for Next Generation Wireless Transceivers

Larry Larson

Univ. California San Diego

1050 Invited speaker

RF/DSP co-designed power amplifiers/transmitters for advanced wireless and satellite applications

Fadhel Ghannouchi

Univ. Calgary

1120

Tuneable technologies for agile microwave systems

S. Gevorgian

Chalmers, Ericsson

Design and Verification of a GaN S-band high power amplifier

J. Nilsson

Saab Microwave Systems

Self-Oscillating RF amplifiers

P. Reynaert, W. Laflere, M. Steyaert, J. Craninckx

KU Leuven, IMEC, Leuven

1200-1300 Lunch and Exhibition

GOLD SPONSOR: Agilent

1300-1500 Workshops Wednesday 5 March 2008

Agile Microwave Systems	RF Power Amplifiers (1)	Microwave Components	THz Technology
Ascom/Catella Moderator: Hans-Olof Vickes Saab Microwave Systems	Runan Moderator: Bo G. Berglund Ericsson	Scania Moderator: Sven Mattisson Ericsson Mobile Platforms	Valdemar/Ledning Moderator: Staffan Rudner Swedish Defence Research Agency - FOI
A method for switchable rejection filters N. Meissner Saab Avionics	The Frequency Spectrum of Bandpass Pulse Width Modulated Signals T. Blocher, P. Singerl, A. Wiesbauer, F. Dielacher Graz Univ., Infineon	Highly Integrated MMICs for mm-wave system application H. Zirath, S.E. Gunnarsson, M. Ferndahl, R. Kozhuharov, C. Kärfelt Chalmers, Ericsson	Invited WS speaker: An introduction to the T4000 terahertz imager C. Mann Thruvision Ltd., Abingdon, UK
60 GHz $\lambda/8$ Phase-Shifter in EFFA Technology X. Rottenberg, P. Ekkels, B. Nauwelaers, W. De Raedt Imec, KU Leuven	The potential of active load and source tuning on base station power amplifiers T. Lejon Ericsson	An Ultra Wide Band LNA in 90 nm CMOS W. Ahmad, A. Axholt, H. Sjöland Lund Univ	
Tuneable Filters for Agile Microwave Systems A. Deleniv, S. Gevorgian Chalmers, Ericsson	Comparing Polar Transmitter Architectures using GaN HEMT Power Amplifier E. Cijvat, K. Tom, M. Faulkner, H. Sjöland Lund Univ., Victoria Univ., Melbourne	Flip Chip for High Frequency K. Boustedt Ericsson.	Novel 220 GHz Slot-Square Substrate Lens Feed Antenna Integrated on MMIC J. Svedin, S. Leijon, N. Wadefalk, S. Cherednichenko, B. Hansson, S. Gunnarsson, I. Kalfass, A. Leuther, A. Emrich FOI, Chalmers, Fraunhofer-IAF, Omnisys Instruments

Agile Microwave Systems (cont')	RF Power Amplifiers (1) (cont')	Microwave Components (cont')	THz Technology (cont')
<p>Microwave MEMS activities at the Royal Institute of Technology J. Oberhammer, N. Somjit, <u>M. Sterner</u>, F. Saharil, S. Braun, G. Stemme KTH</p>	<p>Invited WS speaker:</p> <p>Class MTM Power Amplifier Linearization D. E. Kelly PulseWave RF, Austin</p>	<p>Cryogenic X-band Low Noise Amplifiers N. Goia, M. Kelly, A. Malmros, N. Wadefalk, <u>J.P. Starski</u> Chalmers</p>	<p>Planar antennas for terahertz frequencies S. Cherednichenko Chalmers</p>
<p>Phase-Comparison Monopulse Direction Measurement Antenna Array for 6-18 GHz C. Johansson, T. Eriksson, J. Grabs, T. Windahl Saab Avionics</p>	<p>Different Classes of Power Amplifiers using SiC MESFET S. Azam, R. Jonsson, Q. Wahab Linköping Univ., FOI</p>	<p>Low-Noise Cryogenic Amplifier built using MMIC-like /TRL Technique O. Nyström, <u>E. Sundin</u>, D. Dochev, V. Desmaris, V. Vassilev, V. Belitsky Chalmers, Onsala Space Observatory</p>	<p>Geosynchronous Earth Orbit Atmospheric Sounder S. Andersson, <u>J. Embretsen</u>, A. Emrich, M. Ericson, M. Hjort, J. Riesbeck, C. Tegnander Omnisys Instruments</p>
<p>MEMS Phase Shifters for an Affordable Low-Power Ka-band Multifunctional ESA on a small UAV R. Malmqvist, C. Samuelsson, A. Gustafsson, <u>T. Boman</u>, S. Björklund, B. Carlegrim, R. Erickson, T. Vähä-Heikkilä, P. Rantakari FOI, Millilab-VTT</p>	<p>Modeling of dual-input power amplifiers T. Eriksson, C. Fager, H. Cao, A. Soltani, U. Gustavsson, H. Nemati, H. Zirath Chalmers</p>	<p>Small-Signal Modeling of Narrow bandgap InAs/AlSb HEMTs M. Malmkvist, E. Lefebvre, L. Desplanque, X. Wallart, G. Dambrine, S. Bollaert, J. Grahn Chalmers, IEMN Lille</p>	<p>Back-End Module Demonstrator for radio-astronomy applications J.L. Cano, B. Aja, E. Villa, L. de la Fuente, E. Artal Univ. Cantabria, Santander</p>
<p>An adjustable broadband MMIC equalizer J. Grabs, U. Öhman, N. Meissner Saab Avionics</p>	<p>Invited WS speaker:</p> <p>Recent Advances in GaN HEMT Power Amplifier Technology for Telecommunication Applications</p>	<p>Low-Noise, High-Speed Strained Channel Silicon MOSFET Technology for RF-Applications B.G. Malm, J. Hällstedt, P.-E. Hellström, M. Östling Royal Institute of Technology</p>	<p>ALMA Band 5 (163-211 GHz) Sideband Separating Mixer B. Billade, I. Lapkin, A. Pavolotsky, R. Monje, J. Kooi, V. Belitsky Chalmers, California Institute of Technology</p>
<p>Tunable Impedance Matching Network M. R. Rafique, T. A. Ohki, P. Linnér, A. Herr Chalmers</p>	<p><u>R. Pengelly</u>, S. Wood, D. Farrell, B. Pribble, J. Crescenzi Cree Inc., Central Coast Microwave Design, US</p>	<p>Wideband Microstrip 90° 3-dB Two-Branch Coupler with Minimum Amplitude and Phase Imbalance D. Wang, M. Li, A. Huynh, <u>P. Håkansson</u>, S. Gong Nanjing Electronic Equipment Institute, Linköping University</p>	<p>High Power Photonic MW/THz Generation Using UTC-PD B. Banik, J. Vukusic, H. Hjelmgren, H. Sunnerud, A. Wiberg, J. Stake Chalmers</p>
<p>Coded OFDM in Hybrid Radio Over Fibre Links J.F. Miranda, M. Gidlund Univ. Gävle, Nera Networks</p>		<p>An Ultra-Wideband Six-Port transceiver Covering from 3.1 to 4.8 GHz <u>P. Håkansson</u>, S. Gong Linköping Univ</p>	<p>Towards a THz Sideband Separating Subharmonic Schottky Mixer P. Sobis, J. Stake, A. Emrich Chalmers, Omnisys Instruments</p>
<p>Equivalent Circuit of Metamaterials with a Negative Permeability A. Rumberg, M. Berroth Univ. Stuttgart</p>	<p>Design Consideration for Varactor-Based Dynamic Load Modulation Networks U. Gustavsson, B. Almgren, H. Nemati Ericsson, Chalmers</p>	<p>Gated tunnel diode pulse generator M. Nilsson, M. Ärelid, E. Lind, G. Astromskas, L.-E. Wernersson Lund Univ.</p>	<p>HIFAS: High-Performance full-custom Autocorrelation Spectrometer ASIC A. Emrich, S. Andersson, <u>M. Hjort</u> Omnisys Instruments</p>

1500-1530 Coffee and Exhibition SILVER SPONSORS: Anritsu Ageto MTT
1530-1730 SESSION II Runan Chairman: Piotr Starski, Chalmers
1530 Invited speaker Extremely Low-Noise Amplification with Cryogenic FET's and HFET's: 1970-2006 (Where do we go from here?) Marian W. Pospieszalski National Radio Astronomy Observatory, Charlottesville, VA
1600 560 GHz f_t , f_{max} operation of a refractory emitter metal InP DHBT E. Lind, A.M. Crook, Z. Griffith, M.J. Rodwell Lund Univ., Univ. California Santa Barbara
Low phase-noise balanced Colpitt InGaP-GaAs HBT VCOs with wide frequency tuning range and small VCO-gain variation H. Zirath GHz Centre, Chalmers, Ericsson
Feasibility of Filter-Less RF Receiver Front-End S. Ahmad, N. Ahsan, A. Blad, R. Ramzan, T. Sundström, H. Johansson, J. Dabrowski, C. Svensson Linköping University
Small-Size 2-10 GHz Radar Receiver Si-RFIC H. Berg, H. Thieses, M. Hertz, F. Norling Saab Microwave Systems
High frequency, current tunable spin torque oscillators: experimental characterization S. Bonetti, J. Garcia, J. Persson, J. Åkerman Royal Institute of Technology
N -coupling the capacity of wireless communication using electromagnetic angular momentum B. Thidé Swedish Institute of Space Physics, Uppsala
1730-1830 Visit (optional) MC2 Cleanroom or Microwave Labs, Chalmers (www.chalmers.se/mc2)
1900 Conference Dinner at Universeum (www.universeum.se)

Thursday 6 March 2008
0830- 1000 SESSION III Runan Chairman: Herbert Zirath, Chalmers
0830 Plenary invited speaker The Next Wireless Wave is a Millimeter Wave Joy Laskar GeorgiaTech
0910 Invited speaker High Frequency and Mixed Signal Design for Communication and Remote Sensing applications in advanced technologies Mehran Mokhtari Teledyne Scientific
0940 MMIC design at G-band (140-220 GHz) including a 220 GHz Single-Chip Receiver MMIC with Integrated Antenna S.E. Gunnarsson, N. Wadefalk, M. Abbasi, C. Kärnfelt, R. Kozhuharov, J. Svedin, B.M. Motlagh, B. Hansson, S. Cherednichenko, I. Angelov, D. Kuylenstierna, H. Zirath, S. Rudner, I. Kalfass, A. Leuther Chalmers, FOI, Ericsson, Fraunhofer-IAF
A Quad-Core 130-nm CMOS 57-64 GHz VCO V. P. Goluguri, J. Wernehag, H. Sjöland, N. Troedsson Cambridge Silicon Radio Sweden, Lund University
1000-1030 Coffee and Exhibition SILVER SPONSORS: Amtele AMSKA MicroComp Nordic

1030-1210 SESSION IV Runan Chairman: Niklas Rorsman, Chalmers			
1030 Invited speaker			
GaN HEMT development for microwave power applications- Current status and trends Masaaki Kuzuhara Univ. Fukui			
1100			
Paving the road for integrated gallium nitride transceivers K. Andersson, M. Thorsell, N. Billström, J. Nilsson, J. Holmkvist, A-M. Andersson, M. Südow, M. Fagerlind, P.-Å. Nilsson, A. Malmros, H. Hjelmgren, N. Rorsman, GHz Centre, Chalmers, Saab			
Demonstrator of Class-S Power Amplifier A. Samulak, G. Fischer, R. Weigel Univ. Erlangen-Nürnberg, Alcatel-Lucent			
30/20 GHz Balanced Sub-harmonic MMIC Mixer for Space Applications D. Kleén, J. Thelberg Saab Space			
Water Vapour Radiometer for ALMA A. Emrich, <u>M. Wannerbratt</u> Omnisys Instruments			
European Radio & Microwave Interest Group (EuRaMIG) - An initiative from GHz Centre: Status and Coming Activities P. Olanders, Ericsson, Chairman GHz Centre, J. Grahn, Chalmers, Director GHz Centre			
1210-1300 Lunch and Exhibition PLATINUM SPONSOR: VINNOVA			
1300-1430 Workshops		Thursday 6 March 2008	
Antennas Ascom/Catella Moderator: Per Sjöstrand Saab Avionics	RF Power Amplifiers (2) Runan Moderator: Johan Ståhl Saab Microwave Systems	Measurement - Modeling Scania Moderator: Niclas Keskitalo Ericsson	The GHz Entrepreneur Valdemar/Ledning Moderator: Peter Wahlberg Microwave Road
Integrated Antennas for RF MEMS Routes A. Rydberg, S. Cheng, P. Hallbjörner, S. Ogden, K. Hjort Uppsala Univ., SP, Borås Presented by C. Karlsson, SP	Output Power Density and Breakdown Voltage in Field-Plated Buried Gate Microwave SiC MESFETs P.Å. Nilsson, F. Allerstam, K. Andersson, M. Fagerlind, H. Hjelmgren, A. Malmros, M. Südow, E.Ö. Sveinbjörnsson, H. Zirath, N. Rorsman, Chalmers	Model-Based Pre-distortion for Signal Generators C. Luque, N. Björnell Univ. Gävle	<i>The WS provides some personal reflections on doing business from innovations and IP in RF/Microwave from three small companies, one global company and one venture company. The WS is concluded by a discussion</i>
Microstrip patch antenna for wireless applications N.A. Touhami, B. Aja, A. Tazón, E. Artal Univ. Cantabria, Santander	Silicon-on-SiC hybrid substrate with low RF-losses and improved thermal performance J. Olsson, Ö. Vallin, D. Martin, L. Vestling, U. Smith, H. Norström Uppsala Univ., Infineon	A Comparison of Antenna Diversity Characterization Methods using Reverberation Chambers and Drive Tests D. Nyberg, M. Franzén, P.S. Kildal Chalmers, Bluetest AB	Mikael Reimers, CEO Foodradar Systems AB www.foodradar.com
Small Microstrip Fractal Antenna for RFID Tag P. Enoksson, <u>M. Rusu</u> , A. Curutiu, H. Rahimi, C. Rusu Chalmers, Bucharest Univ., Bonn Univ., Imego	A review of validation criteria for behavioral power amplifier models <u>P. Landin</u> , M. Isaksson, Univ. Gävle	Measuring Relative Receiver Sensitivity of Wireless Terminals in One Minute in a Reverberation Chamber M. Andersson, <u>C. Orlenius</u> , M. Franzén Bluetest AB	Tomas Ornstein, CEO Ranatec Instrument AB www.ranatec.se

Antennas (cont')	RF Power Amplifiers (2) (cont')	Measurement - Modeling (cont')	The GHz Entrepreneur (cont')
Dual-band choke horn Eleven Feed A. Yasin, J. Yang, T. Östling Chalmers, Arkivator AB	CMOS for micro- and millimeter-wave power applications M. Ferndahl, H. Nemati, H. Zirath Chalmers Comparative analysis of the complexity/accuracy tradeoff for power amplifier behavior models A. Tehrani, H. Cao, T. Eriksson, C. Fager, Chalmers	Modeling of SiGe HBT Operation in Extreme Temperature Environment P. Sakalas, M. Ramonas, M. Schroter, A. Kittlaus, H. Geisler, C. Jungemann, A. Shimukovitch Dresden Univ.; Semiconductor Physics Institute, Vilnius; SUSS Microtec, Bundeswehr Univ. Neubiberg; Univ. California San Diego	Johan Lassing, CEO Qamcom Technology AB www.qamcom.se
Optimization of 200-800 MHz Eleven Feed for Use in Reflector Antennas of GMRT Y.B. Karandikar, P.S. Kildal Chalmers	A Computational Load-Pull Investigation of Harmonic Loading Effects on AM-PM conversion O. Bengtsson, L. Vestling, J. Olsson Univ. Gävle, Uppsala Univ.	On-wafer network analyser uncertainty estimation J. Stenarson, K. Andersson, C. Fager, K. Yhland SP Borås, Chalmers	Peter Olanders, Technology Strategist Ericsson AB www.ericsson.com
Method for Circuit Based Optimization of Radiation Characteristics of Multi-port Antennas K. Karlsson, J. Carlsson SP Borås, Chalmers	Identification of Distortions in a RF Measurement System H. Cao, A. Soltani, C. Fager, T. Eriksson Chalmers	Mm-wave device testing using wideband coplanar transitions E. Villa, B. Aja, L. de al Fuente, E. Artal Univ. Cantabria, Santander	Bengt Gustafsson, CEO Microwave Technologies AB
Circular Monopole & Dipole Antennas for UWB Radio Utilizing a Flex-Rigid Structure M. Karlsson, S. Gong Linköping Univ.	Further enhancement of Load pull simulation technique to study non linear effects of LDMOS in TCAD A. Kashif, T. Johansson, C. Svensson, T. Arnborg, Q. Wahab Linköping Univ., Infineon, FOI	High Efficiency using Optimized SOI Substrates L. Vestling, O. Bengtsson, K.-H. Eklund, J. Olsson Uppsala Univ., Univ. Gävle	Open debate and discussion with auditorium
Design, Manufacture and Test of Eleven Feed for 1-13 GHz J. Yang, I. Karlsson, X. Chen, P.S. Kildal Chalmers	GaN device and MMIC development at Chalmers M. Fagerlind, M. Südow, K. Andersson, A. Malmros, P.Å. Nilsson, H. Zirath, N. Rorsman Chalmers	Spin Torque Oscillator Simulations and Circuit Design Y. Zhou, S. Srinivasan, J. Persson, J. Åkerman Royal Institute of Technology	
1430-1500 Coffee			
SILVER SPONSORS: ROHDE & SCHWARZ National Instruments			
1500-1600 SESSION V Runan Chairman: Arne Alping, Ericsson			
1500 Invited speaker Industrial aspects of 100 Gb/s optical communication Bengt-Erik Olsson Ericsson Research			
1530 All-Optical Waveform Sampling with TeraHertz Capacity M. Westlund, P.A. Andrekson, H. Sunnerud Chalmers, Picosolve Inc.			
High Speed 1.3 μm VCSELs for FTTH and RoF P. Westbergh, E. Söderberg, J.S. Gustavsson, P. Modh, A. Larsson, Z.Z. Zhang, J. Berggren, M. Hammar Chalmers, Royal Institute of Technology			
1600 Closing Remarks Jan Grahn, Chalmers; General Chairman GHz Symposium 2008 Henrik Sjöland, Lund University: Next GHz Symposium arranger			
1630-1730 Visit (optional) MC2 Cleanroom or Microwave Labs, Chalmers (www.chalmers.se/mc2)			

Welcome to GigaHertz Symposium 2008

The GigaHertz Symposium is the Nordic meeting place for presenting new findings in GHz technologies: Components, circuits and sub-systems for wireless / wireline communication, and sensing. It is now time for the 9th GigaHertz Symposium. This time, the event is carried out on 5-6 March 2008 at Chalmers campus, Göteborg, Sweden. The arranger is Chalmers University of Technology.

At the GHz Symposium 2008, you can find presentations from a vast range of R&D players extending from 1 GHz to 1 THz and beyond. This time, we are also happy to present outstanding invited speakers who will present RF/microwave communication and sensor technologies for applications ranging from intelligent transmitters for wireless communication to cryogenic cooled receivers for radio astronomy.

The Program Committee for GHz Symposium 2008 decided at its first meeting to test some new concepts. The Proceedings have been replaced by the Abstract book you now have in your hand. Furthermore, we have omitted the poster session and introduced shorter presentations and parallel workshops. Finally, we involved industry by letting distinguished company representatives lead the workshops with dedicated "hot" GHz themes.

Chalmers is proud to announce that this probably is the largest GHz Symposium so far with almost 270 delegates at the time of this writing. Around half of the delegates are from industry representing around 50 companies. Almost 20% of the delegates come from outside Sweden. The aim of the Program Committee to create the GHz mixing zone between academia, research institutes, and companies seems to have been fulfilled at GHz Symposium 2008.

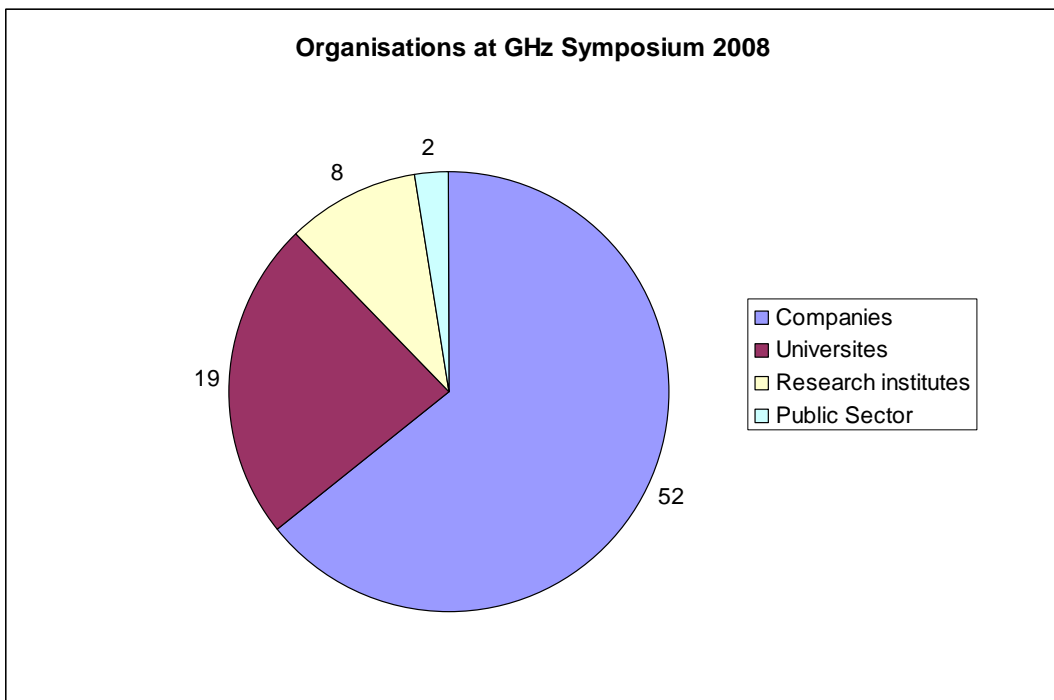
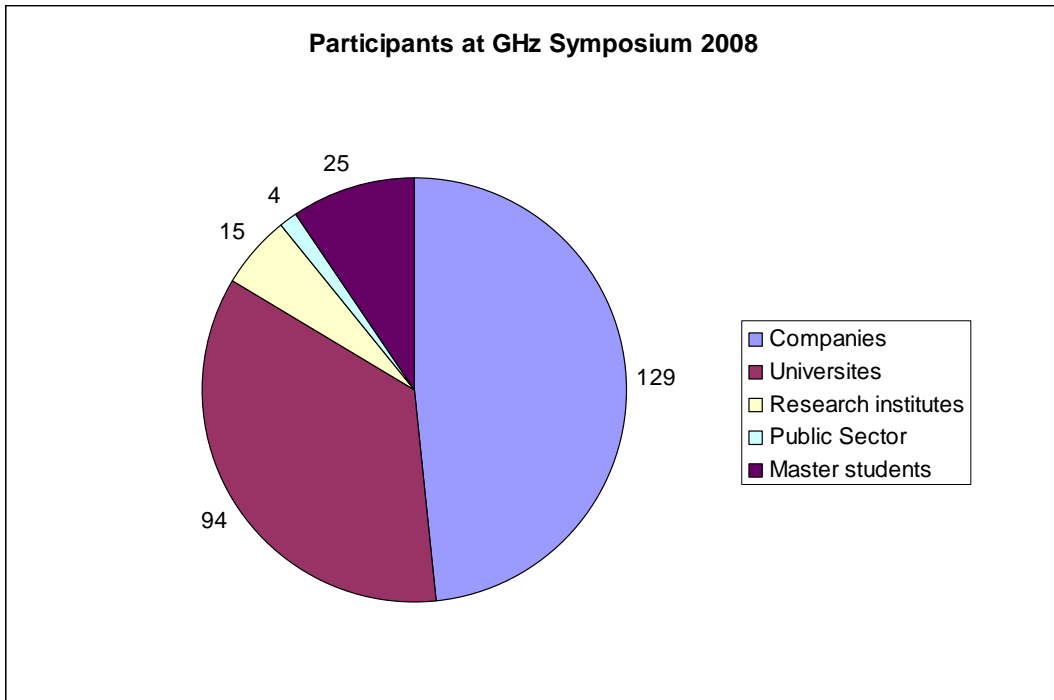
I would like to thank in particular the invited speakers, and all contributors, to make this GigaHertz Symposium 2008 happen. Many thanks to the Program Committee, industrial workshop moderators, Chairmen, and Chalmers employees for keeping this conference together.* I am particularly grateful to the GHz Task Force at MC2 for all practical assistance. Finally, I thank our exhibitors for their sponsoring; Take the time to meet them at the exhibition!

I hope you enjoy GigaHertz Symposium 2008 in Göteborg!

Jan Grahn
General Chairman
GigaHertz Symposium 2008

* Chalmers employees carrying an orange badge are willing to answer questions and/or help our visitors.

Statistics GHz Symposium 2008



Program Committee GHz Symposium 2008

Dr. Jan Grahn (General Chairman)	Chalmers University of Technology
Prof. Anders Rydberg	Uppsala University
Dr. Anders Sjölund	Swedish Foundation for Strategic Research (SSF)
Dr. Gunnar Malm	Royal Institute of Technology (KTH)
Prof. Hans-Olof Vickers	Saab Microwave Systems
Dr. Henrik Sjöland	Lund University and Ericsson Mobile Platforms
Dr. Klas Yhland	SP Technical Research Institute of Sweden
Dr. Maria van Zijl	Business Security
Prof. Niclas Keskitalo	Ericsson, and University of Gävle
Prof. Sheila Galt	Chalmers University of Technology
Prof. Spartak Gevorgian	Chalmers University of Technology, and Ericsson Research
Prof. Staffan Rudner	Swedish Defence Research Agency (FOI)
Dr. Thomas Lewin	Ericsson Research, Ericsson

GHz Task Force at MC2, Chalmers

Jan Grahn
Jeanette Träff
Eva Hellberg

Invited Speakers GHz Symposium 2008

- [Prof. Larry Larson](#)
[Center for Wireless Communications](#)
[University of California at San Diego](#)
Intelligent Transmitter Technology for Next Generation Wireless Transceivers
- [Prof. Joy Laskar](#)
Schlumberger Chair in Microelectronics,
Director [Georgia Electronic Design Center](#)
Georgia Tech, Atlanta
The Next Wireless Wave is a Millimeter Wave
- [Prof. Fadhel Ghannouchi](#)
[iRadio Laboratory](#)
University of Calgary
RF/DSP co-designed power amplifiers/transmitters for advanced wireless and satellite applications
- [Dr. Marian W. Pospieszalski](#)
[National Radio Astronomy Observatory](#)
Charlottesville, VA
Extremely Low-Noise Amplification with Cryogenic FET's and HFET's: 1970-2006 (Where do we go from here?)
- [Dr. Mehran Mokhtari](#)
[Teledyne Scientific and Imaging Company](#)
Thousand Oaks, CA.
High Frequency and Mixed Signal Design for Communication and Remote Sensing applications in advanced technologies
- [Dr. Bengt-Erik Olsson](#)
[Ericsson AB](#)
Ericsson Research, Mölndal, Sweden
Industrial aspects of 100 Gb/s optical communication
- [Prof. Masaaki Kuzuhara](#)
[Department of Electrical and Electronics Engineering University of Fukui, Japan](#)
GaN HEMT development for microwave power applications- Current status and trends
- **Invited Workshop speakers:**
THz Technology: Dr. C. Mann, [Thruvision Ltd.](#): **An introduction to the T4000 terahertz imager**
RF PA(1): D. Kelly: [Pulsewave RF](#), Austin: **Class M Power Amplifier Linearization**
RF PA(1): Dr. R. Pengelly, [Cree Inc.](#): **Recent Advances in GaN HEMT PAs for Telecom Applications**

Abstract Book Contents GHz Symposium 2008

Wednesday 5 March 2008

SESSION I 1000-1200	1
Workshops 1300-1500	
Agile Microwave Systems	7
RF Power Amplifiers (1)	18
Microwave Components	27
THz Technology	38
SESSION II 1530-1730	48

Thursday 6 March 2008

SESSION III 0830-1000	56
SESSION IV 1030-1210	61
Workshops 1300-1430	
Antennas	68
RF Power Amplifiers (2)	77
Measurement - Modeling	87
The GHz Entrepreneur	96
SESSION V 1500-1600	102

Session I

1000-1200 Wednesday 5 March 2008

Intelligent Transmitter Technology for Next Generation Wireless Transceivers

Professor Larry Larson

Department of Electrical and Computer Engineering
University of California, San Diego

Abstract: Future generations of wireless communications are expected to place increasing burdens on the efficiency and linearity of power amplifiers, due to the use of more complex waveforms and wider bandwidths. This has implications for the design of transmitters in portable/mobile devices as well as base stations and access points. Although semiconductor device technology has made rapid progress in fundamental power amplifier transistor performance, the use of digital signal processing techniques to optimize the linearity and efficiency provides enormous potential for further improvement. This paper will summarize the digital techniques that can be employed to improve the performance of wireless power amplifiers.

RF/DSP co-designed power amplifiers/transmitters for advanced wireless and satellite applications

F. M. Ghannouchi, Fellow IEEE
Professor and iCORE/CRC Chair, Electrical and Computer Engineering Department
Director iRadio laboratory, University of Calgary, Calgary Canada
E: mail: fghannouchi@ieee.org

Abstract:

The wireless and satellite communications communities have always been looking for power and -spectrum efficient amplification systems. The design of such power amplifiers has to be considered closely together with the system architecture in order to ensure optimal system level performances in term of linearity and power efficiency. This implies the use of adequate transmitter's architectures that convert the analog base band information to architecture dependent amplifier driving signals such as sigma-delta, EE&R, and LINC architectures. This talk layouts the principles behind software enabled linear and highly efficient power amplifiers/transmitters sub-systems for multi-standard and multi-band applications. Recent advances/trends and practical realizations will also be presented and discussed.

Tuneable technologies for agile microwave systems

S. Gevorgian

Department of Microtechnology and Nanoscience MC2, Chalmers University of Technology
spartak.gevorgian@mc2.chalmers.se

A brief review of tuneable technologies useful for development of components for agile microwave systems will be presented. It includes a comparative analysis of mechanical, electric, magnetic and optical tuning methods. Apart semiconductors (p-i-n diodes, varactors, field effect transistors etc.) the report will focus on technologies not yet compatible with standard semiconductor fabrication processes, such as micromechanical and nanomechanical components (carbon nanotube, nanowires etc.), ferrite/ferromagnetic components, liquid crystals, plasma, ferroelectric and piezoelectric (varactors, thin film bulk acoustic wave resonators) components etc.

Design and verification of a GaN S-band high power amplifier

Joakim Nilsson, joakim.u.nilsson@saabgroup.com

Saab Microwave System, SE-412 89 Göteborg

Summary:

This paper describes the design of a 2.7-3.3 GHz GaN power amplifier. For the design two GaN-power bars with a total gate width of 10 mm each were used. The GaN power bars has been developed by QinetiQ, UK, within a European co-project called Korrigan [1]. The power bars were fitted into packages and characterized at Saab Microwave Systems. For the device characterization, pulsed Load-Pull and S-parameter-measurements were performed on the packaged power bars. The matching networks were then designed using the measured data in Agilent ADS 2006.

Intro:

Future radar systems require more efficient power-amplifier-realizations. Meeting these new requirements, is to use microwave power transistors in WBG-technology. The use of microwave power transistors in WBG-material for power amplifiers in radar systems, is a possible way. With the possibility of high supply-voltage, the system power distribution will be more efficient, resulting in lower losses in voltage-conversion. The high feeding-voltage for the power amplifiers leads to higher output impedance and therefore simpler matching networks with lower losses, which contributes to a higher system-efficiency. Other advantages with microwave power transistors in WBG material are heat-hardiness and high power density. Typical power-density values are 4 W/mm-gatewidth for a 30 W GaN-chip in comparison with below 1 W/mm with Si or GaAs. That gives, for instance, greater possibilities to design smaller MMIC-power amplifiers than with common technologies.

Results:

The measurements were performed under pulsed condition with gate-voltage and RF-signal pulsed with 50-200 μ s pulse-length at 5-20 % duty cycle. The drain-voltage, at the measurements, was varied between 25 and 35 V.

The power amplifier shows, with a drain-voltage at 25 V, an output power of more than 50 W over the whole frequency band with PAE > 35 % and Gain > 10 dB. A peak output power at 75 W was obtained at 3 GHz with a drain-voltage at 35 V. That means a power density at nearly 4 W/mm-total gate width measured at power amplifier level.

Conclusion:

With a peak output power at 75 W and a power density at about 4 W/mm, the power amplifier shows very promising results for further progress within the Korrigan [1] project and for European GaN-component development.

References:

- [1] Project number RTP 102.052 within EDA

Self-oscillating RF amplifiers

P. Reynaert, W. Laflere, M. Steyaert and J. Craninckx*

Katholieke Universiteit Leuven, Belgium

Department of Electrical Engineering, ESAT-MICAS

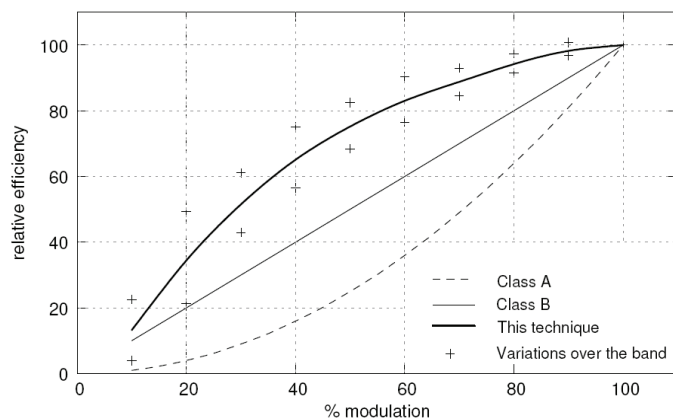
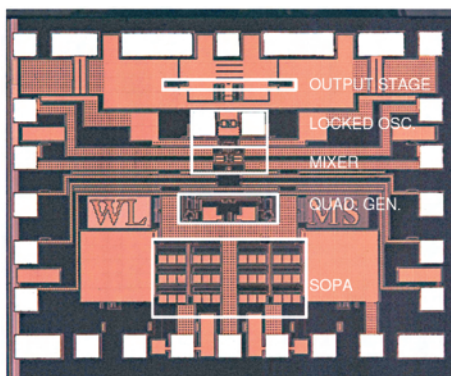
*Imec, Leuven, Belgium

patrick.reynaert@esat.kuleuven.be

Although CMOS RF transceivers for wireless communications have become very common, it somehow seems that CMOS RF power amplifiers have been left behind. Achieving sufficient output power from a low-voltage CMOS technology is for sure a challenge. Furthermore, the high peak-to-average power ratio of today's wireless standards further impedes the design of CMOS PAs. Not to mention the challenges that arises when the PA is integrated together with other RF and analog circuitry.

Several research groups have already demonstrated the feasibility of constant-envelope GHz CMOS PAs. These PAs do not allow linear amplification and can only transmit one single output power level. But when a constant envelope PA is turned on and turned off, the average output power at the fundamental frequency can be modulated according to the duty-cycle. Such a burst-mode operation, driven by a PWM or SD modulator, results in spectral tones at the PWM or SD clock frequency, and these tones obviously need to be suppressed by the antenna filter. The major advantage is that the constant envelope PA is either on or off, and thus always operates at a high efficiency. As such, this technique allows the amplification of amplitude modulated signals at high efficiency.

In this work, we propose a self-oscillating delta modulator to achieve high linearity and to lower the spurious tone of the modulator. To demonstrate this technique, the topology was implemented in 0.18 μ m CMOS. The implemented solution can serve as a power efficient CMOS pre-driver as it achieves up to 8.26dBm with an efficiency of 35%.



Workshop

Agile Microwave Systems

1300-1500 Wednesday 5 March 2008

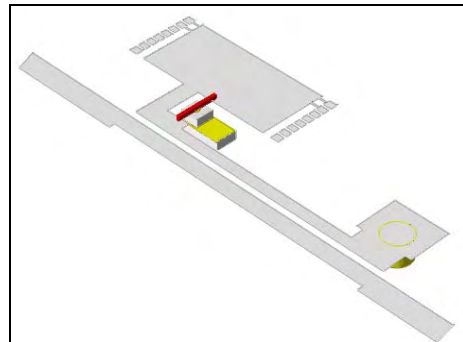
A method for switchable rejection filters

Niklas Meissner (niklas.meissner@saabgroup.com) and Jan Grabs (jan.grabs@saabgroup.com)
Saab Avitronics, SE-175 88 Järfälla, Sweden.

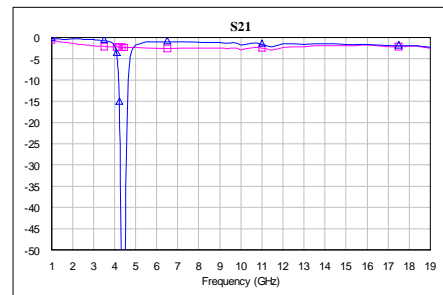
A method is proposed for designing rejection filters that can be switched off. The usual way for switching between passband and rejection band is by using switches and dual channels. With this method a second mode for the filter is introduced. The two modes of the rejection filter can be changed by a diode. With this dual mode filter the frequency passband will be very broad and insertion loss will be kept low without the need for active components.

The development of communication and radar systems using high carrier frequency band for signals is increasing. For applications operating at these frequencies there is a need for suppression of these unwanted signals. Suppression is sometimes the only option for avoiding interference when the power level is high. By introducing rejection filter in the receiver channel they can be rejected. In some cases there are signals within the rejection band that you need to see. This paper gives an example of a design where a method has been used for designing rejection filters that can be transformed into transmission lines. Microstrip technology was used to realize the filter.

Normally when designing rejection filters at microwave frequency stubs of $\lambda/4$ length are used, where λ is the wavelength at the rejection frequency. Here resonators are used instead of stubs for filtering so that the passband will be broadened. To enable the use of the same channel for passband and rejection, low coupling between filter resonators and the main waveguide is needed for the passband mode. The filter consists of a coupling line and a resonator part. The method used introduces a diode between the coupling line and the resonator. The diode is wire bonded into the filter and coupled through a capacitance to ground so it can be DC biased into different modes. When the diode is conducting the microstrip filter will transform into a coplanar transmission line.



In the example in this paper a microstrip rejection filter with eight segments were designed. The insertion loss parameter was measured for the two modes. Here the signals were rejected more than 45 dB in a 200 MHz band around 4 GHz and the passband loss was about 1 dB for the rejection mode and 2.5 dB for the passband mode from 1 to 19 GHz.



A broadband microwave dual mode rejection filter was designed with promising results.

60 GHz $\lambda/8$ Phase-Shifter in EFFA Technology

X. Rottenberg^{1,2}, P. Ekkels^{1,2}, B. Nauwelaers² and W. De Raedt¹

¹IMEC v.z.w., Division MCP, Kapeldreef 75, B3001 Leuven, Belgium

²K.U.Leuven, ESAT, Kasteelpark Arenberg 10, B3001 Leuven, Belgium

xrottenb@imec.be

RF-MEMS technology is widely accepted as a key enabling technology for current and future telecom applications. RF-MEMS devices indeed allow defining high quality, cost effective, highly integrated, low power consumption and tunable passive components. These devices however often rely on fairly complex and/or arguably expensive technologies. Recently, we developed a cheap and extremely low complexity electrostatic RF-MEMS technology involving only two lithographic steps, i.e. EFFA (Electrostatic Fringing-Field Actuator)[1]. The EFFA's rely indeed on the fringing E-field lines for their actuation and not on parallel-plate E-field as conventional devices.

In this paper, we present the design, realization in EFFA technology and characterization of $\lambda/8$ phase shifters for 60GHz application as presented in Figure 1. As conventional EFFA's [1] are too large to be considered lumped at 60GHz, we designed a distributed phase-shifter taking advantage of their electrical length. It consists of a tunable 4mm long multi-stage CPW (CoPlanar Waveguide) realized in a 1 μ m thick Al layer partially suspended 3 μ m above an AF45 glass substrate. The RF-ground consists of fixed semi-infinite planes and suspended strips defined 10 μ m from the signal line. This narrow slot allows actuating the CPW by DC-biasing its signal line vs. its ground. The strip width is designed so that the characteristic impedance of the line, Z_0 , remains close to 50 Ω in idle and actuated states while the total electrical length of the line is strongly modified [2].

The measurement results in Figure 2 show insertion and return loss (IL and RL) respectively better than 2.3dB and 10dB at 60GHz. This IL corresponds to that of a fixed 4mm long CPW. The RL in idle state is slightly above its design goal. The CPW is then too inductive. We attribute this discrepancy to fabrication tolerances of the 10 μ m suspended slots. Finally, the $\lambda/8$ phase shift at 60GHz is perfectly defined. Linear in frequency, the phase shift is expected to reach $\lambda/4$ at 120GHz.

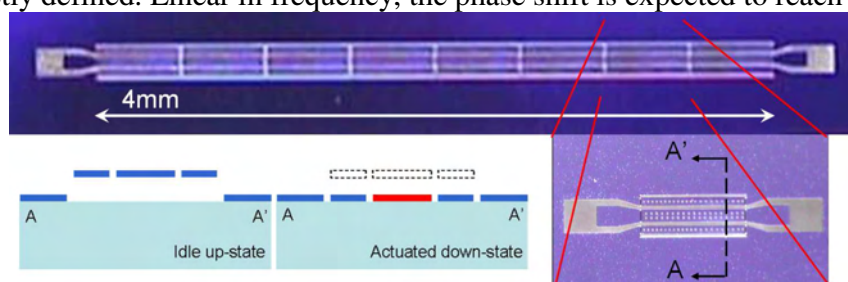


Figure 1 Top view microphotograph of the 4mm long phase shifter and one of its building blocks, along with schematic cross-section of idle and actuated states.

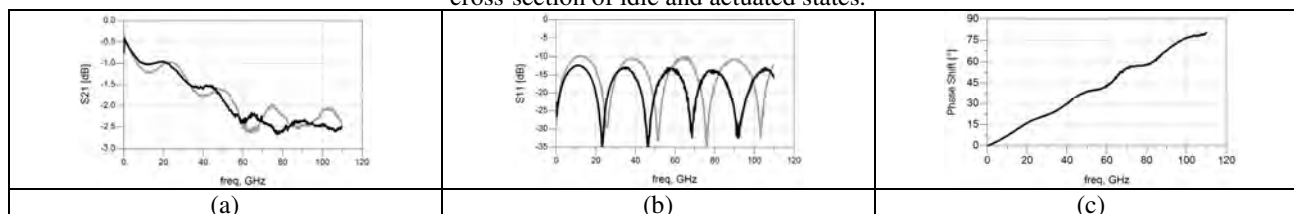


Figure 2 Measurement results of the phase shifter of Figure 1 – (a) and (b) insertion and return loss in idle (grey) and actuated (black) states (c) phase shift between idle and actuated states.

References

- [1] X. Rottenberg et al., "An electrostatic fringing-field actuator (EFFA): application towards a low-complexity thin-film RF-MEMS technology", J. Micromech. Microeng. 17 (2007) S204-S210.
- [2] D. M. Pozar, "Microwave Engineering", Addison-Wesley, 1993.

Tunable Filters for Agile Microwave Systems

A.Deleniv¹, S.Gevorgian^{1,2}

¹Department of Microtechnology and Nanoscience, Chalmers University of Technology, 41296 Gothenburg, Sweden

²Microwave and High Speed Electronics Research Center, Ericsson AB, Mölndal, Sweden

A general approach is developed that allows optimisation of the performance of the tuneable filters by trading between the tuning range and the losses. Tuneable resonators based on tuneable ceramics, semiconductor and ferroelectric varactors are considered as the main enabling technologies.

Tunable filters based on ferroelectrics and semiconductor varactors will be reported. As an example, Fig.1a shows the measured performance of a five-pole tuneable filter using GaAs semiconductor diodes. This is developed for the application at 2GHz and allows 200MHz (10%) tuning range. Another practical example of a tuneable dielectric-waveguide resonator is demonstrated at 15GHz. This uses thin film ferroelectric varactors, which at these frequencies are distinctly better than their semiconductor competitors. The measurement of the resonator revealed $\sim 120\text{MHz}$ tuneability and unloaded $Q=530$. To demonstrate the potential of the ferroelectric varactors a conceptual design of tuneable dual-mode dielectric-waveguide filter is developed with 15GHz centre frequency. The performance of the filter, Fig.1b, obtained using HFSS demonstrates $\sim 240\text{MHz}$ tuneability and $\sim 3\text{dB}$ insertion loss.

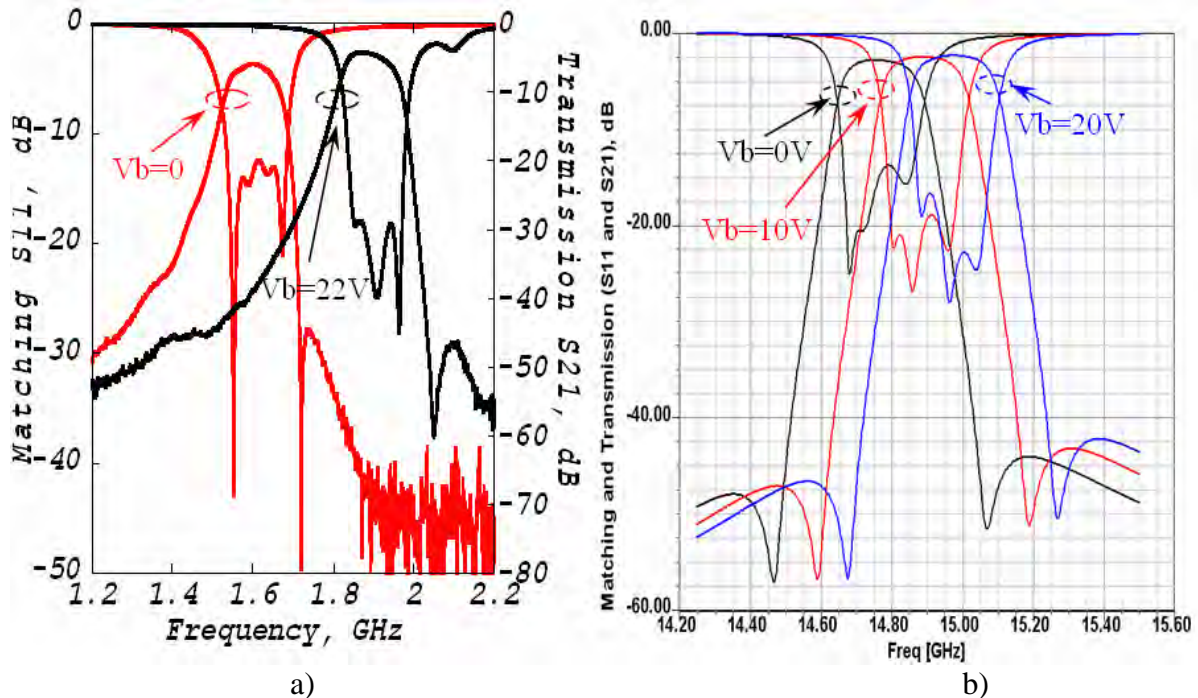


Fig.1 Performances of tuneable filters based on semiconductor (a) and ferroelectric (b) varactors.

Microwave MEMS activities at the Royal Institute of Technology

J. Oberhammer, N. Somjit, M. Sterner, F. Saharil, S. Braun, G. Stemme
 Microsystem Technology Lab, School of Electrical Engineering
 KTH-Royal Institute of Technology, 10044 Stockholm, Sweden
 contact: joachim.oberhammer@ee.kth.se

This paper gives an overview on the ongoing RF and microwave MEMS activities in the Microsystem Technology Lab (MST) at KTH, School of Electrical Engineering.

RF MEMS activities in this group are carried out since 2001, when the development of a special, S-shaped film-actuator based switch design was carried out, which combines the features of large DC and RF isolation in the off-state *and* very low actuation voltages of 12-15 V. This switch design has been adapted for constructing a switch array, consisting of 400 double-pole-single-through microrelays integrated and encapsulated on a single chip of a size of 10x14 mm², for the application of re-configurable telecommunication networks, to be employed in main distribution frames of the copper-wire network infrastructure. A SEM picture and a schematic overview of an array reduced to a 2x2 DPST configuration, is shown in Figure 4.

A further RF MEMS switch project comprises a mechanically bistable switch mechanism, which is based on two interlocking cantilevers (Figure 1), resulting in a switch with true zero-power consumption in the on-state and in the off-state. Figure 1 also shows a SEM picture of a special variant of this switch, where the complete switch mechanism is embedded inside the signal line of a coplanar waveguide, which, in contrast to conventional switch designs where the actuator is built ontop of the waveguide and therefore disturbing the wave propagation, results in an extremely low reflections and loss microwave switch of <0.1 dB switch insertion loss up to 20 GHz. Furthermore, this switch concept is based on a 3D micromachined, 30µm thick coplanar waveguide, which results in extremely low insertion loss, since the major part of the field lines is concentrated above, and not in, the substrate.

Within a NORDITE Scandinavian ICT programme project, novel RF MEMS components for the RF front-end of (automotive) radar beam-steering units at 76-81 GHz are investigated. Figure 2 shows a passive, micro-electromechanically tunable phase-shifter concept based on a moving dielectric block ontop of a transmission line, suitable for handling signals of much higher power as compared to switched delay lines. Figure 3, finally, shows a method of direct beam-steering by a micro-electromechanically tunable high-impedance surface, a tunable meta-material structure developed in collaboration with Helsinki University of Technology.

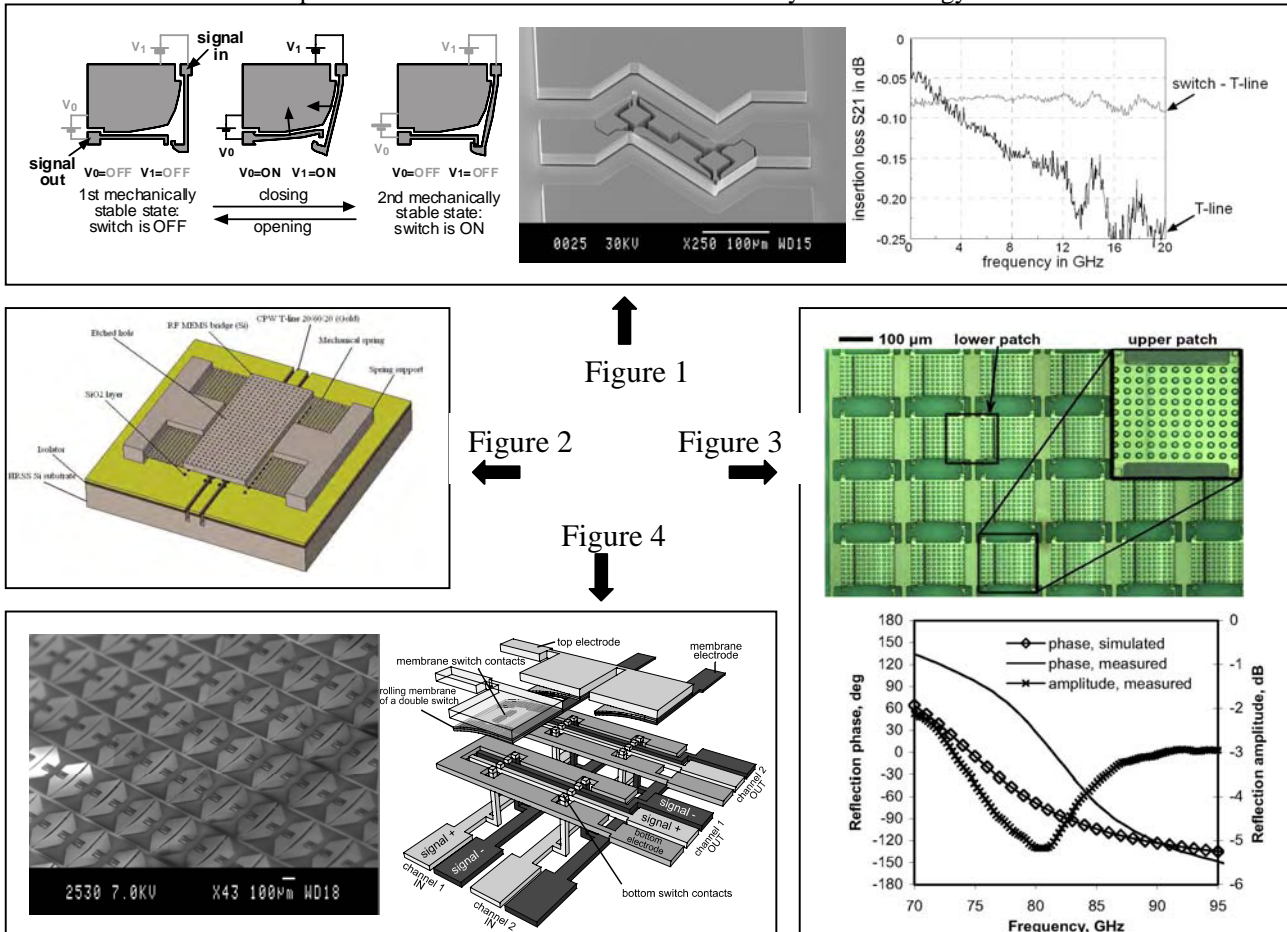


Figure 1

Figure 2

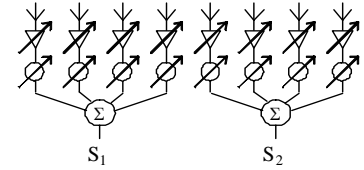
Figure 3

Figure 4

Phase-Comparing Direction Measurement Antenna Array for 6-18 GHz

Christer Johansson (christer.v.johansson@saabgroup.com), Thomas Eriksson (thomas.a.eriksson@saabgroup.com), Jan Grabs (jan.grabs@saabgroup.com), Tomas Windahl (tomas.windahl@saabgroup.com), all at Saab Avitronics, SE-175 88 Järfälla, SWEDEN.

Introduction A direction measurement antenna array aimed at high accuracy measurements of the direction to an emitter by using a single emitter pulse is designed. The antenna array uses 4+4 densely packed spiral antennas for the direction measurement (see the figure to the right) and another 4+4 spiral antennas for the ambiguity resolution. One spiral antenna is used as guard antenna. The signal from each spiral antenna is calibrated in phase as well as in amplitude. The direction of the main antenna lobe is electronically steerable by means of phase shifters. The combined signals from 4 spiral antennas form the signal S_1 and the combined signals from the 4 neighbouring spiral antennas form the signal S_2 . From S_1 and S_2 the phase-comparing monopulse method [1] is used to calculate the direction.



Theory The direction is calculated by the formula

$$(1) \quad \theta_{measured} = \arcsin \left(\lambda_{carrier} \frac{\arctan(\text{Im}(\Delta/\Sigma))}{M\pi a} + \lambda_{carrier} \frac{\sin(\theta_{calibrated})}{\lambda_{calibrated}} \right),$$

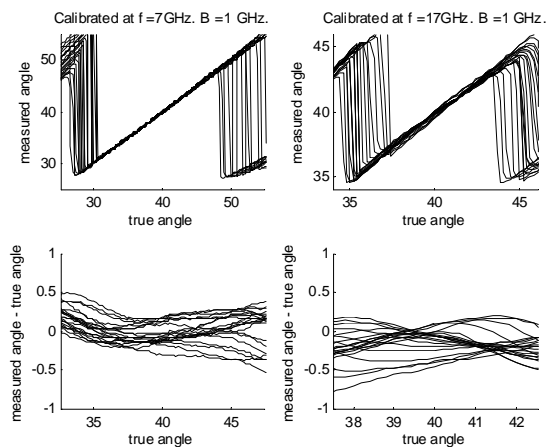
where $\text{Im}(\Delta/\Sigma)$ is the imaginary part of the monopulse quotient, $\theta_{calibrated}$ is the direction of the main lobe for the calibration frequency $c/\lambda_{calibrated}$, M is the number of antenna elements combined in each channel ($M=4$ in this case), a is the spiral antenna element distance ($a=33\text{mm}$ in this case) and $\lambda_{carrier}$ is the carrier wavelength of the emitter. By using perturbation theory and basic probability theory the expected standard deviation of the measurement error due to the phase shift discretization can be derived from Eq (1) as

$$(2) \quad \sigma_{\theta}^2 = \text{Var}[\theta_{measured}] = \frac{\sigma_{phase\ shifter}^2 \cdot \lambda_{carrier}^2}{2\pi^2 a^2 M^3 \cdot \cos^2(\theta_{true})},$$

where $\sigma_{phase\ shifter}$ is the standard deviation of the phase shift error and σ_{θ} is the standard deviation (due to the phase shift error) of the measured direction. Since 5-bit phase shifters are used the phase error is uniformly distributed within $\pm 5.625^\circ$, giving $\sigma_{phase\ shifter} = 11.25^\circ / \sqrt{12} \approx 3.25^\circ$. Eq. (2) can be seen as the theoretical limit of the performance of a monopulse antenna array that is phase calibrated and directionally steered with phase shifters.

Measurements The plots to the right show examples of direction measurements when the main antenna beam is pointing 40° off boresight and when the polarization of the incoming wave is known. The antenna was calibrated at the direction 40° and for this polarization. The upper row in the figure to the right shows two plots of the measured direction versus true direction, and the lower row shows measurement error versus true direction. The two leftmost plots show the result for $f \in [6.5, 7.5]$ GHz, and the two rightmost for $f \in [16.5, 17.5]$ GHz. Eq (2) predicts the measurement error σ_{θ} to be

0.15° (at 7 GHz) and 0.06° (at 17 GHz). Hence, from the lower row it is seen that the measurement error of the antenna array is close to the theoretical limit at 7 GHz, and about twice the theoretical limit at 17 GHz.



Acknowledgements This work was financed by the Swedish Defence Materiel Administration.
References [1]: Skolnik: Radar Handbook, Second edition, McGraw-Hill, 1990

MEMS Phase Shifters for an Affordable Low-Power Ka-Band Multifunctional ESA on a Small UAV

¹Robert Malmqvist, ^{1*}Carl Samuelsson, ¹Andreas Gustafsson, ¹Tomas Boman, ¹Svante Björklund, ¹Börje Carlegrim, ¹Roland Erickson, ²Tauno Vähä-Heikkilä, ²Pekka Rantakari

¹Dept. of Sensor Technologies, FOI Swedish Defence Research Agency, Linköping, Sweden

²Millilab, VTT Technical Research Institute of Finland, Espoo, Finland

(*Presently with Saab Communication AB, Linköping, Sweden)

Abstract—We report on a study of a Ka-band multi-functional electronically steerable antenna (ESA) on a small UAV that is based on using sub-arrays with low-loss RF MEMS phase shifters. Our power estimations show that low phase shifter losses are critical if the dissipated radar hardware DC power should fit within the given system requirements. Simulated results further indicate it can be possible to achieve adequate RF performance with a 4-bits 35 GHz MEMS phase shifter design made on quartz.

I. INTRODUCTION

Unmanned Airborne Vehicles (UAVs) can be deployed to perform various missions such as surveillance, reconnaissance and monitoring by the use of imaging systems. Compared with optical sensors, a radar sensor provides all-weather and all-night capabilities as it can function almost independent of rain, snow, fog and the time of the day. A small UAV equipped with a multifunctional RF system needs to support different radar functions as well as a data link. High resolution images of the ground are obtained with synthetic aperture radar (SAR). The ground-moving-target-indicator (GMTI) mode makes it possible to also detect moving objects on the ground. An on-board all-weather Sense-and-avoid (S&A) capability will be needed for UAVs to avoid collisions with flying objects. This is also a requirement for UAVs to be allowed to operate autonomously in non-segregated airspace. It is also important to achieve low cost, size, weight and DC power for the radar hardware. With the technology of today, the easiest realization would probably include mechanically scanned antennas. However, for the future it is believed that advances in phased array technology can facilitate multi-function and conformal antennas which are integrated in the fuselage. An active electronically scanned antenna is flexible but also complex and

costly to realize since it requires an LNA and PA behind every antenna element which will increase the cost, especially for large arrays. For a more affordable approach we consider instead a passive ESA where a single LNA and PA are used behind a certain subarray. Since commercially available Ka-band phase shifters have too high losses we study here the possibility to use MEMS phase shifters in a Ka-band multifunctional ESA on a small UAV.

II. SYSTEM ARCHITECTURE AND REQUIREMENTS

Beam steering will be needed for SAR/GMTI (spot mode) as well as for S&A. Electronic scanning is more flexible and adaptable to sharing the apertures between multiple functions compared to mechanical scanning. A conformal ESA could also more easily fulfill the demands on low weight and compact size for a small UAV. Meeting the power requirements for the SAR function is found to be limited by the available DC power for the radar hardware (50 W is assumed for a small UAV). Low-loss phase shifters are then key elements in a passive ESA where the number of LNAs and PAs can be minimized using sub-arrays (and thus the cost).

III. RF MEMS PHASE SHIFTERS

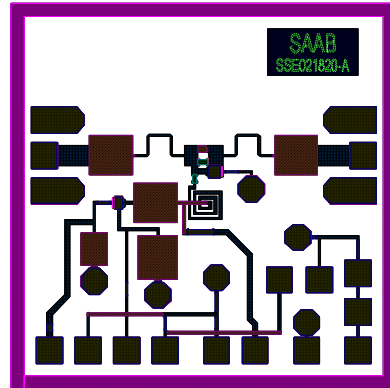
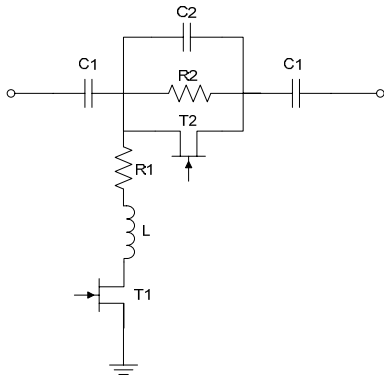
We have designed a 4 bits phase shifter which has been sent to be fabricated at ICT Trento in Italy using their RF MEMS process. The two largest bits were simulated using an EM-simulation tool. According to simulations, the loss for the shortest and longest delays (reference state and close to 360°) equals 1 dB and 3 dB at 35 GHz, respectively. The average loss equals 2 dB. This compares relatively well with a previously reported Ka-band MEMS phase shifter, especially since that the phase shifter design presented in this paper involves one more bit. Measured results of the fabricated MEMS phase shifter will be reported on at the conference.

An adjustable broadband MMIC equalizer

Jan Grabs (jan.grabs@saabgroup.com), Ulf Öhman (ulf.ohman@saabgroup.com)
and Niklas Meissner (niklas.meissner@saabgroup.com)
Saab Avitronics, SE-175 88 Järfälla, Sweden.

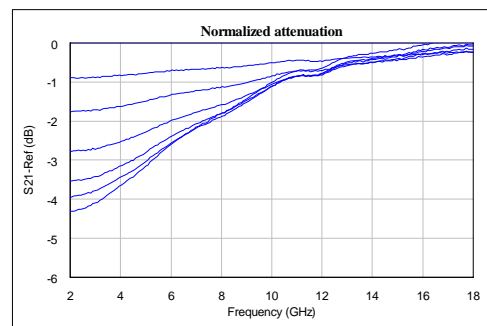
Introduction. Broadband GaAs amplifiers that are used in many microwave circuits have an inherent drawback, the gain changes with temperature. This gain level variation can be handled by temperature controlled attenuators but there is also a change in the frequency slope when the temperature varies. An amplifier covering the 2 – 18 GHz frequency range can have a frequency slope of about 2 dB within the temperature range of -55°C to +120°C. This can cause problems when a number of amplifiers are used in the gain chain. E.g. a circuit with five amplifiers will cause a frequency slope change of about 10 dB. A solution to this problem is to use an equalizer with a positive frequency slope that changes with temperature.

The realisation of the equalizer is an MMIC chip made on GaAs. The circuit consists of a resistive attenuator and two reactive elements, a capacitor and an inductor. These elements are used to bypass the high frequencies and thereby creating a frequency slope. To adjust this slope two FETs are used. These work as tuneable resistors where the resistance is changed by adjusting the bias voltage. The circuit also consists of DC blocking capacitances and bias circuits.



Equivalent circuit of the equalizer

Results. The measured performance of the broadband MMIC equalizer show that the attenuation is adjustable between 4.5 dB and 9 dB at 2 GHz resulting in a tuneable frequency slope change of about 4.5 dB. The attenuation at 18 GHz is about 2.5 dB. The picture to the right shows the normalized gain with different bias voltage settings.



Data showing the improvement using this equalizer chip in a microwave circuit will also be presented at the conference.

Acknowledgements. This work was partly financed by the Swedish Defence Materiel Administration.

Tunable Impedance Matching Network

M. R. Rafique, T. Ohki, P. Linner and A. Herr

Abstract—We present superconducting SQUID based tunable impedance matching networks designed for highly miniaturized filters. The performance of miniaturized filters is very sensitive to parasitic and fabrication related spread. The presented experimental results show that using tunable impedance matching networks, the degraded performances of these types of filters is improved.

I. INTRODUCTION

TUNABLE impedance matching network using serial SQUIDs as a tunable inductance is presented. A tunable impedance matching network is an essential component of high-Q miniaturized superconducting filters. A tunable impedance matching network compensates for the inevitable reflection losses at ports of the filter due to the parasitic and fabrication related spread of parameters. Comparing the other methods of inductance/capacitance tuning, SQUID based tuning is easily achievable at low power applications, as it needs no add-on layers or mechanical setups. From [1], the overall inductance of a dc-SQUID can be varied by control current, I_{con} . The SQUID based tunable impedance matching networks, designed for Hypres 4.5 kA cm⁻² process [2], are theoretically and experimentally verified.

II. THEORY

The total inductance of N SQUIDs in series with a common I_{con} can be expressed as

$$L \propto \frac{N}{A + B \cos(DI_{con})}, \quad (1)$$

where A , B and D are SQUID's parameter dependant constants. From (1), for a required small ΔL , the needed ΔI_{con} is $\propto \Delta L$.

In the tunable impedance matching network, the integration of series SQUIDs can be efficiently done by replacing the inductance, L , of the lumped π -network (Fig. 1(a)). For a filter impedance of Z_f , standard microwave load impedance, $Z_k=50 \Omega$, and shunt capacitors of the π -network, C , the port impedance, Z_p , of the network can be expressed as follows

$$Z_p = \frac{Y_C + Y_L + Y_f}{Y_C(Y_C + Y_L + Y_f) + Y_L(Y_C + Y_f)}, \quad (2)$$

where $Y_L=1/(j\omega L)$, $Y_C=j\omega C$, $Y_f=1/Z_f$. From (1) and (2), at an optimum matching of $Z_k = Z_p$ at the filter's passband, f_0 , the small shift in Z_f , ΔZ_f , can be compensated by tuning I_{con} as $\Delta I_{con} \propto \Delta Z_f$.

Raihan Rafique, Thomas Ohki, Peter Linner and Anna Herr are with the department of Microtechnology and Nanoscience, Chalmers University of Technology (corresponding author, phone: +46317721875; fax: +46317723622; e-mail: raihan.rafiq@mc2.chalmers.se).

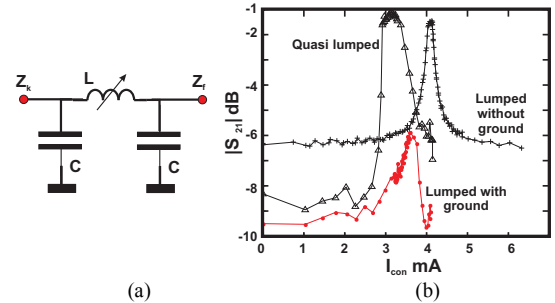


Fig. 1: Equivalent model (a) and measured passband loss (b) of the filters as a function of control current of tunable impedance matching networks.

III. EXPERIMENTAL RESULTS

The developed tunable matching network has been connected to three different superconducting filters presented in [3]. The effect of the matching network tuning has been tested by measuring transmission characteristic of the filters, at 4.2 K using an Agilent E8364B network analyzer. Fig. 2(b) shows the measured maximum transmission, $|S_{21}|$, at the passband of all the filters. The measured current, corresponding to the maximum inductance tunability is 4.1 mA. Table 1 summarizes the measured performance of the filters with passive and tunable impedance matching networks.

TABLE I
COMPARISON OF FILTERS' PERFORMANCES

Filter type		L pH	BW MHz	ripple dB	Losses dB	f_0 GHz
Lumped filter	Passive	161	5	0.15	8.7	2.11
	Tunable	170	3.5	-	5.9	2.15
Lumped filter	Passive	163	28	2.38	2	1.96
	Without ground	Tunable	275	18	-	1.46
Quasi-lumped filter	Passive	190	110	4.3	4.75	4.45
	Tunable	207	75	-	1.12	4.42

IV. CONCLUSION

SQUID based superconducting tunable impedance matching networks for miniaturized microwave high-Q filters are successfully demonstrated. The presented circuits are one of the first examples that demonstrate the SQUID with a highly miniaturized monolithic passive filter to overcome parasitic and fabrication related spreads dependent performance degradation.

REFERENCES

- [1] T. A. Fulton, L. N. Dunkleberger, and R. C. Dynes, "Quantum interference properties of double Josephson junctions," Phys. Rev. B, vol. 6, 1972.
- [2] Hypres Nb Design Rules. [Online]. Available: <http://www.hypres.com/>
- [3] R. Rafique, Towards Superconducting Monolithic Microwave Integrated Circuits. Chalmers: PhD dissertation, 2008.

CODED OFDM IN HYBRID RADIO OVER FIBRE LINKS

Juan F. Miranda M. and Mikael Gidlund*

Center for RF Measurement Technology, University of Gavle, Sweden
and Nera Networks AS, Norway, e-mail: juan_mm24@hotmail.com

Distributed antenna systems based on Radio over Fiber (RoF) has proved to be the most efficient solution to achieve in-building coverage in 3G systems [1]. Today 3G uses an air interface based on WCDMA. However, Coded Orthogonal Frequency Division Multiplexing (COFDM), has been selected in IEEE802.11a, WiMax and the long term evolution of 3G (LTE) due to its flexibility and robustness in fading environments [2]. The objectives of the present investigation are therefore to examine the OFDM reliability in the nonlinearities and multipath posed by the RoF link, and how its performance can be improved by using representative linear block codes.

As a measure of reliability, the Bit Error Rate (BER) of the uncoded and coded OFDM-RoF system for Uplink (UL) and Downlink (DL) was simulated. The system modeling considers multipath fading from radio transmission [3] and Amplitude-to-Amplitude (AM/AM) and Amplitude-to-Phase (AM/PM) distortions produced by the Electrical-to-Optical (E/O) conversion and amplifying stages of the fiber link [4]. Several BCH and Reed-Solomon codes were studied with different code rates [5], complexity and interleaving depth. Their properties are related to system parameters such as Bit Energy per Noise Density, Input Back-Off (IBO) and modulation order.

The Results show that using 4-QAM modulation with a moderate Input Back-Off (i.e. 4-10dB), BCH and small Reed-Solomon codes can reduce BER by a factor even greater than 10 depending on the IBO. However, using 16-QAM modulation BER reduction is poor even if Reed-Solomon is used with large number of bits per symbol. Future work would consider using a more complex model for the E/O conversion and power amplifier, more sophisticated codes such as Turbo or LDPC, and the use of nonlinear channel estimation to further enhance system performance.

References

- [1] Hans Beijner, The importance of in-building solutions in third-generation networks: Ericsson Review, Page(s): 90 – 97 2004
- [2] R. Prasad, *OFDM for Wireless Communication Systems*. New Jersey: Artech House, 2004.
- [3] N. Chayat and Breezecom, "IEEE P802.11 Wireless LANs, Updated Submission Template for TGa - revision 2, doc.:IEEE802.11-98/156r2," March 1998.
- [4] X. N. Fernando and A. B. Sesay, "Higher order adaptive filter based predistortion for nonlinear distortion compensation of radio over fiber links," IEEE International Conference on Communications ICC'00, New Orleans, June 20
- [5] S. B. Wicker, *Error Control Systems for Digital Communication and Storage*. New Jersey: Prentice Hall, 1995.

This work was sponsored by Fiber Optic Valley and EU regional strategic fund under grant X2.304-1135-06.

Equivalent Circuit of Metamaterials with a Negative Permeability

A. Rumberg and M. Berroth

Institute of Electrical and Optical Communications Engineering, Universität Stuttgart,
Pfaffenwaldring 47, 70550 Stuttgart, Germany, axel.rumberg@int.uni-stuttgart.de

Abstract

An equivalent circuit of cut-wire pairs providing a negative permeability is presented. The working frequency is around 10 GHz. The equivalent circuit precisely describes the behavior of the real objects including the magnetic resonance.

Introduction

Veselago [1] investigated theoretically the properties of materials having a negative permittivity and a negative permeability simultaneously describing them with a negative refractive index. In 2001 periodic split ring resonators (SRR) demonstrated the negative index in a metamaterial structure [2]. There are now several modifications of the SRR structure. One of the simplest is the so called cut-wire pair (Fig.1) [3]. It can provide a negative permeability at microwave and optical frequencies.

Simulation, Experiment and Results

The wire pairs work with an LC-resonance. The incident electromagnetic field (Fig.1) excites a current in one wire which is coupled to the other wire by the displacement field. A current loop is generated. The excited magnetic field counteracts the incident magnetic field and can change its direction. The dimensions are as follows: $l = 8.5$ mm, $w_1 = 0.7$ mm, $h = 10.16$ mm, $p = 5.715$ mm, $t = 0.5$ mm. The equivalent circuit describes the resonance of the single wires (L_{EL} and C_{EL}) and the magnetic resonance. The substrate RO4003C is modeled with L_{TL} and C_{TL} . The wire pair is coupled to this transmission line by the mutual inductance $M = F \cdot L_{TL}$. F is the fraction of the unit cell occupied by the wire pair. Fig. 2 shows the results. The simulation is done with the FEM solver HFSS at normal incidence and in a waveguide with oblique incidence. The equivalent circuit simulation shows good agreement with the normal incidence simulation. The permeability is retrieved from the S-Parameters [4]. The measurement is done in a waveguide as here only small pieces of substrate are needed. The HFSS simulation agrees well with the measurement. The overall transmission is lower because of the oblique incidence. The magnetic resonance can be seen clearly.

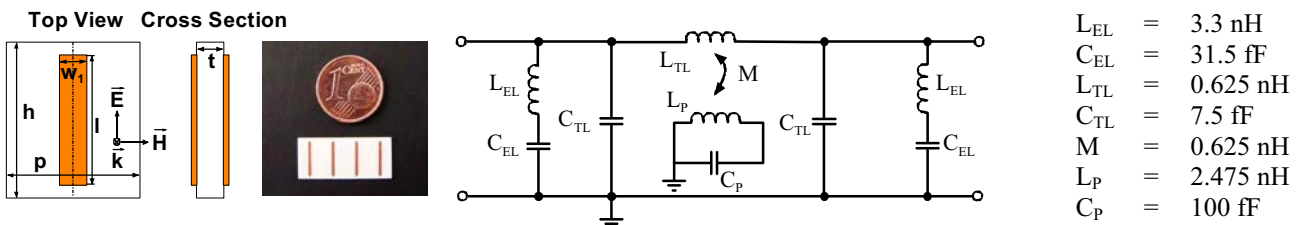


Fig. 1. Top view, cross section, measured piece and equivalent circuit of the cut-wire pair.

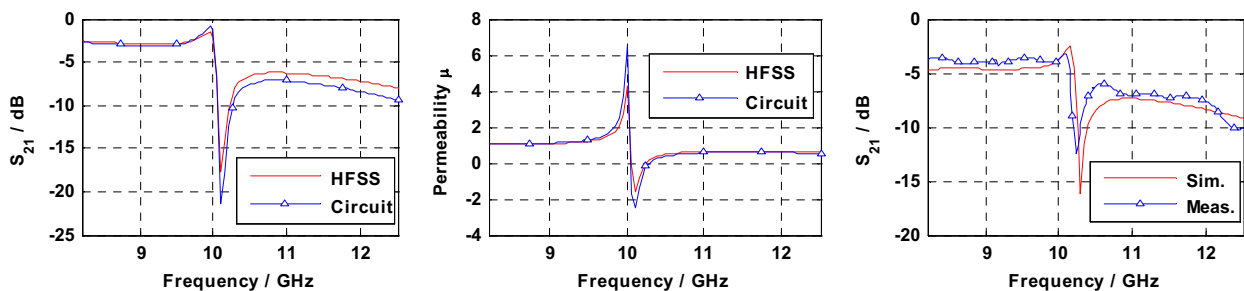


Fig. 2. Transmission at normal incidence, retrieved permeability and waveguide measurement.

Conclusion

The equivalent circuit describes the transmission behavior of the cut-wire pair very well. Also the retrieved permeability matches. The equivalent circuit provides a good understanding of the structure and allows in this way a simple optimization.

[1] V. Veselago, Sov. Phys. Usp., vol. 10, pp. 509-514, 1968.

[2] R.A. Shelby, D.R. Smith, and S. Schultz, Science, vol.292, pp. 77-79, 2001.

[3] J. Zhou, L. Zhang, G. Tuttle, T. Koschny, C.M. Soukoulis, Phys. Rev. B, vol.73, p. 41101, 2006.

[4] X. Chen, T.M. Grzegorzczuk, B.I. Wu, J. Pacheco, J.A. Kong, Ph. Rev. E, vol.70, p. 16608, 2004.

Workshop

RF Power Amplifiers (1)

1300-1500 Wednesday 5 March 2008

The Frequency Spectrum of Bandpass Pulse Width Modulated Signals

Thomas Blocher¹, Peter Singerl², Andreas Wiesbauer² and Franz Dielacher²

¹Christian Doppler Laboratory for Nonlinear Signal Processing

Graz University of Technology, Austria, E-mail: Thomas.Blocher@tugraz.at

²Infineon Technologies Austria AG

I. INTRODUCTION

Third generation radio transmitters generally uses bandwidth efficient modulation techniques to provide the required high data rates. Because such modern modulation formats generates signals with high peak-to-average power ratios, linear power amplifiers (PAs) are needed to meet the spectral requirements. Unfortunately, such linear power amplifiers have very low efficiencies which directly affects the operational costs of a radio basestation. Switched mode PAs have the potential to increase the efficiency considerably. Because such switched mode PAs can only be operated with a limited number of different input signal amplitudes, the modulated (amplitude and phase) RF signal must be modified accordingly. One method is to encode the envelope and the phase of the RF signal into a binary signal with different pulse widths and pulse positions where the original spectrum can be recovered with a simple bandpass filter.

F. H. Raab presented in [1] the bandpass pulse width modulation (BP-PWM), which generates such binary signals. The pulse train $x_p(t)$ in Fig. 1 depicts a BP-PWM encoded signal. The binary signal possess exactly one pulse per carrier period, where the widths of the pulses are proportional to the envelope $a(t)$ and the positions of the pulses depend on the phase $\phi(t)$. The block diagram of the BP-PWM proposed by Raab is shown at the top of Fig. 2, where the envelope is compared with the 90° phase shifted and rectified carrier. A pre-distortion with the arcsin function of the reference signal U_{Ref} and the input signal does not change the modulator output. If the trigonometric function arcsin is applied to the rectified sine-wave reference signal, we obtain a triangular signal. The BP-PWM block diagram with pre-distortion (as used in [2]) is shown at the bottom of Fig. 2. If the reference signal is not phase-modulated, the BP-PWM corresponds to a PWM with pre-distorted input [3].

II. RESULTS

We derive the BP-PWM output spectrum for sinusoidal input signals with a two-dimensional Fourier transform. This analytically derived spectrum is identical to the spectrum of the PWM, where the input is pre-distorted and the PWM reference frequency is replaced by the phase modulated reference signal. Numerical simulations have shown that BP-PWM spectra contains the original signal plus an additional noise. Fortunately, most of the distortion is distributed close

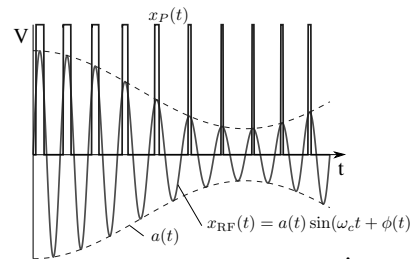


Fig. 1. RF signal, its envelope and the corresponding BP-PWM output

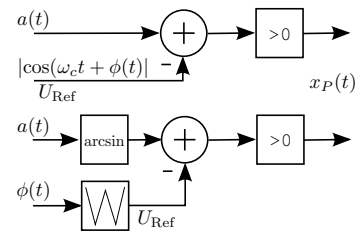


Fig. 2. Block diagram BP-PWM (top), BP-PWM with pre-distortion (bottom)

to the carrier harmonics far away from the frequency band of interest. Due to the discrete-time nature of the proposed modulator architecture we introduce some additional magnitude and phase noise which is primary caused by the time discretization process of the binary signal. Therefore we show the fundamental relationships between the sampling frequency, carrier frequency and the dynamic range.

III. CONCLUSION

Switched mode power amplifiers are suitable to increase the efficiency of new generation radio transmitters considerably. To drive such PAs, we need new modulation schemes which are able to encode the amplitude and phase information e.g. into binary signals. Bandpass PWM generates such signals where the desired information can be recovered with simple low-order bandpass filters. The drawback of bandpass PWM is the short average pulse duration of the PA driving signals.

REFERENCES

- [1] F. H. Raab, "Radio frequency pulsewidth modulation," *Communications, IEEE Transactions*, vol. 21, no. 8, pp. 958–966, 1973.
- [2] S. Rosnell and J. Varis, "Bandpass pulse-width modulation," *Microwave Symposium Digest, 2005 IEEE MTT-S International*, p. 4, 2005.
- [3] Z. Song and D. V. Sarwate, "The frequency spectrum of pulse width modulated signals," *Signal Process.*, vol. 83, no. 10, pp. 2227–2258, 2003.

The potential of active load and source tuning on base stations power amplifiers

Thomas Lejon, Ericsson AB

thomas.lejon@ericsson.com

Summary

This paper addresses the potential in active impedance tuning network for power amplifiers used in base stations for cellular networks.

Abstract

The cellular networks nowadays need to operate in several frequency bands, this threatens to generate a product portfolio with many variants because of the narrow bandwidth of the power amplifier used in the transmitters. There is also a need for high efficiency to reduce the operating cost (OPEX) of the network and large bandwidth for high data rates or multi carrier scenarios. Because of this it is interesting to try to find solutions for an electrically controlled low loss and low Q impedance transformation network that can handle the RF voltage swing created by the amplifier. If we can create such a network it would open possibilities to retune the amplifiers both in frequency and/or increase the efficiency in back off at high modulation bandwidth. This paper will address the need for such a network, the requirements of it, some challenges in creating it and also the potential if it could be created.

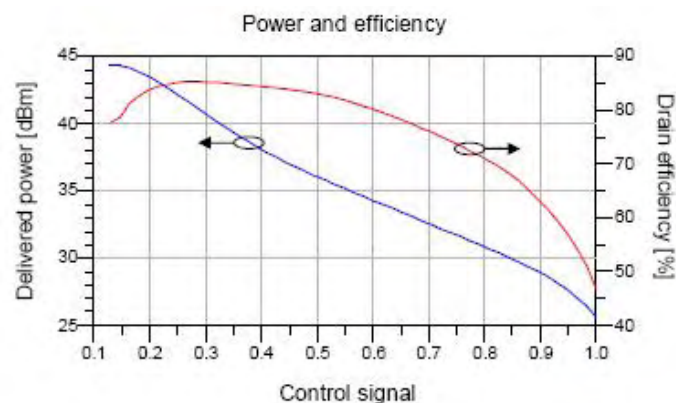


Figure 1 Load modulated class F amplifier

Comparing Polar Transmitter Architectures using a GaN HEMT Power Amplifier

Ellie Cijvat¹, Kevin Tom², Mike Faulkner² and Henrik Sjöland¹

¹Dept. of Electrical and Information Technology, Lund University, Sweden
P.O. Box 118, SE-221 00 Lund, Sweden. e-mail: ellie.cijvat@eit.lth.se

²Centre for Telecommunications and Micro-Electronics (CTME), Victoria University, Australia
P.O. Box 14428 MCMC, Melbourne 8001, Australia

Short summary - A power amplifier (PA) with variable gate bias is compared to an Envelope Elimination and Restoration (EER) configuration. Each use the low-frequency envelope and high-frequency phase component of the signal. The test circuit is implemented using a discrete GaN HEMT power device. Measurements show that the EER architecture maintains a relatively high drain efficiency for a wide output power range, while the PA with variable gate bias shows a significant drop in efficiency for lower output powers.

I. INTRODUCTION

The power amplifier is a critical component in the transmitter. Many architectural solutions have been investigated and implemented, such as Envelope Elimination and Restoration (EER) and Envelope Tracking (ET) [1]. On the circuit design level, an increased interest in switched-mode power amplifiers (PA) has been shown.

Power amplifier architectures suitable for transmission of separated envelope (low-frequency) and phase (high-frequency) signals are compared. First, we discuss a power amplifier with variable gate bias [3]. The PA is switch-mode, and both the low- and high-frequency signal operate on the gate of the device; The phase signal thus causes the transistor to be switched on for a shorter or longer period of time, resulting in a pulse-width modulated signal at the drain of the device, which is then filtered by the output network, giving a variation in output power. Unfortunately, this amplifier structure is not linear, so linearization will be required.

This architecture is compared to a more conventional polar transmitter architecture, that is, EER. Both EER and ET architectures need a supply modulator [1], commonly implemented as a DC-DC converter or class-S amplifier followed by a low-pass filter. However, this modulator is not included in the design, nor in the efficiency.

II. RESULTS

A power amplifier was implemented with a discrete GaN HEMT device [2]. In Fig. 1 the output power and efficiency for the variable gate

bias and EER architecture, respectively, are shown. The variable gate bias shows a maximum output power of 29dBm, with a maximum drain efficiency of 59%. However, the efficiency decreases quite rapidly for decreasing output power. For the EER architecture the efficiency stays high over a large range of output power.

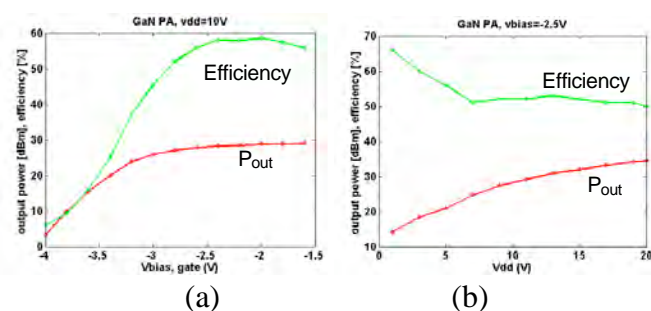


Fig. 1. Measurement results, (a). Output power and drain efficiency as a function of gate bias voltage, with $V_{dd} = 10V$ and $f_{in} = 360MHz$, (b). Output power and efficiency as a function of varying supply voltage (EER), with $V_{bias} = -2.5V$ and $f_{in} = 360MHz$.

III. CONCLUSIONS

The variable gate bias and EER transmitter architectures were compared, using a power amplifier implemented with a discrete GaN HEMT device.

Measurements show an efficiency of 66 to 50% for the ideal EER architecture, for an output power of 14 to 34 dBm, while the variable gate bias PA has a slightly larger range of output power but shows a significant drop in efficiency for lower output power: from 6 to 59% for an output power range of 3 to 29 dBm.

REFERENCES

- [1] F. Wang et al., "An Improved Power-Added Efficiency 19-dBm Hybrid Envelope Elimination and Restoration Power Amplifier for 802.11g WLAN Applications", *IEEE Trans. on Microwave Theory and Techniques*, Vol. 54 no. 12, pp. 4086-4099, December 2006.
- [2] Cree Inc, CGH40010 product specification. Available: http://www.cree.com/products/pdf/CGH40010-Rev1_4.pdf
- [3] E. Cijvat, et al., "A GaN HEMT Power Amplifier with Variable Gate Bias for Envelope and Phase Signals", in *Proc. of the 25th Norchip Conference, November 2007*.

Class MTM Power Amplifier Linearization

David E. Kelly

PulseWave RF, Austin, TX 78746 USA

Vice President of Engineering – dkelly@pwr.com – 001 (512) 437-2600; fax 001 (512) 437-2601

Abstract - An asynchronous noise-shaping modulator is employed to convert high crest factor analog signals into a data stream. This digital data stream can be directly applied to a broad-band switch mode power amplifier wherein linearity is accomplished via real-time RF feedback. The same Class MTM system can also be applied in a plurality of linear control systems such that it processes distortion signals only. These methods can offer advantages in coding efficiency and device utilization.

Index Terms — Class MTM is a proprietary linearization technology developed by PulseWave RF.

I. INTRODUCTION

For the past decade, perhaps longer, considerable effort has been channeled into improving the power added efficiency, PAE, of linear power amplifiers. Capital and operating expenses, reliability, and radio talk time are but a few of the motivations to improve PAE.

The modern digital cellular communications standards are optimized to extract best utilization from the available spectrum. Since spectrum is the scarce resource, bandwidth efficiency is the first item on a large list of challenges to address. The obvious solution for the systems engineer is to increase modulation coding. Higher data rate calls for higher spectral efficiency, which translates to signals with higher peak to average ratios or PAR. This in turn drives higher linearity requirements on the transmit link, especially, the output power amplifier, or PA. Several techniques have evolved, including novel hardware design and digital signal processing, which reduce the burden of high PAR on the PA. The short summary list of these techniques reads something like;

1. Crest Factor Reduction
2. Analog Predistortion
3. Digital Predistortion
4. Linear Feed-forward Amplifier
5. Doherty Amplifier
6. Envelope Tracking
7. Envelope Elimination and Restoration (EER)
8. LINC (linearization w/ non linear components) or out-phasing

Traditional linear RF PA design begins with a class AB output stage biased for the peak signal power it must deliver. In order to improve PAE one, or more, of the preceding methods is employed to facilitate operating the device deeper into compression without sacrificing linearity in the process. The limit case approach is hard switching at the carrier frequency, as in the LINC method. Both of the envelope methods listed involve amplitude modulation of the output stage and are special cases of switch-mode operation.

One subject of this paper is hard switching at the carrier frequency up to, and including, the output stage. A noise shaping modulator is employed to frequency translate and encode a modulated analog carrier. The amplitude and phase information from the modulated signal are conveyed in pulse density fashion to a switching amplifier. Non idealities in the switching amplifier are mitigated through loop feedback. A sample of the output is routed back through the modulator, in real-time, wherein the effects of distortion and loop delay are minimized. Note the simplified block diagram in figure 1. This is a digital amplifier that encodes an analog input signal and compares it to the output signal on a bit by bit basis. The modulator provides correction signals to maintain linearity as necessary.

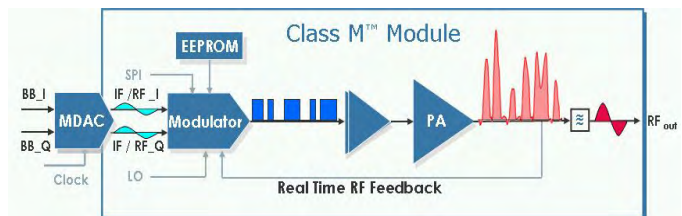


Figure 1 – Class M Amplifier System

Additional examples of CLASS MTM amplifier embodiments, along with their supporting laboratory measurements, will be discussed in the full workshop presentation.

Different Classes (A, AB, C & D) of Power Amplifiers using SiC MESFET

Sher Azam¹, R. Jonsson², Q. Wahab^{1,2}

¹ Department of Physics (IFM), Linköping University, Linköping, Sweden

² Swedish Defense Research Agency (FOI), Linköping, Sweden

ABSTRACT:

In this abstract we are presenting wide bandgap semiconductor transistors (SiC MESFET) in different classes of amplifiers. The results are based on designing and fabrication of class-AB power amplifiers using ADS and simulation of physical transistor structure (after optimization) in TCAD for class-A and switching response in class -C & D power amplifiers.

1): Class-A Power Amplifier results

In class-A, The limiting frontier of DC voltage at the drain of an enhanced version of previously fabricated and tested SiC microwave power transistor is studied at 1 GHz. An increase in the power dissipation (W/mm) and decrease in PAE (%) with the increase in DC drain voltage is observed. The PAE (%) at 1 GHz, at $V_{dc}= 50$ V is 25.6 %, reduced to 16.8 % at $V_{dc}= 70$ V (34.4 % decrease). The power dissipation is increased from 8.41 W/mm at $V_{dc}= 50$ V to 11.25 W/mm at $V_{dc}= 70$ V (36.36 % increase). Thus DC voltage applied at the drain of SiC MESFET greater than 50 V is disadvantage in class-A power amplifier.

2): Class-AB Power Amplifier results

In class-AB, We designed and fabricated three power amplifiers (30-100 MHz, 200-500 MHz and 0.6-1.8 GHz). The designs are based on measured S-parameters. The 30-100 MHz amplifier showed 45.6 dBm (~36 W) power at 1 dB compression (P_{1dB}), at 50 MHz. The power added efficiency (PAE) is 48 % together with 21 dB of gain. The maximum output power at 2 dB gain compression was 46.1 dBm (~41 W). One power sweep was performed at a drain bias of 60 V, $V_g = -8.5$ V, and at this bias point the P_{1dB} was 46.7 dBm (~47 W).

The typical results obtained in 200-500 MHz are; at 60 V drain bias the P_{1dB} is 43.85 dBm (24 W) except at 300 MHz where only 41.8 dBm was obtained. The maximum output power was 44.15 dBm (26 W) at 500 MHz corresponding to a power density of 5.2 W/mm. The PAE @ P_{1dB} [%] at 500 MHz is 66 %.

Preliminary measured results obtained in 0.6-1.8 GHz amplifier are; S11 is below -4 dB, S22 below -9 dB and gain is above 9 dB upto 1.2 GHz and above 7 dB for the rest of the band.

3): Class-C & D Switching Power Amplifier results

In class-C, the switching response of SiC MESFET is studied by applying square pulses of 5 % duty cycle at the gate. The results are; efficiency of 71.4 %, power density of 1.0 W/mm with a power gain of 31 dB and switching loss was 0.424 W/mm.

In class-D, a square pulse of 30% duty cycle is applied at the gate and at the same time a square pulse of same duty cycle is applied at the drain (instead of applying sin wave) at 1 GHz. A V_{dc} voltage of 10 V is applied at the drain to keep the transistor above turn ON. The results are; an efficiency of 49.3 %, power density of 2.1 W/mm with a power gain of 29.3 dB is obtained. The switching loss is 2.15 W/mm.

The device shows resistive loss behavior at the crossing point of the drain current and voltage waveforms in both amplifiers. It is due to the sudden increase in drain current during the turn off. The space charge accumulation at the channel and buffer layer interface and near the gate on drain side and electron current density in the channel at gate voltage pulse off and drain voltage pulse rise time (which is observed using Tech plot software) is also found to be responsible for the switching losses and resulting reduction in the efficiency.

Modeling of dual-input power amplifiers

Thomas Eriksson[†], Christian Fager, Haiying Cao, Ali Soltani[†], Ulf Gustavsson, Hossein Nemati and Herbert Zirath
[†]Department of Signals and Systems Department of Microtechnology and Nanoscience
 Chalmers University of Technology, Göteborg, Sweden

I. INTRODUCTION

In many communications systems, most of the electrical power is consumed by the final RF power amplifier (PA) stage of the transmitter. Maximizing efficiency is therefore a fundamental concern in design of such PAs. There has recently been an increased interest in polar modulation architectures, where the envelope of the communication signal is extracted and separately used to amplitude-modulate the RF amplifier, for example based on well-known techniques such as Envelope Elimination and Restoration (EER) [1] or Envelope Tracking (ET) [2]. Load modulation (LM), where the output signal is modulated by dynamically altering some parameter in the amplifier network, can also be used [3]. Polar modulation and load modulation has the potential advantage of allowing the RF amplifier to work in its most efficient mode (close to saturation) at all times.

The above techniques have in common that they divide the communication signal into two parts, an RF part and a baseband modulation part, and feed the signals to different inputs of the power amplifier circuitry. To achieve the highest efficiency, the RF and modulation signals should be jointly optimized. Such optimization requires good amplifier models including two paths, i.e. dual-input amplifier models [4], which is the main topic of this paper.

II. OUR WORK

In our research, we study dual-input black-box amplifier models of different accuracy and complexity. In this paper, we study two approaches, as described in the following subsections.

A. Approach 1: A simple combiner

The simplest dual-input model consists of two single-input models combined by multiplication, see Figure 1. With this

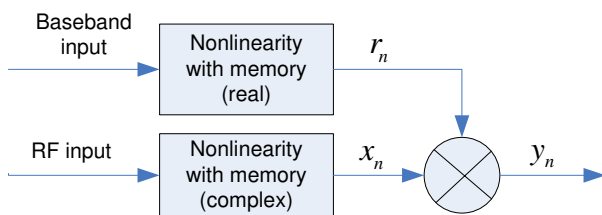


Fig. 1. A simple dual-input model with two single-input models combined with a multiplier.

model, the output is given by the simple equation $y_n = r_n x_n$. The identification is simple, since the two paths can be identified separately. First, the RF path of the amplifier is fed with a pure sinusoidal input, leading to x_n being a complex

constant. Now, by feeding the baseband path with an arbitrary signal that can fully excite the amplifier, we can identify the baseband path model. Second, we use a constant input at the baseband path, and feed the RF path with the desired signal, making identification of the RF model possible.

B. Approach 2: Combination by a static nonlinearity

The model above is, albeit simple, able to model all nonlinear and memory effects of both the RF path and the baseband path. However, it cannot model conceivable nonlinearities in the combination circuitry. To overcome this difficulty, one must include nonlinearity in the combination of the two paths, see Figure 2. With this approach, the output is given by

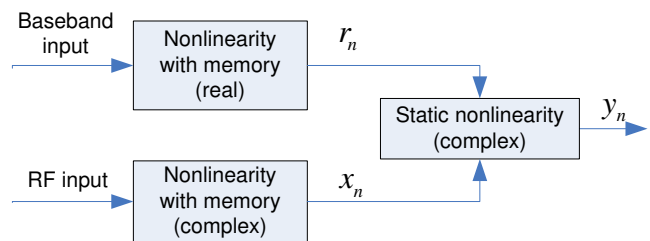


Fig. 2. A dual-input model with two single-input models combined with a static nonlinearity.

$$y_n = \sum_{k=0}^K \sum_{l=0}^L a_{k,l} |x_n|^{2k} x_n r_n^l. \quad (1)$$

The identification is more involved compared to the previous case. A working approach is to start similar to the identification above, by a simple initialization of the combination model and separately identify the two paths, followed by identification of the combination model. This must then be iterated until convergence.

III. SUMMARY

In the final version of our paper, the performance of different approaches will be compared, together with description of identification and complexity of the models.

REFERENCES

- [1] L. R. Kahn, "Single-sideband transmission by envelope elimination and restoration," *Proceedings of the IRE*, vol. 40, no. 7, pp. 803–806, 1952.
- [2] A. A. M. Saleh and D. C. Cox, "Improving the power-added efficiency of fet amplifiers operating with varying-envelope signals," *IEEE Trans. on Microwave Theory and Techniques*, vol. 83, no. 1, pp. 51–56, 1982.
- [3] F. H. Raab, "High-efficiency linear amplification by dynamic load modulation," *Microwave Symposium Digest, 2003 IEEE MTT-S International*, vol. 3, pp. 1717–1720, 2003.
- [4] J. C. Pedro and S. A. Maas, "A comparative overview of microwave and wireless power-amplifier behavioral modeling approaches," *IEEE Transactions on Microwave Theory and Techniques*, vol. 53, no. 4, pp. 1150–1163, 2005.

Recent Advances in GaN HEMT Power Amplifier Technology for Telecommunication Applications

Raymond Pengelly¹, Simon Wood¹, Donald Farrell¹, Bill Pribble¹
and James Crescenzi²

1 Cree Inc.

2 Central Coast Microwave Design LLC.

Abstract

The recent evolution of GaN HEMT transistors has opened up a range of power amplifier architectures for the various telecommunication bands that have, in the past, been limited to lower frequencies. Following a description of the characteristics of wide bandgap technologies, the unique advantages of GaN HEMTs applied to Class A/B, Doherty, drain modulated and switch mode amplifiers will be detailed particularly in respect to efficiency and bandwidth.

Practical examples of Class A/B amplifiers will be compared with a number of Doherty amplifiers employing digital pre-distortion with peak power handling up to 150 watts in the 2500 to 3500 MHz frequency range. The Doherty amplifiers feature hundreds of megahertz of RF bandwidth with wide video bandwidths accommodating multiple simultaneous signals.

Efficiency improvements with waveform engineered amplifiers including Class J, Class E, Class F and inverse Class F, covering frequencies from 900 to 3500 MHz, will also be described.

The specific design approach for envelope tracking (drain modulated) power amplifiers in the 2100 to 2700 MHz frequency range will be described where peak power levels from 10 to 150 watts can be produced with average efficiencies of greater than 60%.

Finally, the development of wideband efficient amplifier “modules”, covering 700 to 900 MHz, 1800 to 2200 MHz and 2100 to 2700 MHz, using harmonic matching and novel power combining approaches will be described. These same modules can be employed in a variety of configurations to further boost efficiency.

Design Considerations for Varactor-Based Dynamic Load Modulation Networks

Ulf Gustavsson^{#*}, Björn Almgren[#], Hossein Mashad Nemati^{*}

[#]Ericsson AB, ^{*}Chalmers university of technology, Department of Microtechnology and nanoscience

I. INTRODUCTION

In modern wireless communication systems, one of the key component regarding both performance and energy efficiency, is the RF power amplifier. Measures are therefore taken in order to meet the requirements of high efficiency, high bandwidth and re-configurability that these systems need.

II. OUR WORK

A high linearity varactor network suitable for dynamic load modulation is presented in [1]. A way of implementing this is suggested in [2] and [3]. While studying the capacitance voltage dependence in combination with the applied RF voltage from the amplifier, one quickly realises the problematic situation. The problematic scenario will be illustrated using $C(V) = C_0 \cdot (1 - V_c / \phi)^{-M}$ to describe the C-V characteristics of the varactor stack. By applying the voltage of the amplifier as shown in Figure 1, across the selected varactor topology with C-V characteristics shown in Figure 2, one can easily discover that the hyper-abrupt behaviour of the C-V curve will not contribute to the decrease of the said amplifier output voltage needed, thus during parts of each RF cycle, one of the varactors will be biased in a forward direction.

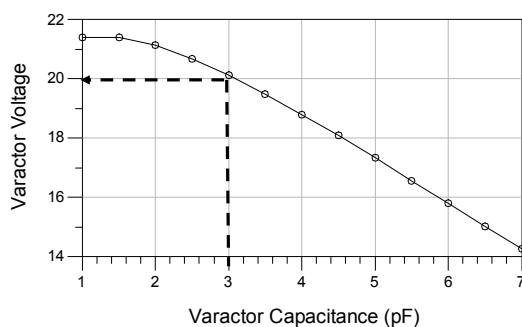


Figure 1 – RF PA output voltage dependence of the capacitive load.

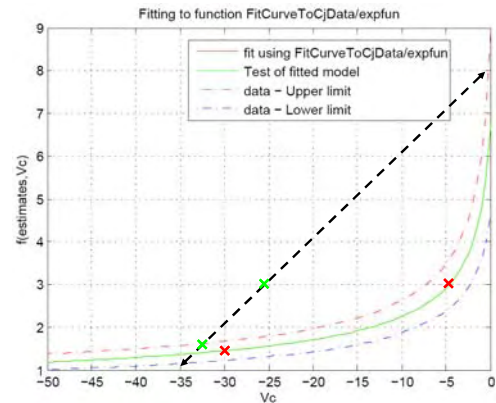


Figure 2 - Example of a hyper-abrupt varactor C-V characteristic and the "wanted" C-V characteristic (dashed line). Points of 1 and 3 pF are marked out.

Using a variable capacitor from Johansson tech., the output of the amplifier can be statically altered. This method of verifying the controllability of the amplifier is described in [2]. Simulations have shown the need for linear varactors in order to successfully implementing a dynamic load modulation network.

III. CONCLUSIONS

As shown during this work and the work referred to here, dynamic load modulation shows high potential, but is in need of variable capacitive elements with linear characteristics. This will also decrease the non-linearity for which one needs to compensate for as well as the amplitude needed to supply the control voltage to the said varactor network.

REFERENCES

- [1] K. Buisman, et al., "'Distortion free' varactor diode topologies for RF adaptivity," *IMS 2005, Long Beach, CA, Jun. 2005*, pp. 157-160.
- [2] Lepine, Fabiene; Zirath, Herbert; Jos, Rik: "A Load Modulated High Efficiency Power Amplifier." *European Microwave Conference 2006 Manchester*
- [3] Almgren, Björn; "Dynamic Load Modulation", *Master thesis in microwave engineering at Gävle university*

Workshop

Microwave Components

1300-1500 Wednesday 5 March 2008

Highly integrated MMICs for millimeterwave system application

Herbert Zirath^{1,2} Sten E. Gunnarsson¹, Mattias Ferndahl¹, Rumen Kozhuharov¹, Camilla Kärnfelt¹

¹Chalmers University of Technology, Department of Microtechnology and Nanoscience
Microwave Electronics Laboratory, Göteborg, Sweden.

²Ericsson AB, Microwave and High Speed Electronics Research Centre, Mölndal, Sweden.

Abstract — In order to reduce the manufacturing cost for future 60 GHz products, a high integration level is necessary. Recent results on mHEMT and pHEMT multifunctional receiver/transmitters realized at Chalmers University are reported. Multifunctional MMICs utilizing single ended, subharmonically pumped, balanced and single sideband mixers are reported. Other chipsets for additional applications such as radiometers are reported as well. Most recently, a 220 GHz integrated receiver utilizing mHEMT technology was demonstrated.

Various receiver and a transmitter chips were recently developed based on pHEMT and mHEMT processes from WIN Semiconductors, with following applications in mind

- 1 60 GHz Wireless LAN
- 2 53 GHz radiometer for earth observation
- 3 24 GHz radar chip

A block diagram of a typical receiver MMIC is shown in Fig 1, with the corresponding chip photo in Fig. 2. The chip measures 5.7×5 mm. The RX chip possesses a 3 dB RF bandwidth of 8 GHz between 55 and 63 GHz with an optimal conversion gain, G_C , of 8.6 dB at 58 GHz. The image reject ratio is larger than 20 dB between 59.5 and 64.5 GHz. Transmitter chip were also developed and will be reported. Due to the general architecture of the chipset any modulation format can be used. A test bench for system tests was setup where general modulation signals can be calculated and loaded to the ESG. Due to the limitation in the measurement setup, we used ASK for higher bitrates than 200Mbit/s. This chipset was implemented in both a pHEMT and an mHEMT version with similar RF-performance. The power consumption was cut to 420 mW and 450 mW for the mHEMT-based receiver and transmitter respectively. A modified version of the 60 GHz receiver was designed for a 53 GHz radiometer application. The mixer has I-Q wideband intermediate frequency output which is sampled by a high speed spectrometer processor. The measured 3-dB bandwidth is 7 GHz.

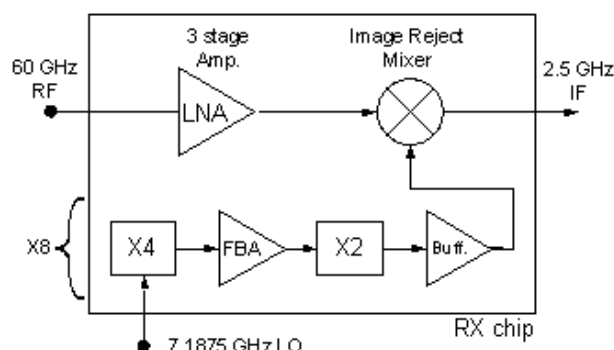


Fig. 1 Block diagram of the receiver MMIC

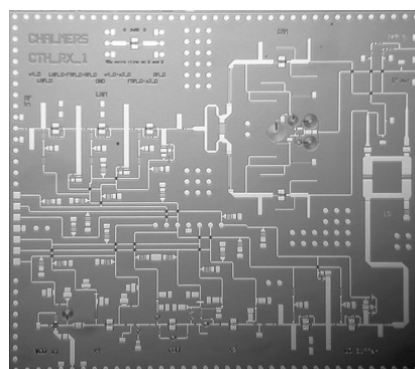


Fig. 2 Photo of the receiver chip. (5.7×5.0 mm²)

Integrated receiver for 220 GHz radiometer

Multifunctional MMICs for frequencies 118, 183, and 220 GHz with a similar approach as the 60 GHz chipset, are being developed at Chalmers University at the moment, utilizing an mHEMT-process from IAF. In a recent 220 GHz receiver design, the antenna was integrated on 'chip'. The receiver noise figure of the MMIC-frontend is less than 10 dB. To the best knowledge of the authors, this represents the highest frequency of any multifunctional active MMIC.

An Ultra Wide Band LNA in 90nm CMOS

Waqas Ahmad¹, Andreas Axholt², Henrik Sjöland²

¹Master's student at the faculty of engineering, Lund university, sx06wa7@student.lth.se

²Dept. of electrical and information technology, Lund university, Sweden

{Andreas.Axholt, Henrik.Sjoland}@eit.lth.se

Abstract— This paper presents a design of a two-stage LNA in 90nm CMOS targeted for the ultra wide band frequency range, 3.1GHz - 10.6GHz. Post-layout simulations show a gain of 23dB±1dB, a noise figure of 4dB, input reflection S_{11} below -10dB, and an IIP3 above -10.4dBm over the entire band of interest, with a total power consumption of 14.4mW from a supply voltage of 1.2V. The circuit measures just 310x410 μm^2 including pads.

I. INTRODUCTION

IN 2002 FCC allocated a 7.5GHz frequency band for ultra wide band applications with restricted transmission masks. Since then UWB has gained a large momentum in both academia and industry. This new wide frequency span allows for low cost, high data rate, and low power short range communications.

II. CIRCUIT TOPOLOGY

The schematic of the UWB LNA is shown in Fig 1. The input stage is realized using a common-gate amplifier to achieve broadband input matching to 50 Ω . The load resistor value R_1 is chosen such that the DC gate voltage of transistor M_2 ensures that it operates in the saturation region. Both noise figure and input impedance are functions of g_{m1} , hence a compromise must be made in noise figure to fulfill the $S_{11} < -10$ dB requirement.

The second stage is a cascode common-source stage with inductive load. To achieve wideband gain in the second stage, a shunt feedback technique has been adopted, implemented by capacitor C_1 and resistor R_2 in Fig. 1.

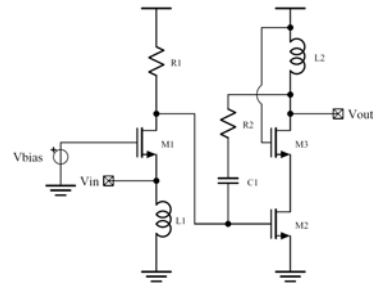


Fig. 1. Two-stage UWB low noise amplifier

III. RESULTS

The circuit was simulated using SpectreRF with BSIM4 transistor models. The inductors were modeled using Indentro [1]. The circuit consumes 14.4mW and measures 310x410 μm^2 including pads. Simulated results are presented in Fig. 2. The circuit is currently under fabrication.

IV. CONCLUSION

A two-stage UWB low noise amplifier implemented in UMC 90nm CMOS process has been presented together with simulation results. This paper is the result from a master's thesis performed by Waqas Ahmad at Lund University, Sweden [2].

REFERENCES

- [1] Niklas Troedsson, <http://www.indentro.com>
- [2] Waqas Ahmad, "Front-End for Ultra Wide-Band (UWB) Wireless Receivers in 90nm CMOS"

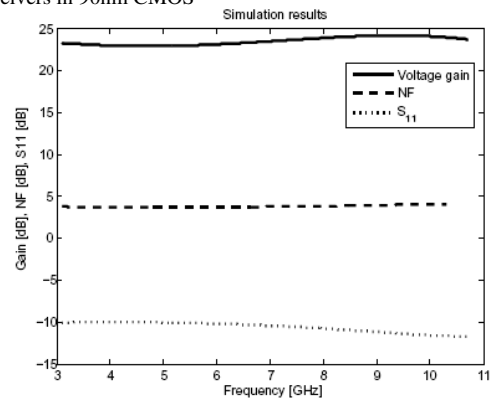


Fig. 2. Simulated gain, noise figure, and S_{11}

Flip Chip for High Frequency

Katarina Boustedt

Microwave and High Speed Research Center
Ericsson AB, Mölndal, Sweden
Katarina.boustedt@ericsson.com

Die interconnect through wire bonds is the most often employed process for high and low-frequency chips. The die is soldered or adhesively joined to a carrier, and gold or aluminum wires connect the die bond pads to corresponding pads on the carrier. When high-frequency operation is considered, the wires cannot be disregarded electrically, since they cause significant parasitic losses, primarily due to inductance, resulting in undesirable signal disturbances, unless compensated for during the design phase. As a rule of thumb, one adds a 1-nH inductance for the bond-wire effects, but this approximation is too coarse for sensitive cases.

Flip chip offers some very important benefits over wire bonding, for example better electrical performance and a smoother assembly process. This facilitates reduction of production costs and makes low-cost, high-volume production possible. Another considerable factor in choosing an interconnect method for high frequency operation is the fact that the geometrical shape of flip-chip interconnects is very predictable and repeatable. Bond wires vary in length, leading to variations in parasitics, which makes compensation in the die design more difficult. The benefits of flip-chip interconnect for lower frequency applications are well-known.

Microwave chips typically have much fewer interconnect pads than other dice. Therefore, the need for flip chip does not typically come from a need for more I/Os per unit area, even though the die surface area is normally smaller than typical silicon dice. An edge length of a few millimeters is common. It has been stated that MMIC cannot be assembled on a chip carrier with short interconnection lengths using an automated wire bond tool. Hence, a significant driver for implementing flip-chip dice in high-frequency applications is the simplified chip assembly and the improved performance stemming from the short and consistent lead lengths, i.e., the interconnect bumps.

There are many variations deemed feasible when implementing flip-chip GaAs die for high-frequency applications. These are variations in materials and methods for fabricating carriers and bumps, die design, techniques for simulation, and production.

The flip-chip interconnect builds on three fundamental elements, bumps on a chip, the chip carrier or substrate, and the method of joining a die to a carrier. These building blocks are interdependent, thus it is vital to take all of them into account, in order to select the optimal flip-chip system for a given application. The possible use of an encapsulant will be another consideration. Recent literature provides many variations for high-frequency flip-chip systems, some of which are discussed in this presentation.

CRYOGENIC X-BAND LOW NOISE AMPLIFIERS

Naiara Goia, Matthew Kelly, Anna Malmros, Niklas Wadefalk, and J. Piotr Starski

*Chalmers University of Technology, Department of Microtechnology and Nanoscience
Microwave Electronics Laboratory, SE-412 96 Göteborg, Sweden*

Abstract - This paper describes a number of cryogenic low noise amplifiers with very low noise for the frequency band 8.4-8.5 GHz. The amplifiers have been designed with different inputs: standard coaxial and waveguide

At 10 K ambient temperature the three-stage InP-based amplifiers have a gain of 33.0+/-0.5 dB and a noise temperature of 5 -7K.

The InP transistors used in the amplifiers were processed at Chalmers clean room facility in our own proprietary process.

INTRODUCTION

InP based High Electron Mobility Transistors (HEMTs) have extremely good low-noise performance and superior high frequency performance. In this study we have designed, manufactured, and measured amplifiers with low noise and different input circuits. Amplifiers with different input circuits are of interest for combinations with different types of isolators (coaxial/waveguide) to obtain the lowest possible noise for a combination of the isolator/amplifier in cases where the input match of the amplifier is not sufficient. The amplifiers are of a three-stage design in microstrip. The first stage is always equipped with an InP HEMT transistor processed at Chalmers. The remaining transistors are commercially available GaAs based HEMTs from Mitsubishi.

HEMT FABRICATION AND CHARACTERISTICS

A lattice matched structure on InP grown by molecular beam epitaxy was used in the fabrication of the Chalmers HEMT. The transistors have a 40Å AlInAs spacer, whose purpose is to separate the 300Å thick 53% InGaAs channel from the planar silicon doping. We use a 200Å thick AlInAs Schottky barrier and a cap layer consisting of 50Å undoped InGaAs. The measured transconductance at room temperature is close to 550mS/mm, which gives $g_m \approx 110\text{mS}/200\mu\text{m}$ device.

AMPLIFIER DESIGN AND MEASUREMENTS

A three-stage, 8.4-8.5GHz, single-ended amplifiers with specified gain of 33dB were designed. We have designed, manufactured and measured three amplifiers with different input circuits: standard coaxial, coaxial followed by a high directivity 30 dB microstrip coupler, and waveguide. All amplifiers had coaxial output. Typical measured values for noise and gain at 15K are shown in Fig. 1, the photograph of amplifier is shown in Fig.2.

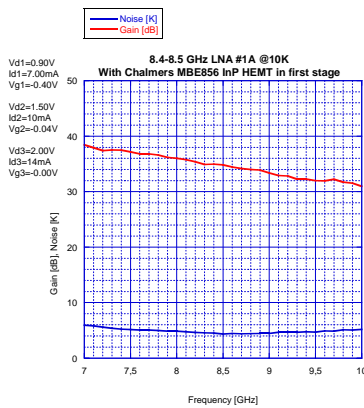


Fig. 1. Measured noise and gain of the amplifier with standard coaxial input at 15K.

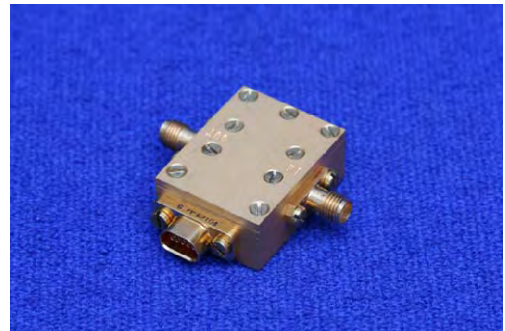


Fig. 2. 8.4-8.5 GHz LNA

SUMMARY AND CONCLUSION

Recent work on cryogenically cooled HEMT-based amplifiers with different inputs has been presented. The lowest noise temperature of around 5K has been achieved with an InP-based amplifier over the 8.4-8.5GHz band with an associated gain of 33+/-0.5dB. The InP HEMTs have been manufactured at Chalmers.

Low-Noise Cryogenic Amplifier built using Hybrid MMIC-like / TRL Technique

O. Nyström, E. Sundin, D. Dochev, V. Desmaris, V. Vassilev, V. Belitsky

Group for Advanced Receiver Development (GARD), Department of Radio and Space Science
with Onsala Space Observatory, Chalmers University of Technology, Gothenburg, Sweden,
E-mail: olle.nystrom@chalmers.se

HEMT cryogenic low-noise amplifiers are an important part of instrumentation: the amplifiers use as a front-end for different measurements and as IF amplifiers in heterodyne receivers. During last few years the low-noise limit has reached as low level as approximately 0.5 K/GHz for GaAs [1] and 0.25 K/GHz for InP HEMT [2]. However, besides electrical performance improvement there were not many improvements on mass and dimension side of such amplifiers as they were built based on standard TRL technology with discrete active and passive components. Mass and dimensions are also very important for real applications. When ultimate low-noise performance is placed in focus, pure MMIC technology seems to loose against design using discrete components. With this in view, pioneered work by E. F. Lauria, et. al. [3] have successfully demonstrated a design employing MMIC approach while using discrete components and based on a microstrip on Cufalon with lumped bias network. Encouraged by this work, we propose a compact design of a 4-8 GHz cryogenic low noise amplifier using a combination of standard TRL and lumped element technology to achieve both ultimate noise performance over the specified band and a very compact size. In our design, the size reduction of the amplifier is realized by selecting an alumina substrate with a high dielectric constant, ($\epsilon_r = 9.9$), but also by taking advantage of the lumped networks in the matching and bias circuitries. Avoiding quarter wave transformers and instead use a lumped element design approach opens up for the possibilities to reach greater bandwidths and simultaneously obtain a more compact design. In order to make optimum design, we have performed extensive simulations. Each amplifier stage has been simulated in Agilent EMDS, 3D electromagnetic field simulation package, including the single layer capacitors, and then implemented in the ADS circuit simulations as an S-parameter file. Over the 4-8 GHz band, the simulations predict noise temperature, $T_{\text{average}} < 4.3$ K, $S_{11} < -12$ dB, $S_{22} < -15$ dB, and a gain, $S_{21} > 35$ dB. The transistors selected for the design are commercial InP HEMT (HRL) chosen due to their excellent noise performance [2], but also for the very low power consumption, which is of great importance at cryogenic temperatures. All the components used in the RF-signal path and in the bias circuits are mounted with conductive epoxy. Apart from the RF-signal path, all components are interconnected via bond-wires. Fine tuning is done by adjusting the length and loop heights of the bond-wires. At the conference we plan to report results of measurement and characterization of the prototype amplifier.

[1] C Risacher, et. al., "Low Noise and Low Power Consumption Cryogenic Amplifiers for Onsala and Apex Telescopes", Proceedings of Gaas 2004, October 2004, Amsterdam.

[2] N. Wadefalk, et. al., "Cryogenic Wide-Band Ultra-Low Noise IF Amplifier Operating at Ultra-Low DC-Power", IEEE Transactions on Microwave Theory and Techniques, vol. MTT-51, no. 6 June 2003.

[3] E. F. Lauria, et. al., "A 200-300 GHz SIS Mixer-Preamplifier with 8 GHz IF Bandwidth", 2001 IEEE International Microwave Symposium, Phoenix, AZ, May 2001.

Small-signal modeling of narrow-bandgap InAs/AlSb HEMTs

Mikael Malmkvist¹, Eric Lefebvre¹, Ludovic Desplanque², Xavier Wallart², Gilles Dambrine², Sylvain Bollaert², and Jan Grahn¹

¹Microwave Electronics Laboratory, Department of Microtechnology and Nanoscience (MC2), Chalmers University of Technology, SE-412 96 Göteborg, Sweden

²Institute of Electronics, Microelectronics and Nanotechnology (IEMN), P.O. Box 60069, 59652 Villeneuve d'Ascq, France

(mikael.malmkvist@chalmers.se)

The small-signal model (SSM) of $2 \times 50 \mu\text{m}$ gate-width InAs/AlSb HEMTs with gate-length variation from 225 nm to 335 nm has been investigated. To account for the relatively high gate-leakage current I_G in InAs/AlSb HEMTs, the conventional FET SSM has been extended by shunting C_{gs} and C_{gd} with R_{gs} and R_{gd} , respectively. By utilizing this modeling approach the gate-length dependence of C_{gs} and C_{gd} was analyzed. When reducing the gate length from 335 nm to 225 nm, C_{gs} and C_{gd} were reduced by 40% and 35%, respectively.

Owing to its semiconductor properties and type-II energy-band alignment, the InAs/AlSb HEMT exhibits superior electron mobility and carrier channel confinement. This makes the InAs/AlSb HEMT suitable for high-frequency, low-noise and ultra-low power applications [1]. To be able to evaluate and improve the device as well as to implement it in an MMIC, an accurate SSM is required. Furthermore, to improve the HEMT figures-of-merit f_T and f_{max} it is important to reduce C_{gs} but also to keep a low C_{gd}/C_{gs} ratio.

On-wafer DC measurements revealed a transconductance g_m as high as 1300 mS/mm at $V_{DS} = 0.5 \text{ V}$ and a g_m above 900 mS/mm at V_{DS} of only 0.3 V, as shown in Fig. 1(a). At $V_{DS} = 0.1 \text{ V}$ and $V_{GS} = -0.9 \text{ V}$ an I_G of $7 \mu\text{A}$ was measured, whereas at $V_{DS} = 0.5 \text{ V}$ the value was as high as $210 \mu\text{A}$. Due to this high I_G the conventional SSM is insufficient. In Fig. 1(b), the measured and modeled K is presented with and without shunting C_{gs} and C_{gd} with R_{gs} and R_{gd} , respectively. A significant discrepancy is observed below 10 GHz when omitting R_{gs} and R_{gd} . By applying the extended SSM, the C_{gs} and the C_{gd} behavior versus gate length were studied. Within the studied gate-length interval, C_{gs} and C_{gd} were reduced by 40% and 35% respectively, with an increased C_{gd}/C_{gs} ratio of 6%, see Fig 1(c). The different gate lengths were obtained through FIB-SEM measurements, see inset in Fig. 1(c). If the gate length is further reduced, the improvement with respect to f_{max} will not be as significant due to degradation in the C_{gd}/C_{gs} ratio.

InAs/AlSb HEMTs with gate-lengths ranging between 225 nm and 335 nm have been investigated by extending the conventional SSM accounting for the elevated I_G present in this narrow-bandgap HEMT technology. As the gate length was reduced, C_{gs} was reduced by 40% and the C_{gd}/C_{gs} ratio was only slightly increased warranting improved RF performance.

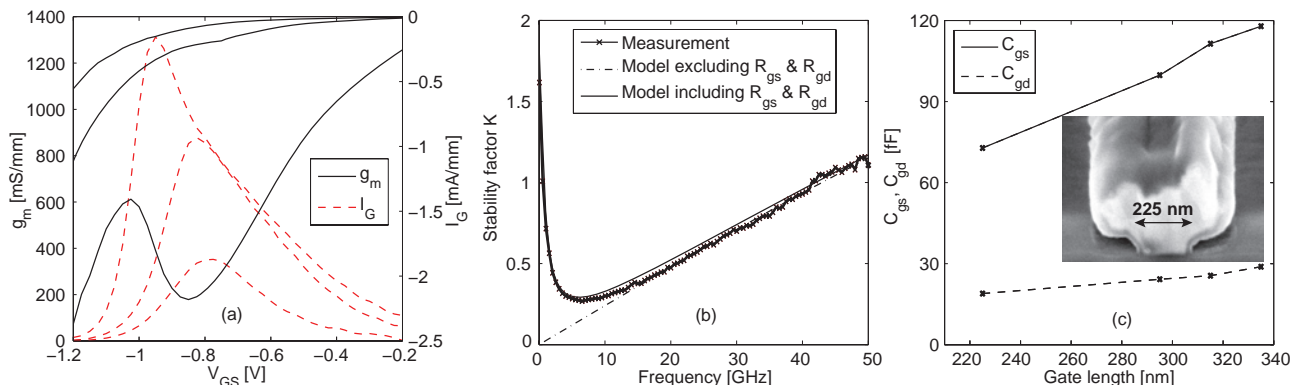


Fig.1. $2 \times 50 \mu\text{m}$ gate-width InAs/AlSb HEMT characteristics of (a) $g_m(V_{GS})$ and $I_G(V_{GS})$ with a 225 nm gate length at $V_{DS} = 0.1, 0.3$ and 0.5 V , (b) the influence on stability factor K with or without R_{gd} and R_{gs} shunting C_{gd} and C_{gs} , respectively, and (c) the gate-length dependence on C_{gd} and C_{gs} (inset: FIB-SEM image of a 225 nm gate).

- [1] B. Y. Ma, J. Bergman, P. Chen, J. B. Hacker, G. Sullivan, G. Nagy, and B. Brar, "InAs/AlSb HEMT and its application to ultra-low-power wideband high-gain low-noise amplifiers," *IEEE Transactions on Microw. Theory Tech.*, vol. 54, no. 12, pp. 4448-4455, 2006.

Low-Noise, High-Speed Strained Channel Silicon MOSFET Technology for RF-Applications

B. Gunnar Malm, Julius Hällstedt, Per-Erik Hellström, and Mikael Östling
 KTH - Royal Institute of Technology, School of ICT, Kista, Sweden, E-mail: gunta@kth.se

Strained channel silicon MOSFETs on virtual substrates (VS) are a promising technology for high performance RF and analog applications. Significantly increased electron mobility can be achieved by growing a tensile strained silicon layer on top of a relaxed $\text{Si}_{1-x}\text{Ge}_x$ buffer layer, where the composition x is in the range of 20-30%. The hole mobility is also improved but to a smaller degree [1]. The high mobility improves transconductance as well as RF-parameters such as cut-off frequency (f_T) and power gain (f_{MAX}), and the improvement is maintained at deca-nanometer gate lengths. Furthermore, for high quality strained layers the low-frequency ($1/f$) noise is preserved or lowered as compared to unstrained silicon technology [1]. For devices operating at high current densities, such as a MOSFET biased for maximum cut-off frequency, the poor thermal conductance of the SiGe buffer layer is a potential drawback [2]. To solve this problem special epitaxial growth techniques have been suggested to decrease the layer thickness and improve heat removal. We present results from nMOSFETs fabricated using a sidewall transfer lithography technology [3], to achieve a physical gate length of 50-80 nm, as shown in Fig. 1. Both thin and thick virtual substrates have been investigated. Multifinger RF nMOSFETs demonstrate f_T above 100 GHz, see Fig. 2. The high resistance of the 50 nm length/10 μm width gate fingers limits the f_{MAX} , devices with finger width of 5 μm showed f_{MAX} close to 50 GHz. Devices fabricated with a so-called supercritical thickness of the strained Si layer (110 nm) on thick 20% SiGe buffers show excellent junction leakage [4] and the $1/f$ noise is almost identical to the silicon reference, shown in Fig. 3.

This work was supported by SSF and Vinnova. We acknowledge our partners in the SiNano network (Univ. of Stuttgart and Warwick) for epitaxial growth.

- [1] M. von Haartman, B. G. Malm, P. E. Hellström, M. Östling, et al, "Impact of strain and channel orientation on the low-frequency noise performance of Si n- and pMOSFETs," *Solid-State Electronics*, vol. 51, pp. 771-777, 2007.
- [2] S. H. Olsen, E. Escobedo-Cousin, J. B. Varzgar, R. Agaiby, et al, "Control of self-heating in thin virtual substrate strained Si MOSFETs," *IEEE Transactions on Electron Devices*, vol. 53, pp. 2296-305, 2006.
- [3] J. Hällstedt, P.-E. Hellström, Z. Zhang, B.G. Malm, et al "A robust spacer gate process for deca-nanometer high-frequency MOSFETs," *Microelectronic Engineering*, vol. 83, pp. 434-439 2006.
- [4] J. Hällstedt, B. G. Malm, P.-E. Hellström, M. Östling, M. Oehme, J. Werner, K. Lyutovich, and E. Kasper, "Leakage current reduction in 80 nm biaxially strained Si nMOSFETs on in-situ doped SiGe virtual substrates," presented at ESSDERC, Munich, 2007.

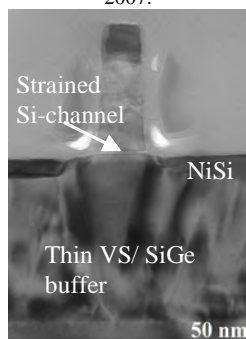


Fig. 1. XTEM image showing a 50 nm s-Si channel nMOSFET on 200 nm thin SiGe virtual substrate.

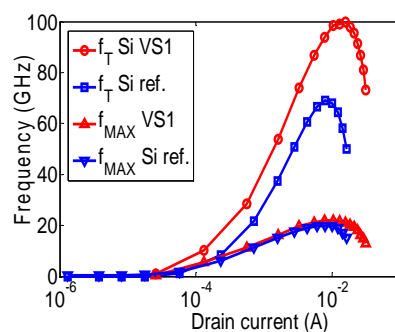


Fig. 2. HF-characteristics of RF nMOSFET on a silicon reference and thin VS, gate width ($4 \times 10 \mu\text{m}$), V_{DS} 1.0 V. The f_T increase is about 40 %.

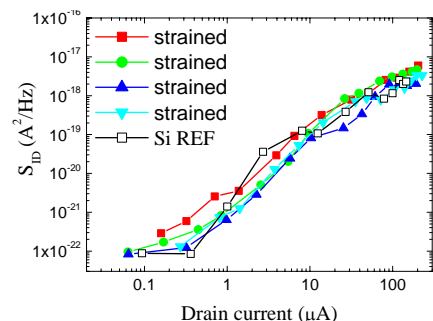


Fig. 3. Drain current noise S_{ID} for strained channel nMOSFETs L_G 80 nm compared to unstrained reference.

Wideband Microstrip 90° 3-dB Two-Branch Coupler with Minimum Amplitude and Phase Imbalance

Duxiang Wang^{1,2}, Ming Li¹, Allan Huynh², Pär Håkansson² and Shaofang Gong²

¹Nanjing Electronic Equipment Institute, P.O.Box 1610, Nanjing, 210007 Jiangsu, P.R.China

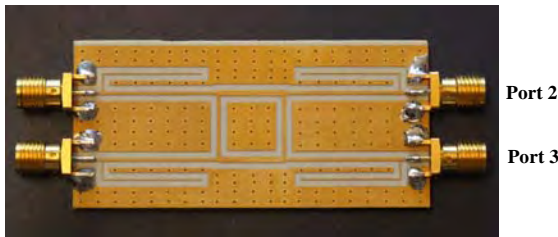
Phone: +86-25-84638544, Fax: +86-25-84498353, E-mail: wangduxiang@hotmail.com

²Linköping University, Department of Science and Technology, SE-60174 Norrköping, Sweden

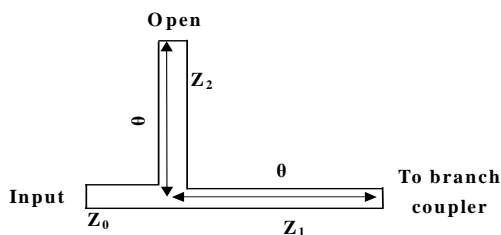
Phone: +46-11-363089, Fax: +46-11-363270, E-mail: allhu@itn.liu.se

A wideband 90° 3-dB directional-coupler is one of the key components in a six-port transceiver circuit for wireless ultra-wideband (UWB) or other communication systems. For the Mode 1 band group of UWB communications, the frequency band ranges from 3.1 to 4.8 GHz, i.e., a 43% relative bandwidth. However, conventional two-branch 90° 3-dB directional-couplers are typically limited to a relative bandwidth of 10%, which does not fulfill the UWB requirement. In this work, a new branch coupler has been designed, manufactured and measured. Both simulation and measurement results show that it has low insertion loss, and small amplitude and phase imbalances in a relative bandwidth of 59 % from 3.0 to 5.5 GHz.

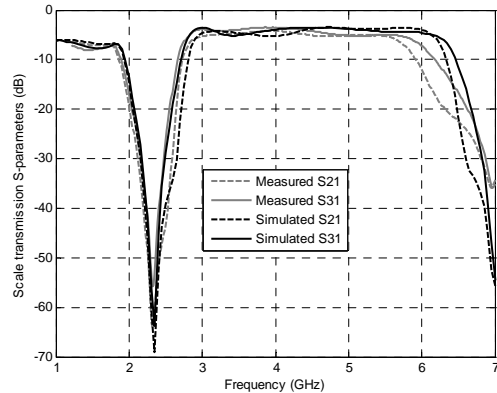
As shown in Fig. 1a this wideband microstrip coupler is made of an ordinary two-branch coupler but with matching networks at the 4 ports. The matching network, as shown in Fig. 1b, consists of a half wavelength transformer and an open stub to broaden the bandwidth of the conventional two-branch coupler. This method was reported before by other authors, but their focus has been on the amplitude balance. This work has been focused on both amplitude and phase balances to cover the 43% relative-bandwidth required by UWB. This two-branch coupler uses higher impedance line, with Z_1 and Z_2 to be $1.36Z_0$ and $1.71Z_0$, respectively, to achieve the minimum amplitude and phase imbalance in the frequency range of 3.0-5.5 GHz, as shown in Figs 1c and 1d, respectively.



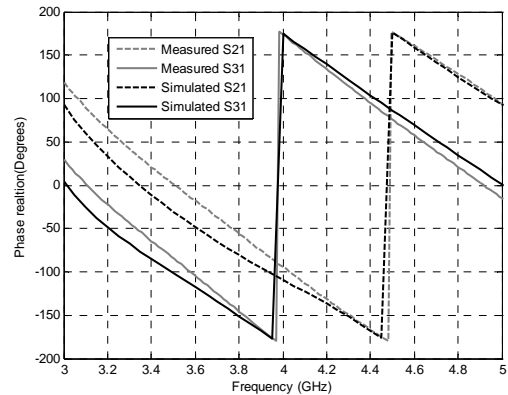
(a)



(b)



(c)



(d)

Fig 1. Branch coupler with match networks, having a relative bandwidth of 59 % from 3.0 to 5.5 GHz.: (a) prototype, (b) matching network, (c) amplitude balance, and (d) phase balance.

It is concluded that the conventional two-branch coupler has a relative bandwidth of 10 %. However, with matching networks connected to the four ports of the two-branch coupler the bandwidth can be enlarged to a 59 % relative-bandwidth within the frequency range of 3.0-5.5 GHz. The phase imbalance must be considered when considering the amplitude balance. This new coupler has low insertion loss, and both small amplitude and phase imbalances in the frequency range of 3.0-5.5 GHz, which exceeds the UWB requirement for the Mode 1 band group 3.1-4.8 GHz. Therefore, this coupler can be used in a UWB six-port transceiver design.

An Ultra-Wideband Six-port Transceiver Covering from 3.1 to 4.8 GHz

Pär Håkansson and Shaofang Gong

Linköping University, Department of Science and Technology, SE-60174 Norrköping, Sweden

Phone: +46-11-363089, Fax: +46-11-363270, E-mail: parha@itn.liu.se

This paper presents an ultra-wideband transceiver based on the six-port technique. The six-port transceiver covers the frequency spectrum from 3.1 to 4.8 GHz, i.e., it covers the lower band of the UWB spectrum. The transceiver has thus an relative bandwidth of 43%. A key component in the six-port transceiver is the correlator which utilizes three ultra-wideband 3-dB 90° branch couplers and one 3-dB 0° Wilkinson power divider. It is manufactured utilizing microstrips on a printed circuit board. It is shown that the transceiver is able to demodulate high order modulations such as 64-QAM and modulate QPSK signals.

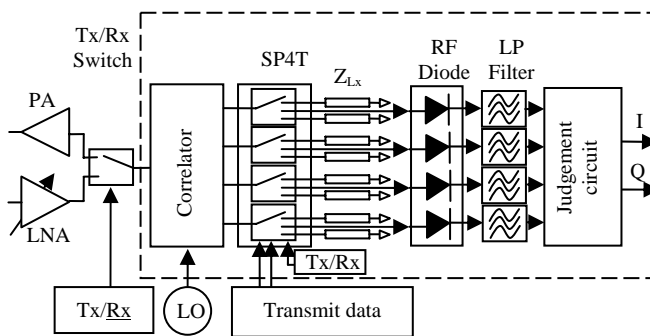


Fig. 1 Block diagram of the transceiver, the circuitry within the dashed lines is implemented in this work.

Fig. 1 shows the block diagram of the six-port transceiver. The received path consists of a low noise amplifier (LNA), Tx/Rx switch, correlator, SP4T switch, four radio frequency diodes, four low-pass filters and a judgment circuit. The judgement circuit is implemented utilizing two instrumentation amplifiers. In the transmit mode the SP4T switch is switched between the different impedance loads Z_{Lx} shown in Fig. 1.

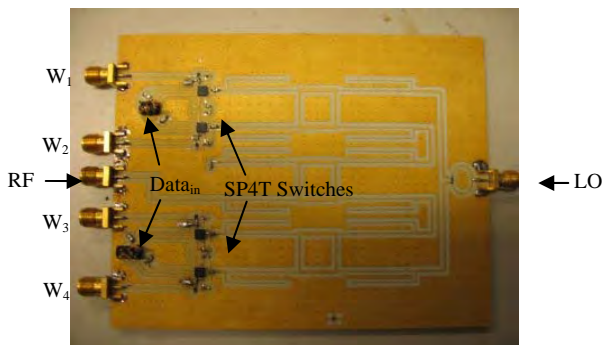


Fig. 2. Photo of the manufactured six-port transceiver.

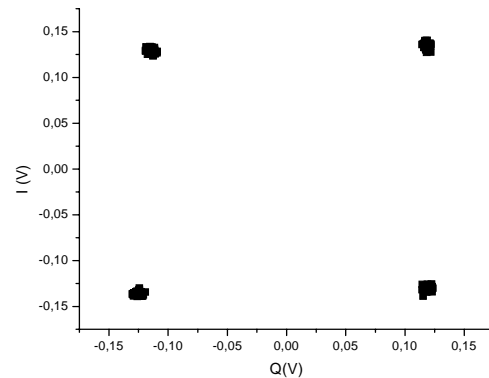


Fig. 3. Measured I/Q constellation diagram of a QPSK signal at 3.96 GHz and a data rate of 1 Mbps.

TABLE I. MEASURED PROPERTIES OF THE TRANSCEIVER

$f_{lo} = f_{rf}$	3.432 GHz	3.96 GHz	4.488 GHz
Error Vector Mag (%RMS)	15.2	5.3	9.6
Mag. Error (%RMS)	8.6	4.6	8.6
Phase error (°)	7.6	1.56	2.3
Quadrature Error (deg)	-10	4.8	9.8
Gain imbalance (dB)	-2.1	0.4	0.5

Fig. 3 shows the measured I/Q diagram when the data is transmitted by the transceiver in the transmit mode and received by the receiver (another six-port receiver module). The power of the transmitted signal is -12 dBm and the power of the receiver LO is 3 dBm. Table I summarizes the measured results at the center frequencies of the three UWB sub-bands, i.e., 3.432, 3.96 and 4.448 GHz when the data is transmitted by the transceiver shown in Fig. 2 and received by another receiver. The quadrature error, i.e., the phase error between the I- and Q- paths, ~10% at the lower and higher bands. This can be improved by further optimization of the six-port correlator.

The small phase and amplitude imbalances of the ultra wideband correlator, i.e., 7° and 1.4 dB, make it possible to produce a high quality RF signal receiver and transmitter without using any calibration technique in the UWB frequency band 3.1 – 4.8 GHz which has never been reported before.

Gated tunnel diode pulse generator

M. Nilsson, M. Ärlelid, E. Lind, G. Astromskas, and L.-E. Wernersson.

Abstract—We demonstrate the function of a gated tunnel diode as a high frequency pulse generator. The maximum oscillation frequency is 22 GHz and the shortest pulse length is 1 ns. The output voltage swing delivered to a 50 ohm load is 100 mV. The technique is scalable and will be used for ultra wide band communication experiments.

I. INTRODUCTION

THE negative differential resistance (NDR) property of resonant tunneling diodes (RTDs) has been exploited in various high frequency applications such as oscillators and pulse generators. These applications uses plain RTDs integrated into an electrical circuit. Instead we have integrated an RTD into a field effect transistor, the gated tunnel diode (GTD). The device IV-characteristics is shown in figure 1, for further details regarding the GTD refer to [1]. By integrating the GTD in parallel with an coplanar resonance circuit, an oscillator circuit has been constructed. The possibility to tune the resonance frequency with the gate and collector bias to form a voltage controlled oscillator (VCO) is one of the many features of the GTD oscillator.

II. RESULTS

When biased in the NDR region the oscillator generates a tunable -10 dBm signal, the highest frequency being 22 GHz. The main application of the circuit is not to use it as a continuous oscillator but rather as a pulse generator. This is motivated by the recent development toward low power ultra wide band (UWB) wireless communication, and especially impulse radio (IR) UWB. Pulse generator operation is achieved by biasing the device in the NDR region and then applying a square wave to the gate. The GTD is then forced out off its NDR region and instead enters a region of positive differential resistance. This switches the oscillations off, figure 2.

M. Nilsson, E. Lind, G. Astromskas and L.-E. Wernersson are with the Department of Solid State Physics, Lund University, Lund. M. Ärlelid is with the Department of Electroscience, Lund University, Lund, (e-mail: Mikael.Nilsson@ftf.lth.se).

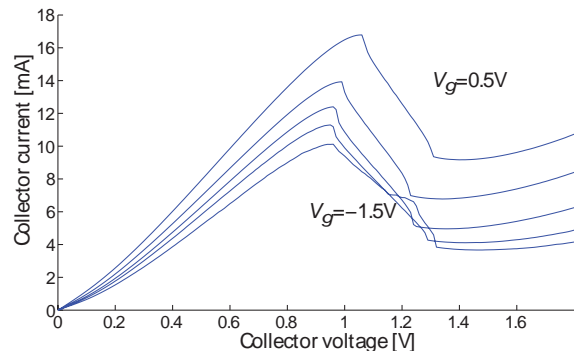


Fig. 1. IV-characteristics of the GTD. The gate voltage is increased in steps of 0.5 V.

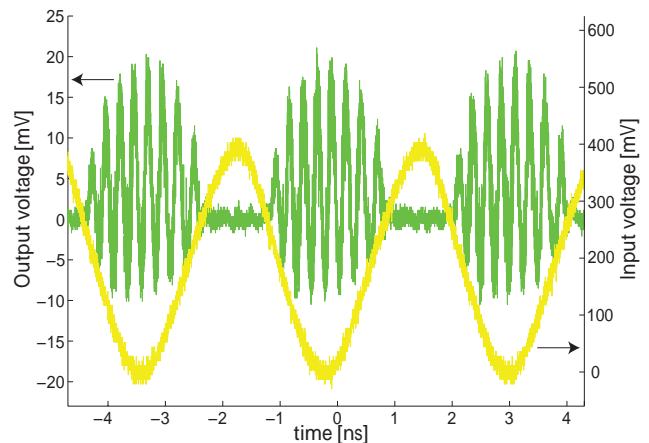


Fig. 2. Output from the pulse generator, the 16.4 GHz output signal is down converted with a 13.1 GHz signal. Due to the bias stabilization network the bias conditions are 1.9 V and 377 mA.

III. CONCLUSIONS

We have constructed a pulse generator using a gated tunnel diode. The pulse generator shows promising features such as the possibility to generate very short pulses at a high frequency. So far the output pulse length is limited by the input pulse length. The main goal is to construct a wireless IR-UWB system for the 60 GHz regime capable of transmitting at least 3 Gbps.

REFERENCES

- [1] E.Lind, P. Lindström, L.-E. Wernersson. *Resonant tunneling permeable base transistor with high transconductance*, IEEE Electron Device Lett. **25**, 678 (2004),

Workshop

THz Technology

1300-1500 Wednesday 5 March 2008

Introduction to the T4000 Passive Terahertz Imager

Chris Mann, Chief Technical Officer

ThruVision Ltd, 17-18 Central 127, Milton Park, Abingdon, Oxon OX14 4SA

chris.mann@thruvision.com, www.thruvision.com.

Passive millimetre wave imaging is now an established and accepted technology that is finding viable commercial applications in many areas, particularly security and border control. The upper frequency of operation has largely been governed by the availability of solid state uncooled detectors to around 100GHz. Passive operation at higher frequencies potentially offers some unique features such as higher optical resolution for a given system size, increased depth of focus and improved material contrast. However, the technological challenges involved in realising arrays of terahertz detectors with the required sensitivity, packing density, repeatability and reliability are considerable.

ThruVision's T4000 passive imager incorporates such arrays which are combined with proprietary optics and scanning. The imager has some unique capabilities which make it highly attractive for emerging security and civil applications such as the detection of concealed contraband and firearms at a remote distance. This talk provides an introduction to ThruVision's products and associated technology.

A Novel 220 GHz Slot-Square Substrate Lens Feed Antenna Integrated on MMIC

J. Svedin¹, S. Leijon¹, N. Wadefalk², S. Cherednichenko², B. Hansson², S. Gunnarsson²,
I. Kalfass³, A. Leuther^{3,4}, and, A. Emrich⁴

¹Dept. of Microwave Technology, Swedish Defense Research Agency (FOI), SE-581 11 Linköping, Sweden

²Dept. of Microtechnology and Nanoscience, Chalmers Univ. of Technology, SE-412 96 Göteborg, Sweden

³Fraunhofer Institute for Applied Solid State Physics (IAF), Freiburg, Germany

⁴Omnisys Instruments AB, SE-421 30 Västra Frölunda, Sweden

Email: jan.svedin@foi.se

I. ABSTRACT

For several decades the interest for applications at millimetre wave frequencies has been increasing. This mainly concerns sensor- and communication systems for military use and the corresponding for space based systems. More recently emerging applications such as e.g. imaging systems for detection of concealed weapons has suggested the use of the atmospheric windows, e.g. at 220 GHz.

To reduce the cost, weight and volume of such systems, MMIC based solution are preferred compared to discrete solutions. In terms of price per unit and manufacturing repeatability it would be highly advantageous to have a single-chip solution. By also integrating the antenna on-chip, only low-frequency inputs and outputs would be required on the MMIC. The loss associated with traditional bond wire connections at 220 GHz would then be completely avoided.

In this work, which is done within the NanoComp project, a Swedish/German Research Collaboration supported by FOI, we aim to design a 220 GHz single-chip receiver MMIC with integrated antenna. The MMIC will aside from the integrated antenna (this paper) include a full mm-wave front-end, i.e. a low noise amplifier (LNA), a mixer, and an X8 LO multiplier chain [1]. All designs are manufactured in a 0.1 μm gate length GaAs mHEMT MMIC process offered by the Fraunhofer Institute for Applied Solid-State Physics (IAF) in Germany.

The novel slot-square antenna will be used to feed a high-resistivity Si substrate lens. The thickness of the thinned GaAs substrate, 50 μm , roughly corresponds to 0.13λ . This rather high thickness would be problematic for a planar antenna because of the excitation of surface wave modes. However, by using a substrate lens the excitation of surface waves is prohibited and moreover, the field of view of the antenna system is easily tailored to the application by choosing a suitable diameter of the lens, see the conceptual drawing in Fig. 1.

The 220 GHz slot-square feed antenna was designed with requirements on the impedance bandwidth, a dual polarization capability and compatibility with a microstrip (MS) environment. The substrate lens under the MMIC focuses the

radiation and feeds the slot-square on-chip antenna through a square opening in the ground plane of the MMIC. The antenna was derived from a co-planar waveguide (CPW) fed slot-square antenna by moving the ground plane to the backside of the chip, shorting it and using the CPW signal line as the MS feed line, see a 3D schematic view in Fig. 2.

The measured impedance of some manufactured 220 GHz antenna break-out circuits was found in good agreement with simulations.

Noise factor measurements (using the hot/cold load Y-factor method) on an MMIC with the novel slot-square feed antenna, an LNA and a mixer positioned on top of a 12 mm Si lens showed a total DSB NF < 10 dB at 220 GHz [1].

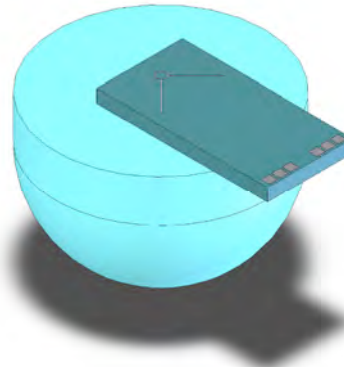


Fig. 1. Conceptual drawing of an MMIC with feed antenna on top of a substrate lens antenna.

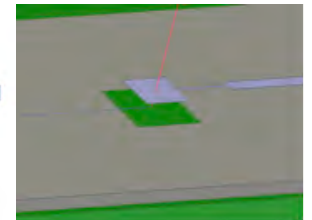


Fig. 2. A 3D view of the novel MS fed slot-square substrate lens feed antenna.

REFERENCES

- [1] S. E. Gunnarsson, N. Wadefalk, J. Svedin, S. Cherednichenko, I. Angelov, H. Zirath, I. Kalfass, and A. Leuther, "A 220 GHz Single-Chip Receiver MMIC with Integrated Antenna", submitted to *IEEE Microwave and Wireless Components Letter*, Oct. 2007.

Planar antennas for terahertz frequencies

Sergey Cherednichenko

Chalmers University of Technology, Dep. Microtechnology and Nanoscience, Fysikgrand

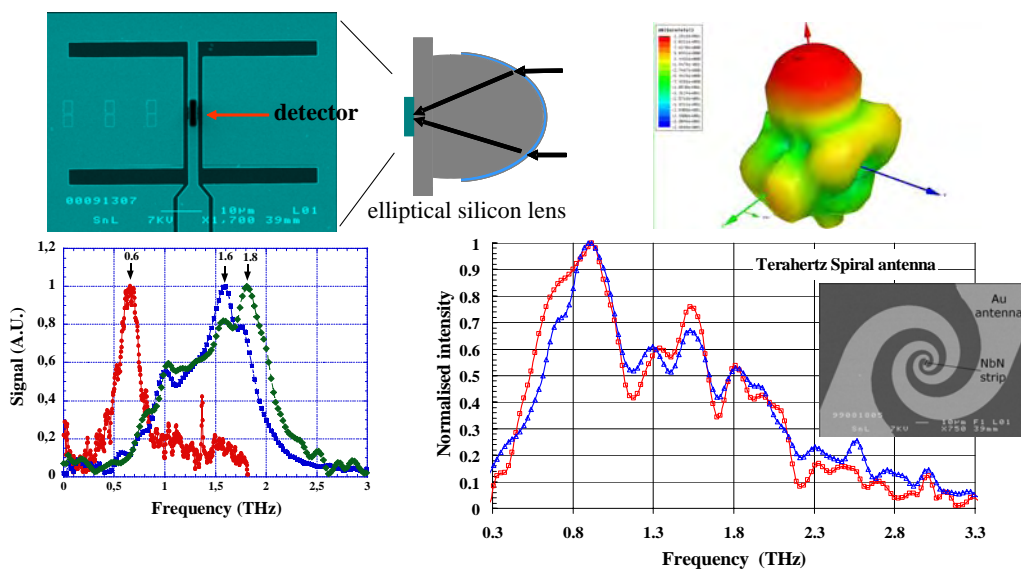
3, SE-41296, Gothenburg, Sweden

serguei@chalmers.se

During the last years, terahertz frequencies got much interest due to the progress in the electronic and photonic devices for terahertz wave detection and generation. Many applications require free space wave launching and re-collection. It brings up a question of an effective antenna, suitable for integration with THz devices, and presenting required properties, among of which high gain and polarization sensitivity are often named. A high level of expertise has been reached in the field of radio astronomical receivers, which can now be adopted for terrestrial applications.

Planar antennas are very efficient for integration not only with two terminal but, as it was recently demonstrated with a subMM MMIC receiver, even with three terminal devices. A narrowband response with a X-pol level below -20dB can be obtained with either double-slot (see figure below) and double-dipole antennas. Clamped to a silicon lens a high gain of about 20dB can be achieved. Due to a high symmetry of the beam pattern this antennas can be efficiently (90%) coupled to a Gaussian telescope for a long distance signal transmission. On contrary, logarithmic spiral (see the figure below) or logo-periodic antennas have very broadband response, covering a few octaves.

We will present results of different antenna simulations using modern 3D simulating software. Theoretical results will be compared with experimental once.

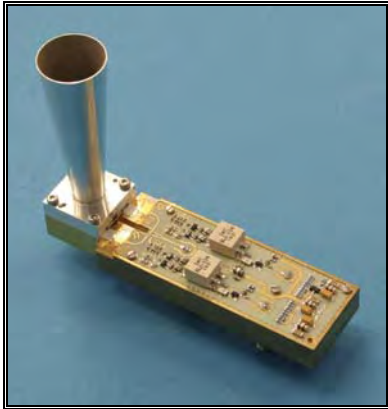


Geosynchronous Earth Orbit Atmospheric Sounder

*S. Andersson, J. Embretsén, A. Emrich, M. Ericson, M. Hjorth, J. Riesbeck, C. Tegnander
Omnisys Instruments AB, Contact: je@omnisys.se*

ABSTRACT

Omnisys Instruments is currently developing a system which will demonstrate an innovative instrument concept for future atmospheric microwave sounding. The instrument concept's primary objective is to achieve accurate observation at significant spatial resolution with microwave and (sub) millimetre wave sensors from Geosynchronous Earth Orbit (GEO).



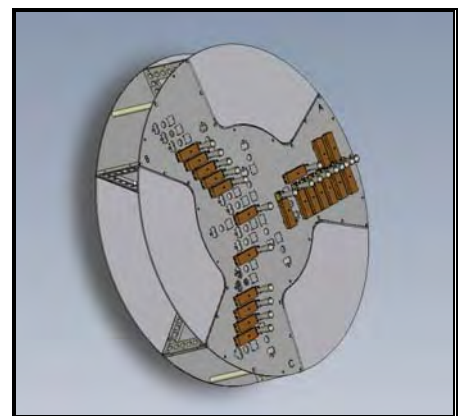
A 50 GHz receiver front-end

Atmospheric sounders measure the distribution of radiation emitted by the atmosphere. From this information vertical profiles of temperature and humidity through the atmosphere may be obtained. Current generation of sounders, which are embarked on-board low Earth orbit (LEO) satellites, provide meteorological data for weather forecasting and global observations for climate monitoring. Geostationary observations have the key potential advantage for providing real-time continuous coverage of a region, which is essential for now casting.

Omnisys has led an ESA study to select candidate breakthrough concepts to meet the requirements. In terms of performance, the specification is: 30 km resolution over the earth disc (400x400 map), covering the frequency bands 53, 118, 166, 183, 340, 380 GHz, and an update rate of 30 minutes. Due to the large aperture size required to achieve 30 km horizontal resolution from GEO, its use has so far been restricted to the case of LEO satellites. This will now be accomplished with a synthesised aperture using over 500 (sub) millimetre receivers mounted on booms. The deployed booms stretch over an 8 meter diameter.

The overall objective of the GEO Atmospheric Sounder activity is to develop and demonstrate enabling instrument concepts to achieve accurate observation at significant spatial resolution with microwave and (sub) millimetre wave sensors from GEO. This will entail the development and demonstration of the required innovative technologies as part of a demonstrator.

The demonstrator will consist of 20 dually polarised 50 GHz receiver front-end units with multi-functional single-chip receiver MMIC. These front-end units will be mounted in a Y-shaped sparse array on a rotating, 900 mm in diameter, mechanical structure.



The instrument concept demonstrator

The central processing core of the demonstrator performs IF conditioning, quantisation and cross correlation of all combinations of the 40 (2x20) down converted signals. Adding to this are the phased locked local oscillator with distribution, power conditioning and distribution unit and electronics control unit.

Back-end module demonstrator for radio-astronomy applications

Juan Luis Cano, Beatriz Aja, Enrique Villa, Luisa de la Fuente, Eduardo Artal
(juanluis.cano@unican.es)

Departamento de Ingenieria de Comunicaciones. ETSIIT. Avenida de los Castros, s.n.
Universidad de Cantabria. Santander (Spain)

Summary

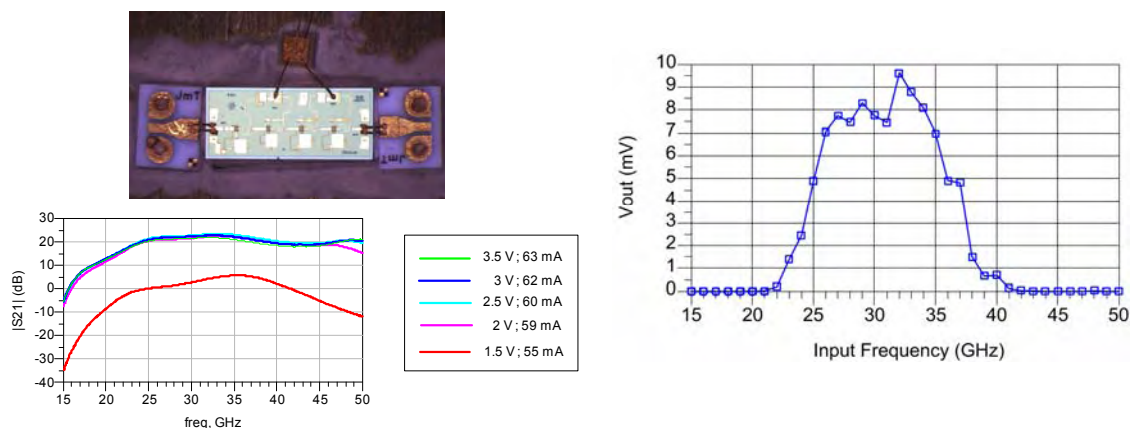
A broadband back-end module demonstrator for a Ka-band radiometer has been designed and tested. It is a direct conversion receiver based on low noise amplification, band pass filtering and Schottky diode detection. Simulations of the system are based on individual subsystems measurements using a coplanar probe station and broadband coplanar to microstrip transitions.

Introduction

Radio-astronomy radiometers for scientific applications, such as Cosmic Microwave Background observations [1], are very sensitive and broadband receivers. Their front-end module is a very low noise amplifier operated at cryogenic temperature. A back-end module at room temperature provides extra gain and direct detection. The branch demonstrator is composed of two cascaded MMIC LNA, band pass filter and Schottky diode detector. The receiver bandwidth is from 26 up to 36 GHz.

Results

The figure on the left shows a LNA assembled in a test fixture for its characterisation, and its gain for different bias points. The plot on the right depicts the back-end output response versus frequency for -53 dBm input power, which is the nominal power output coming from the front-end.



Conclusion

A broadband back-end module demonstrator has been assembled. Its behaviour has been adequately predicted by a prior test of each individual subsystem.

References

[1] M. Bersanelli et al., "Planck-LFI: instrument design and ground calibration strategy", Proc. of the European Microwave Association", Vol. 1, Issue 3, September 2005, pp. 189-195.

This work has been supported by the Ministerio de Educación y Ciencia (Spain), grant references ESP2004-07067-C03-02, AYA2007-68058-C03-03 and BES-2005-6730.

ALMA Band 5 (163-211 GHz) Sideband Separating Mixer

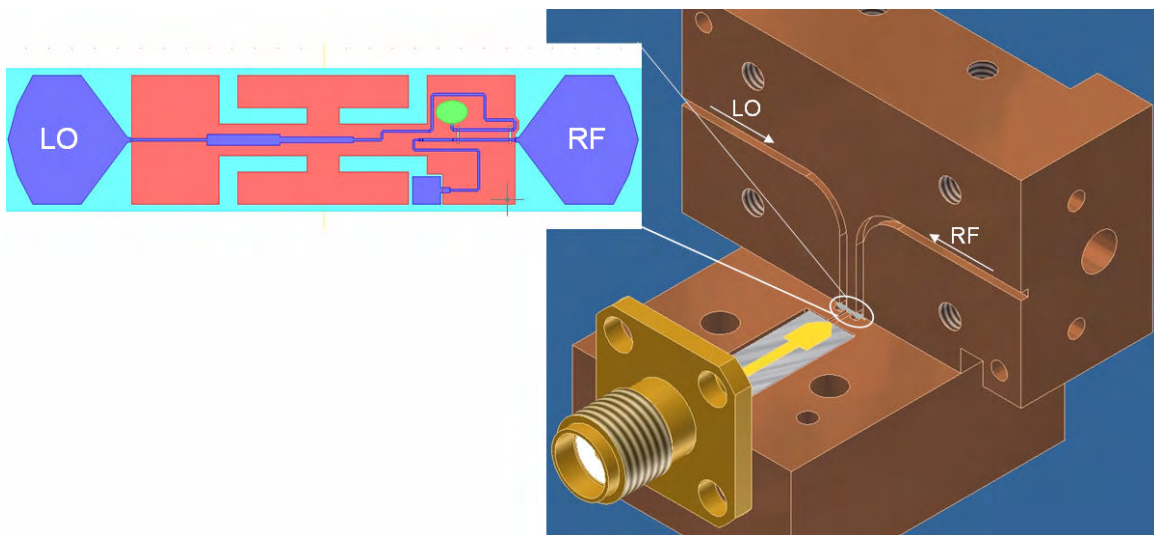
B. Billade¹, Igor Lapkin¹, A. Pavolotsky¹, R. Monje¹, J. Kooi², and V. Belitsky¹.

¹Group of Advanced Receiver Development(GARD), Chalmers University of Technology, Gothenburg, Sweden.

²California Institute of Technology, Pasadena, USA

Email: bhushan.billade@chalmers.se

The ALMA radio telescope is a multi-antenna interferometric instrument under construction by an international consortia consisting of European countries, USA, Canada, and Japan. ALMA will use receivers in 10 different bands and this report presents work on ALMA Band 5, which will be a dual polarization sideband separating heterodyne receiver for 163-211 GHz with 4 - 8 GHz IF. For each polarization, Band 5 receiver employs sideband rejection quadrature layout (2SB) with SIS mixers. In such receiver, the RF signal appears with 90 degree phase difference at the two mixers and LO appears in phase. In our design we use a 90-degree 3-dB waveguide branch-line hybrid for RF and waveguide E-plane power divider for LO. In order to achieve specified -15dB side band rejection the amplitude and phase imbalance of the quadrature scheme should not be more than -2.5dB and 12 degrees respectively, which puts strict constrain on the RF and IF hybrids. We have performed extensive simulations of all components of the 2SB SIS mixer, including 3D EM modeling using Agilent EMDS and ADS circuit simulator. Our simulation shows that the RF hybrid can be designed with 0.8 dB amplitude and 3 degree phase balance at the best case, while the IF hybrid employing Lange coupler attains 0.7 dB amplitude and 5 degree phase balance. The SIS mixer employs MMIC-like approach with all mixer components integrated on the same crystal quartz substrate. The waveguide-to-microstrip transition is done using an E-probe extending into the waveguide; the RF choke at the end of the probe provides a virtual ground for the RF signal. The LO injection is done using a microstrip line directional coupler with slots in the ground plane. The mixer itself consists of two SIS junctions with area 3 square microns each, in twin junction configuration, followed by a quarter wave transformer to couple it to the probe. This circuitry provides optimum matching of the SIS junctions at RF frequencies though the problem with such architecture is that there is no natural cold point to extract the IF. A high inductive line is therefore used using additional layer of SiO₂. A bias-T is integrated with the IF hybrid.



At the time of the conference we plan to present details of the mixer design and results of the first experimental verification of the DSB mixer performance.

High Power Photonic MW/THz Generation Using UTC-PD

Biddut Banik, Josip Vukusic, Hans Hjelmgren, Henrik Sunnerud, Andreas Wiberg and Jan Stake

Department of Microtechnology and Nanoscience, Chalmers University of Technology; SE-41296 Göteborg, Sweden (e-mail: biddut.banik@chalmers.se).

Summary: The ongoing research work concentrates on extending the previously accomplished UTC-PD fabrication and modelling techniques to 340 GHz and above. We have fabricated and characterized UTC-PDs intended for high power MW/THz generation. Several integrated antenna-detector circuits have been designed and characterised.

Introduction: Because of the inherent difficulty to generate power in the frequency range 0.1-10 THz, the term ‘THz-gap’ has been coined [1]. Among a number of MW/THz generation techniques, the photomixer based sources hold high potential offering wide tunability and decent amounts of output power. The photomixing technique relies on the nonlinear mixing of two closely spaced laser wavelengths generating a beat oscillation at the difference frequency. In recent years, there has been an increasing interest in the UTC-PD [2] for photomixing, photo receivers, mm- and sub-mm-wave generation, fibre-optic communication systems, and wireless communications. UTC-PDs have become very promising by demonstrating output powers of 20 mW at 100 GHz [2] and 25 μ W at 0.9 THz [3].

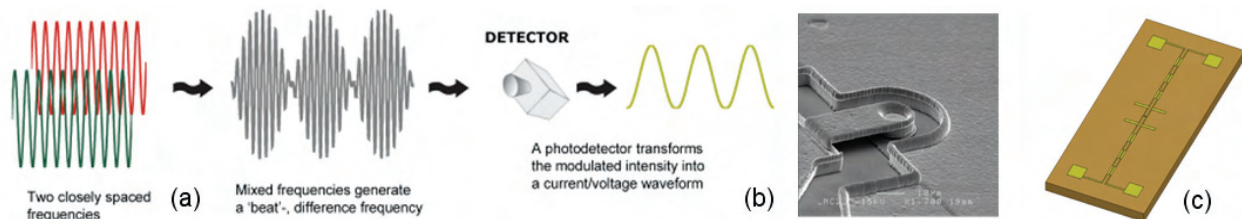


Fig. 1. (a) The principle of photomixing (b) SEM of a fabricated UTC-PD (c) Integrated UTC-PD-antenna.

Results: In order to understand the device behaviour and its dependence on various factors, we have developed an accurate device model [4] implementing hydrodynamic transport model. The model has also enabled us to design and optimise the device for any specific application and target frequency. With the aim to realise and evaluate the performance of the UTC-PD in terms of high power MW/THz generation, several antenna and bias circuit integrated UTC-PDs have been designed and fabricated. The characterisation and measurement results of those devices will be presented.

Conclusion: We have designed, fabricated and characterised UTC-PDs and antenna integrated UTC-PDs. Several other design methodologies, e.g. optimised optical coupling, thermal management, waveguide integration etc. will be investigated in future.

References:

- [1] P. H. Siegel, "Terahertz technology," *IEEE Transactions on Microwave Theory and Techniques*, vol. 50, pp. 910-28, 2002.
- [2] H. Ito, T. Nagatsuma, A. Hirata, T. Minotani, A. Sasaki, Y. Hirota, and T. Ishibashi, "High-power photonic millimetre wave generation at 100 GHz using matching-circuit-integrated uni-travelling-carrier photodiodes," *Optoelectronics, IEE Proceedings*, vol. 150, pp. 138-142, 2003.
- [3] C. C. Renaud, M. Robertson, D. Rogers, R. Firth, P. J. Cannard, R. Moore, and A. J. Seeds, "A high responsivity, broadband waveguide uni-travelling carrier photodiode," *Proceedings of the SPIE*, vol. 6194, pp. 61940C, 2006.
- [4] S. M. M. Rahman, H. Hjelmgren, J. Vukusic, J. Stake, P. Andrekson, and H. Zirath, "Hydrodynamic simulations of uni-traveling-carrier photodiodes," *IEEE J. Quantum Electron.*, vol. 43, pp. 1088-1094, 2007.

Towards a THz Sideband Separating Subharmonic Schottky Mixer

Peter Sobis^(1,2), Jan Stake⁽¹⁾ and Anders Emrich⁽²⁾

⁽¹⁾ Chalmers University of Technology
Department of Microtechnology and Nanoscience
SE-412 96, Göteborg, Sweden
Email: peter.sobis@chalmers.se
Email: jan.stake@chalmers.se

⁽²⁾ Omnisys Instruments AB
Gruvgatan 8, SE-421 30, Västra Frölunda, Sweden
Email: ps@omnisys.se
Email: ae@omnisys.se

GaAs Schottky mixers with state of the art planar submicron diodes are used for THz-detection up to 3 THz today [1]. GaAs Schottky diodes can operate in room temperature which makes them good candidates for space applications and an interesting low cost alternative to low noise cryogenic SIS and HEB technologies. The main advantage of a sideband separation scheme besides that the lower and upper sidebands are indeed separated, is that the IF bandwidth is increased by a factor of two. Moreover, there is no need for image rejection filters on the RF input, which can be bulky and increase the weight and cost of the overall receiver system. Sideband separation mixers have been implemented at THz frequencies before [2], however up to this point they have never been tried with Schottky diodes in a subharmonic mixer configuration. We will present the current status of the development of a novel sideband separating subharmonic receiver topology operating at 340 GHz, see Fig1. The design of a subharmonic mixer and the LO and RF waveguide hybrids will be presented followed by an account of measured results of the individual components.

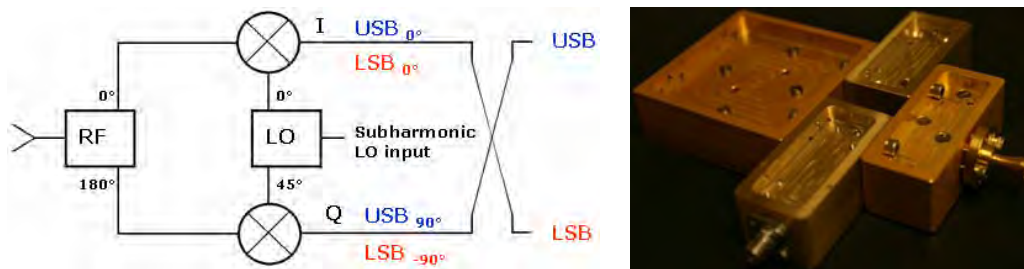


Fig1. Schematic of the sideband separation mixer (left) and modular assembly (right).

[1] J.L. Hesler, T.W. Crowe, W.L. Bishop, R.M. Weikle, R.F. Bradley and Pan Shing-Kuo, "The development of planar Schottky diode waveguide mixers at submillimeter wavelengths", IEEE MTT-S International Microwave Symposium Digest, vol 2, pp. 953-6, 1997.

[2] C. Risacher, V. Vassilev, V. Belitsky, A. Pavolotsky, "Design of a 345 GHz Sideband Separation SIS Mixer", Proceedings of 3rd ESA Workshop on Millimeter Wave Technology and Applications: Circuits, Systems and Measurement Techniques, 21-23 May 2003, Espoo, Finland

HIFAS: High-performance Full-custom Autocorrelation Spectrometer ASIC

A. Emrich, S. Andersson, J. Dahlberg, L. Landén, M. Hjorth, Omnisys Instruments;
T. Kjellberg, Chalmers/MC2; N. Andersson, Acreo
Contact email: mh@omnisys.se

ABSTRACT

Autocorrelation spectrometers are often employed for radio astronomy and atmospheric research applications, due to their high bandwidth and stability. The major advantage of the autocorrelator over other types of spectrometers is that the real-time signal processing can be implemented using relatively simple digital logic, which allows for compact implementations with very high clock speeds and corresponding bandwidths (or low bandwidth, low power implementations where that is preferred).

For the Odin research satellite, launched in 2001 and still in operation, Omnisys designed an autocorrelation spectrometer. The core of the spectrometer consists of two ASICs, a sampler and an autocorrelator. Each pair of such chips has 100 MHz of bandwidth and consumes 0.4 W of power. This performance-power ratio was outstanding at the time and is still impressive.

HIFAS, Omnisys fifth generation autocorrelation spectrometer ASIC is being developed. It is a full-custom design with over two million transistors, designed for IBM's 180 nm SiGe Bi-CMOS process. Unlike earlier generations, it contains both the bipolar 3-level ("1.5-bit") A/D converter and the CMOS correlator on the same chip. Thereby, the sensitive high-speed digital interface between the two parts gets integrated on the chip.

The chip supports as input either a complex I/Q input signal pair, measuring its spectrum from $-f_{\text{clk}}/2$ to $+f_{\text{clk}}/2$ or a single baseband signal sampled on both clock edges, measuring from 0 to f_{clk} . This choice gives flexibility for the system level design.

The first batch of the chip was produced in 2007. Unfortunately it turned out to have a logic bug that makes it necessary to do a re-run. A second revision of the chip is being designed at the time of this writing, and tape-out is planned for early 2008.

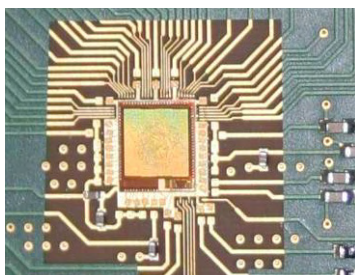


Fig. 2: ASIC wire-bonded on test board.

Despite these initial problems with the chip, most of the chip's functions have been tested and shown to work. The analog parts work in both of the two input modes with up to 8 GHz sample clock, and most of the digital features are also working correctly.

The goal is to reach a bandwidth of 8 GHz, a resolution of 1024 channels, and a power consumption of 3-5 W. When finished, this chip will set a new world record in autocorrelator performance, and open for new possibilities in radiometry on both space and ground.

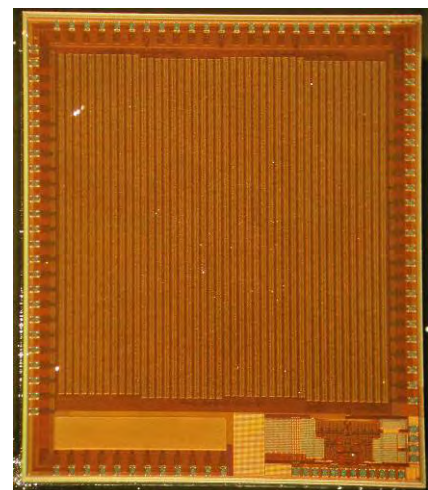


Fig. 1: Photo of the HIFAS ASIC. ADC is in bottom right corner.

Session II

1530-1730 Wednesday 5 March 2008

**Extremely Low-Noise Amplification with Cryogenic FET's and
HFET's: 1970-2006
(Where do we go from here?)**

Marian W. Pospieszalski
National Radio Astronomy Observatory
2551 Ivy Road, Ste. 219
Charlottesville, VA 22903

SUMMARY

Improvements in the noise temperature of field-effect transistors (FET's) and, later, heterostructure field-effect transistors (HFET's) over the last several decades have been quite dramatic. In 1970, a noise temperature of 120 K was reported at 1 GHz and physical temperature of 77 K; in 2003, noise temperatures of 2, 8 and at 35 K were reported at 4, 30 and 100 GHz, respectively, for physical temperatures of 14 to 20 K.

In the first part of the talk the developments in this field are briefly traced and an attempt is made to identify important milestones. Examples of experimental results obtained with different generations of FET's (HFET's) are compared with the model predications. The current state of the art in cryogenic low noise InP HFET amplifiers is presented and some gaps in our understanding of experimental results are emphasized. Random gain fluctuations of these amplifiers important for applications in broadband continuum radiometers for radio astronomy are also shortly discussed.

In the second part the question whether rapidly advancing technologies of microwave heterostructure bipolar transistors (HBT's) and CMOS can in the future offer alternatives to the extremely low noise performance of InP HFET's is addressed. For that purpose noise models of unipolar and bipolar transistors are reviewed with emphasis on their common noise properties. Simple close-form approximate expressions for the noise parameters are given and comparison is made of calculated results with the available experimental data.

560 GHz f_t , f_{max} operation of a refractory emitter metal InP DHBT

Erik Lind*

Solid State Physics, Lund University
Lund University, Sweden
Erik.Lind@ftf.lth.se

* work performed in part while at UCSB

Adam M. Crook, Zach Griffith, Mark J. Rodwell
ECE Department, University of California
Santa Barbara, CA, USA

Abstract—We present results of a hybrid dry/wet-etched type I InGaA/InP DHBT using a refractory emitter metal. Simultaneously high f_t and f_{max} of 560 GHz is obtained, with a breakdown voltage BV_{ceo} of 3.4V.

I. INTRODUCTION

Scaling theory [1] of HBTs indicate that a 2:1 increase in bandwidth requires a 4:1 reduction in emitter and collector widths – for THz operation this requires emitter widths below 125nm. Traditional lift-off techniques and wet etching techniques used for triple-mesa HBTs are difficult to *reliable* scale below 300 nm emitter widths. We have developed a hybrid dry/wet etch technique that reliable scales to emitter widths below 250nm. First results on a 22nm base thickness, 70 nm collector thickness with ~200 nm emitter width produced record simultaneous f_t and f_{max} of 560 GHz [2].

II. FABRICATION

The epitaxial material was grown on 4" S.I. InP wafers at commercial vendor IQE. The fabrication starts with a blanket sputtered deposited $Ti_{0.1}W_{0.9}$ film, which is subsequently patterned using a SF_6/Ar dry etching. Using the emitter metal as mask, the emitter is dry etched in a Cl_2/N_2 plasma, stopping just short of the base. A InP wet etch is then used to clear the $In_{0.53}Ga_{0.47}As$ base. The transistors are finished using self aligned base ohmics, forming a triple-mesa transistor. A cross-section SEM image is shown in Fig. 1. Emitter junctions with widths down to 200 nm could controllable be fabricated, showing a substantial improvement over fully wet etched processes.

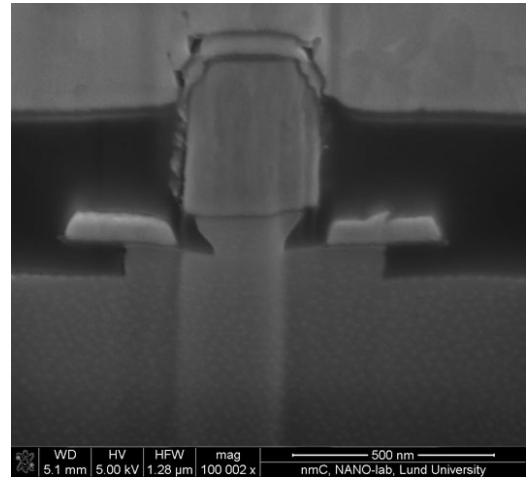


Figure 1. Cross section view (52° tilt) of a DHBT

III. MEASUREMENTS & CONCLUSIONS

The transistors were characterized from DC-67 GHz. The DC current gain was ~ 25 . The Breakdown voltages were $BV_{ceo} \sim 3.4V$, and $BV_{cbo} \sim 3.6 V$, limited by band-to-band tunneling. For devices with emitter widths of 200 nm, a simultaneous extrapolated f_t and f_{max} of 560 GHz was obtained, which is the first report of a device with *both* f_t and f_{max} above 500 GHz. Peak f_t was 600 GHz for a device with lower (430 GHz) f_{max} .

ACKNOWLEDGMENT

This work was supported by the DARPA SWIFT program and a grant from the Swedish Research Council.

REFERENCES

- [1] M. Rodwell et.al., IPRM 2007, pp. 9-13
- [2] E. Lind et.al., DRC 2007, Late News

Low phase-noise balanced Colpitt InGaP-GaAs HBT VCOs with wide frequency tuning range and small VCO-gain variation

Herbert Zirath

Ericsson AB, Microwave and High Speed Electronics Research Centre, Mölndal, Sweden.

Microwave Electronics Laboratory, Göteborg, Sweden Chalmers University of Technology, Department of Microtechnology and Nanoscience, GHz Centre Email: herbert.zirath@chalmers.se

Abstract—Low phase-noise InGaP-GaAs HBT VCOs, utilizing an on-chip ‘wide tuning range varactor’, have been designed, fabricated, and characterized. The primary design goals were low phase noise, wide continuous frequency tuning and small VCO-gain variation. Two types of varactor were compared, a square varactor and a finger varactor. The square varactor achieves a frequency tuning of 27%, and the finger varactor 21%. The phase noise is typically -100dBc/Hz at 100kHz offset frequency. A VCO gain (sensitivity) of 160 MHz/V is obtained with a variation of less than 10%. The power consumption is controlled by the core dc-current and is of the order 50-100mW.

I. THE MMIC TECHNOLOGY

The MMIC-technology used in this study is a modified commercially available InGaP-GaAs HBT MMIC-technology with an emitter width of 3 μm . The base-collector doping profile is specially designed and optimized for high $C_{\text{max}}/C_{\text{min}}$ ratio and a linear oscillation frequency versus varactor voltage characteristic, i.e. a constant VCO gain.

II. DESIGN OF THE VCO

The schematic of the VCO is shown in Fig 1. The VCO consist of two Colpitt oscillators which are coupled together with the capacitor C2. The complimentary outputs are taken from the emitters in order to minimize the loading of the VCO. By controlling the dc-current of the oscillator core, the amplitude in the tank can be controlled as well as the output power. The current in the oscillator is controlled by the voltage applied at R_{B2} . This control voltage can be used for amplitude level control of the VCO. In order to improve the Q-value of the tank, the varactor geometry was optimized by using a finger structure. A VCO with a square varactor was also designed for comparison. The varactor is realized by using the base-collector junction of the HBT. In this work, a specially tailored doping profile in the base-collector junction is utilized. The goal is to achieve a linear frequency-varactor voltage characteristic as well as a large capacitance variation.

III. MEASUREMENT RESULTS AND DISCUSSION

The output power and oscillator frequency versus the varactor voltage at a collector supply of 8V and a core current of 20 mA is plotted in Fig. 2. The oscillation frequency versus varactor voltage is linear throughout the varactor control range which is highly required in PLL-applications. The ‘square varactor VCO’ can be tuned continuously from 6.8 to 8.9GHz.

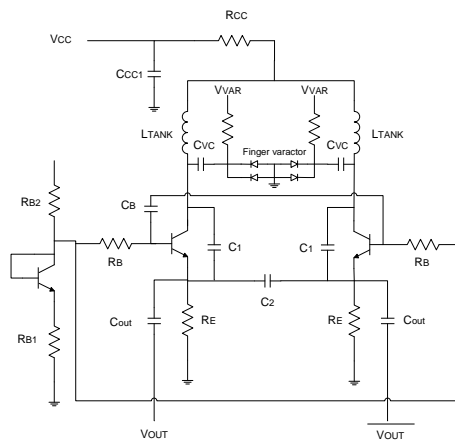


Fig 1 Schematic of the VCO

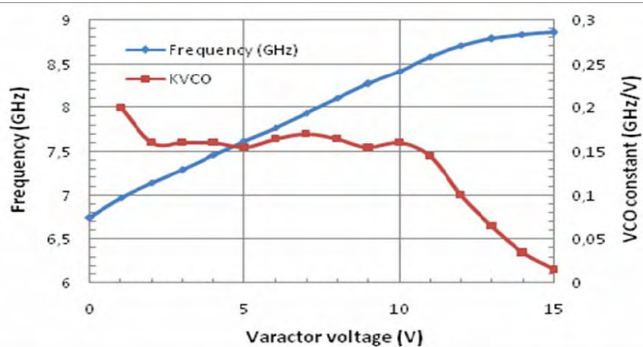


Fig 2 VCO with square varactor. 26% frequency tuning

A minimum phase noise of -99.5 and -101.5 dBc/Hz is obtained with approximately 4 dB variation over the frequency band for a fixed bias. The simulated minimum phase noise is -102 and -104.5 dBc/Hz @100kHz offset respectively i.e. 2.5/3 dB lower than the measurements. The use of finger varactor resulted in a measured improvement of phase noise with 2 dB, close to the simulated value of 2.5 dB. The phase noise as a function of offset frequency was measured utilizing an Agilent E5052A Signal Source Analyzer.

This work shows that encouraging results on wideband tuned Colpitt VCOs can be obtained if a special ‘tailored’ base-collector doping profile is utilized. The measured phase noise is below most reported VCOs in the literature when the oscillation frequency is normalized, and the variation in K_{VCO} is to the knowledge of the author the smallest reported in the literature

Feasibility of Filter-less RF Receiver Front-end

S.Ahmad, N.Ahsan, A.Blad, R.Ramzan, T.Sundström, H.Johansson, J.Dąbrowski, C.Svensson
Department of Electrical Engineering, Linköping University

This work is a feasibility study on a radio receiver design where RF filters are avoided or considerably simplified. The problem originates from the idea of a *software defined radio* (SDR), capable of receiving any radio standard in any frequency band. Following the traditional radio paradigm towards multi-band SDR, we would end-up in a bunch of highly selective band-preselect filters placed between antenna and the RF front-end. This is an expensive, bulky and lossy solution. Similarly if we try to develop tunable passive filters.

In a receiver with no band-preselect filter the wanted signal would be accompanied by strong interferers (blockers). The idea is to receive the entire signal and convert it to the digital domain where the interferers can be effectively removed by digital filtering. As both signal and blocker are simultaneously present at the receiver input, automatic gain control does not help. Instead, dynamic range of the front-end and the ADC, and their linearity and noise floor must meet the full dynamic requirement.

For the receiver noise floor both the thermal and ADC quantization noise are vital. We find the receiver dynamic range $DR = P_{bl} / (F_{Rx} N_{ref}) = (P_{bl} \times SNR_{out}) / (S \times \gamma)$ where P_{bl} is the blocker power maintained by the receiver, N_{ref} is the reference thermal noise, SNR_{out} is the required SNR at the demodulator input, S is the receiver sensitivity and γ stands for the despreading factor (if any). F_{Rx} reflects the contribution both by thermal and quantization noise. The solution we suggest is a combination of a highly linear LNA/mixer (for large blockers there may be very little room for LNA gain), followed by a low-pass $\Sigma\Delta$ -ADC with very high sampling rate (of the order of the carrier frequency). This architecture could be used as a homodyne or as a low IF superheterodyne with digital IF. By using a very high sampling rate, we mitigate the need for antialias filters and we gain dynamic range through the high oversampling ratio. We will give results on estimated requirements on the components and parameters of such a solution.

To demonstrate the concept we have designed a zero-IF/low-IF RF front-end composed of a highly linear wideband LNA and a quadrature mixer with a simple antialiasing lowpass filter at its output, followed by a 1st order 4-bit $\Delta\Sigma$ ADC, which operates in current mode. The front-end is intended for frequencies 1-6 GHz while the largest signal bandwidth is assumed to be 20 MHz. In this way we aim to combine GSM900/1900, UMTS FDD, DECT, and WLAN 802.11a,b standards in one hardware. The ADC sampling frequency is 2.4GHz so the images at $k \times 2.4$ GHz can be easily suppressed with the 2nd order low pass filter. The circuit has been designed for a 90 nm CMOS process and sent for fabrication at CMP.

Simulations indicate the following results for this demonstrator at 2.4/5.2 GHz:
Gain = 6dB/5dB, NF=6dB/7.5dB, S11= -15dB, and IIP3= -4.5dBm, $P_{bl} \leq -10$ dBm. The NF including the ADC is by about 3dB larger. These data are not sufficient to meet the required specifications, but show the feasibility of the concept.

Small Size 2-10GHz Radar Receiver Si-RFIC

Håkan Berg, Heiko Thiesies, Marie Hertz, Fredrik Norling

Microwave Technology, Saab Microwave Systems, Saab AB
SE-412 89 Göteborg, Sweden

Introduction

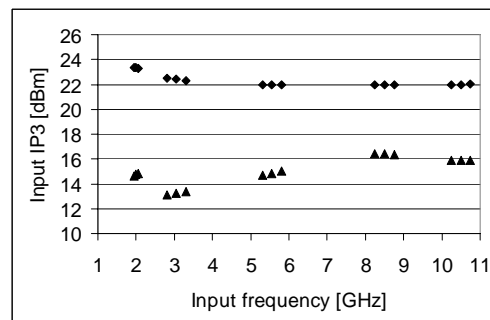
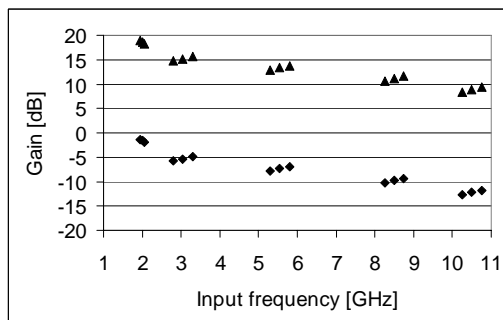
Using traditional RFIC design architecture a radar receiver IC is designed. Traditional low frequency architectures allow for a dramatic size reduction compared to microwave design [1]. Furthermore, since there are no matching networks between the circuits on-chip the bandwidth is limited by transistor performance only. This gives a larger bandwidth and the opportunity to cover the radar bands at S-, C-, and X-band using the same receiver. The IF bandwidth is 200-2500 MHz. Due to the large bandwidth at both in- and output the IC is well suited for superheterodyne radar receivers where it can be used for both frequency conversions.

The IC is manufactured by austriamicrosystems in their 0.35 μ m SiGe-BiCMOS process with an f_T of 60 GHz and is packaged in a 4x4 mm QFN plastic package.

Results

Simulations have been performed at five different input frequency bands as shown below. The gain and IP3 of these simulations are presented with different gain settings. The noise figure is simulated to be less than 13 dB at all frequencies at maximum gain.

RF [GHz]	IF [MHz]	LO [GHz]	Application
3.05 \pm 0.25	2000 \pm 250	5.05	S-band to IF
5.55 \pm 0.25	2000 \pm 250	7.55	C-band to IF
8.50 \pm 0.25	2000 \pm 250	10.50	X-band (low end) to IF
10.5 \pm 0.25	2000 \pm 250	12.50	X-band (high end) to IF
2 \pm 0.05	250 \pm 50	2.25	IF to Baseband



Simulated gain and input referred IP3 for the maximum gain (triangles) and at 20 dB attenuation (diamonds).

Conclusions

A broadband receiver IC has been developed. It is shown to be a potential replacement component for several single-band components and help building generic receivers. It has utilized RFIC design techniques rather than microwave ones; this makes it possible to combine the small-size with broadband performance. The simulated performance is well compatible to the requirements of future radar systems.

- [1] H. Berg, H. Thiesies, M. Hertz, and F. Norling, "A High Linearity Mixed Signal Down Converter IC for C-band Radar Receivers" 2nd European Microwave Integrated Circuits Conference, pp 255-258, Okt. 2007.

High frequency, current tunable spin torque oscillators: experimental characterization

S. Bonetti*, J. Garcia, J. Persson, and Johan Åkerman

Materials Physics, Department of Microelectronics and Applied Physics,
Royal Institute of Technology, Electrum 229, 16440 Stockholm-Kista, Sweden

*e-mail: bonetti@kth.se

We present characteristics of high frequency and current tunable spin torque oscillators (STOs), and give a description of the experimental setup we implemented for their characterization. Our setup allows an automated investigation of magneto-resistance and frequency response as a function of varying applied magnetic field (both in magnitude and in-plane/out-of-plane angle) and driving current. We could measure oscillators with Q-values (resonance frequency / bandwidth) up to 2700 and high tunability range (10-26 GHz). Since we reached the upper frequency limit of the spectrum analyzer (26.5 GHz) at far from critical values of current and field, we expect to observe even higher tunability ranges (up to an estimated 65 GHz) with improvement of the setup.

State-of-the-art oscillators in wireless devices, such as bluetooth chips, use inductive coils in order to generate microwave power. These coils consume large chip area and it has been estimated that more than 75% of the silicon could be saved using a Spin Torque Oscillator (STO). The working principle of this device lies in the interaction between a spin polarized dc current and the magnetization of the various magnetic layers in the STO, resulting in an angular precession of the magnetization itself. As the resistance of the device is proportional to the magnetization angle, the device is an ac resistor, and the dc current causes an ac voltage output. Predictions suggest oscillations ranging from 1 GHz up to 60 GHz with high Q-values (up to 18,000) [1].

In order to measure the signal generated by these devices, one must be able to vary the applied magnetic field and current in an accurate way. Our setup can generate magnetic fields up to 1.7 T and since samples are mounted on a holder fixed on a turntable, the direction of the magnetic field can be varied continuously in the direction in-/out-of- plane of the sample. A pulsed and stepped current source and nanovoltmeter solution replaces the need of a more expensive lock-in amplifier, still allowing a very accurate reading of the magneto-resistance. In order to connect to the sample, non-magnetic ground/signal/ground high frequency (up to 40 GHz) probes are used. The signal from the probe is amplified by a low noise, broadband (1-26 GHz), +45 dB amplifier before connecting to a signal analyzer (20 Hz – 26.5 GHz frequency range). The dc current is applied to the STO by means of a bias-T, connected in the vicinity of the amplifier in the transmission line. All instruments are GPIB controlled and the measurements are fully automated.

A highly advantageous feature of these devices is that the oscillation frequency can be tuned in a linear way with the applied dc current and field (typically 100 Mhz/mA and 20 GHz/T). We observe oscillations up to 26.5 GHz only limited by the microwave amplifier and the signal analyzer. In the literature, the highest oscillation frequency observed to date is 35 GHz [1], but higher values are not theoretically precluded. From extrapolations of our results we find a maximum operation frequency as high as 65 GHz. At present, the highest Q-value observed in our STOs is 2700 at 12 GHz, but Q values above 18,000 [1] at about 34 GHz have been observed in similar devices. Thanks to all these characteristics (linear current tunability, high Q, broadband frequency range), STOs promise to be attractive devices for applications where the operational frequency of the oscillator is required to vary on a wide range, on the order of tens of GHz.

We gratefully acknowledge financial support from The Swedish Foundation for Strategic Research (SSF), The Swedish Research Council (VR), The Göran Gustafsson Foundation and The Knut and Alice Wallenberg Foundation.

References: [1] W. H. Rippard *et al*, Phys. Rev. B **70**, 100406(R) (2004).

N-tupling the capacity of wireless communications using electromagnetic angular momentum

Bo Thidé*

Swedish Institute of Space Physics
P. O. Box 537, SE-751 21 Uppsala, Sweden
E-mail: bt@irfu.se

Physically, electromagnetic radiation consists of two quantities: the well-known electromagnetic linear momentum (or power/Poynting) flux and the less well-known electromagnetic angular momentum flux, both of which are carried by radio beams all the way out to the far zone and are detectable there.

Conventional radio communications has so far relied primarily on the transfer of linear momentum/power/Poynting flux from a transmitting antenna to a receiving antenna. However, one often makes use of the spin part of the angular momentum (SAM), better known as wave polarisation. SAM spans two orthogonal rotational states, corresponding to the (one and the same) left-hand and right-hand rotation of the electric field of all of the waves (photons) in the radio beam. Using wave polarisation, the communication capacity in a given (oscillatory) frequency bandwidth can therefore be effectively doubled.

However, as demonstrated in numerous experiments carried out during the past 15 years it is also possible to make use of the orbital part of the electromagnetic angular momentum (OAM), a much subtler, differential polarisation quantity, related to but distinctly different from SAM. Since OAM spans $l + 1$ orthogonal rotational states, where l can be a large number, this effectively allows an N -tupling of the communication capacity in a given frequency bandwidth, where $N = 2l + 1$. A capacity increase of $N > 100$ has been experimentally demonstrated.

We have been able to show that it is possible to use essentially conventional radio techniques to endow radio beams with OAM, thus allowing for a dramatic increase in the capacity of wireless point-to-point communications. We report the latest results in this area.

*Also at LOIS Space Centre, MSI, Växjö University, SE-351 95 Växjö, Sweden

Session III

0830-1000 Thursday 6 March 2008

The Next Wireless Wave is a millimeter Wave

Joy Laskar PhD
Schlumberger Chair in Microelectronics at Georgia Tech
Director Georgia Electronic Design Center
joy.laskar@ece.gatech.edu

The past few years has witnessed the emergence of CMOS based circuits operating at millimeter wave frequencies. Integrated on a low cost organic packaging, this technology has the promise for high volume fabrication, lowering the cost and opening substantial markets for communications, sensing and radar. As standardization efforts catalyze the interest and investment of industry and agencies, one can be assured of ubiquitous millimeter-wave technology in the consumer electronic market place in the fairly near future. In this talk we will review our developments of radio technology with the highest speed (15Gbs), robustness (better than 20dB link margin with bit-error rates better than 10^{-9}), agility (beam steering and shadowing resistant) and lowest cost per bit. These links are enabled by digital mmw radio technology which leverage new layer fusion radio architectures.

HF and Mixed Signal Challenges/Design for Communication and Remote Sensing

(Invited talk)

Mehran Mokhtari

GigaHertz Symposium, 5-6 March 2008, Göteborg, Sweden

Abstract

Performance improvements in Communication- and remote sensing- systems and related applications are strongly related to front-end capabilities in terms of Linearity, spectral purity and noise, power consumption, size and weight, etc.

While, in most cases, the bulk of the complex signal processing is performed in the digital domain, the significance of the analog front-ends, as well as mixed signal blocks become apparent, in the overall performance and characteristics of the systems.

Digital signal processing utilizes the immense capabilities in constantly improving CMOS technologies. Power consumption, device speed, and interconnect technology, as well as the cost, in high volume production, in CMOS processes have been, amazingly well, following the road maps set for DSP requirements, and appear to have more to offer in the coming years. Mixed signal circuits, in the broader sense, in CMOS/BiCMOS technologies, and circuit techniques, have satisfied the bulk of the immediate needs in most high volume applications, and appear to have room for considerable improvements, in the years to come.

However, some applications (mostly high-end and relatively low-volume), require linearity and spectral purity beyond the capabilities of main stream circuit techniques and technologies, especially in realizing analog and mixed signal functions that commonly set the ultimate performance and capabilities of the systems.

The advancement of these systems, require technologies, circuit techniques, and overall signal processing that rely on careful study of fundamental physical limitations set by Solid-State Physics and Electromagnetics, for the boundary conditions of the desired application, primarily in the micro-/millimeter- wave domain.

The presentation will recapture some of these fundamental limitations in the image of application requirements. Some device technologies (Compound Semiconductor, Si), and circuit approaches, will be covered and discussed.

MMIC design at G-band (140-220 GHz) including a 220 GHz Single-Chip Receiver MMIC with Integrated Antenna

Sten E. Gunnarsson¹, Niklas Wadefalk¹, Morteza Abbasi¹, Camilla Kärfelt¹, Rumen Kozhuharov¹, Jan Svedin³, Bahar M. Motlagh¹, Bertil Hansson¹, Sergey Cherednichenko², Iltcho Angelov¹, Dan Kuylenstierna¹, Herbert Zirath^{1,4}, Staffan Rudner³, Ingmar Kallfass⁵, and Arnulf Leuther⁵

¹Chalmers University of Technology, Microwave Electronics Laboratory, MC2, Göteborg, Sweden.

²Chalmers University of Technology, Physical Electronics Laboratory, MC2, Göteborg, Sweden. ³Swedish Defense Research Agency (FOI), Linköping, Sweden. ⁴Ericsson AB, MHSERC, Mölndal, Sweden,

⁵Fraunhofer Institute for Applied Solid State Physics (IAF), Freiburg, Germany

Email: sten.gunnarsson@chalmers.se

I. ABSTRACT

Systems operating beyond 100 GHz have gained increased academic and commercial interest over the recent years. Traditional applications include radiometers measuring the absorption lines of e.g. oxygen (118 GHz) and water (183 GHz) for environmental studies. Emerging applications has been proposed using the atmospheric windows at 94, 140, and 220 GHz. These applications include e.g. very high-speed (> 10 Gbps) wireless communication, high-resolution passive and active millimeter wave (mm-wave) imaging applications, and systems for detection of concealed weapons, plastic explosives, and biological weapons. In order to enhance the usefulness of such systems, mobility is a key factor and the systems should ideally be small and lightweight. Thus, an MMIC based solution would be favourable over a traditional discrete design due to its smaller size and weight. Furthermore, an MMIC solution with its lower price per unit and high manufacturing repeatability opens up the possibility of multi-pixel array systems for enhanced system performance.

G-band (140-220 GHz) MMICs have been designed and measured in the MMIC group at Microwave Electronics Laboratory (MEL), MC2, Chalmers University of Technology. This work has been done within the NanoComp project, a Swedish/German Research Collaboration supported by the Swedish defense agency, FOI, together with the Swedish Foundation for Strategic Research (SSF) through the High Speed Electronics and Photonics (HSEP) program. The goal is to design single-chip receiver MMICs operating at 220 GHz which includes the full mm-wave front-end, i.e. on-chip antenna, low noise amplifier (LNA), mixer, and an X8 LO multiplier chain. All designs are manufactured in a 0.1 μm gate length GaAs mHEMT MMIC process offered by the Fraunhofer Institute for Applied Solid-State Physics (IAF) in Germany, (www.iaf.fraunhofer.de).

So far, different antennas, LNAs, mixers of different types, frequency multipliers, and power amplifiers have been designed and characterized in the 200 to 220 GHz band. Furthermore, different combinations of the former have also been tested such as the 220 GHz single-chip receiver MMIC with integrated antenna found in Fig 1, [1] and a fundamentally pumped resistive mixer with integrated slot-antenna. The receiver MMIC consists of a novel slot-square substrate lens feed antenna, a three-stage LNA and a sub-harmonically pumped resistive mixer. The receiver MMIC is mounted on a 12 mm silicon substrate lens which focuses the radiation from the calibration loads to the on-chip antenna through an opening in the backside metallization of the MMIC. The double sideband noise figure of this quasioptical receiver is as low as 9.7 dB (2470 K) at 220 GHz including the losses in the antenna and in the lens. Other measured results include a fundamentally pumped resistive mixer with less than 10 dB of loss between 200 and 220 GHz, [2].

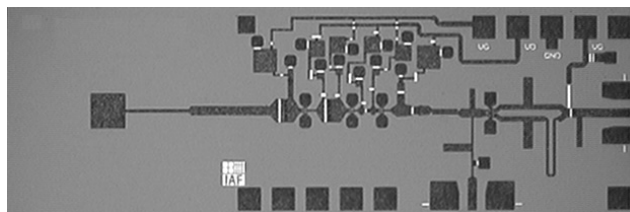


Fig. 1. Chip photo of the 220 GHz single-chip receiver MMIC. The chip measures $3.0 \times 1.0 \text{ mm}^2$.

REFERENCES

- [1] S. E. Gunnarsson, N. Wadefalk, J. Svedin, S. Cherednichenko, I. Angelov, H. Zirath, I. Kallfass, and A. Leuther, "A 220 GHz Single-Chip Receiver MMIC with Integrated Antenna", Submitted to *IEEE Microwave and Wireless Components Letter*, October 2007.
- [2] S. E. Gunnarsson, N. Wadefalk, I. Angelov, and H. Zirath, "A 220 GHz (G-band) Microstrip MMIC Single-Ended Resistive Mixer", Accepted for publication in *IEEE Microwave and Wireless Components Letter*.

A Quad-Core 130-nm CMOS 57-64 GHz VCO

Vara Prasad Goluguri*, Johan Wernehag[†], Henrik Sjöland[†] and Niklas Troedsson[§]

*Cambridge Silicon Radio Sweden AB, Emdalav. 16, 223 69 Lund

[†]Department of Electrical and Information Technology

Lund University, Box 118, 221 00 Lund Sweden

Email: Johan.Wernehag@eit.lth.se

[§]UMC, 488 DeGuigne Drive, Sunnyvale, CA 94085, USA

Abstract—In this paper a quad-core 130-nm CMOS oscillator is presented covering the license free 57-64 GHz frequency band. Each core consists of an LC-oscillator, the supply for the separate cores is switched on and off by a combinatorial network using digital gates. The oscillator core consumes 3.1 mA from a 1.2 V supply and outputs an average power of -5.3 dBm. The phase noise is simulated to -110 dBc/Hz at 3 MHz offset.

I. INTRODUCTION

A 7 GHz wide unlicensed band around 60 GHz is available [1]. This spectrum allocation will permit communication at several gigabits per second. Also in Japan and Europe [2] frequency bands at 60 GHz are opened for unlicensed WLAN communications with a 5 GHz world wide overlap.

II. SIMULATION RESULTS

The circuit topology is the well known LC-oscillator with a tail current source [3] separate for each core. The supply to only one core is active at the same time. The supplies are controlled by a digital network with two bit input control word. This digital network is built of NAND-gates and inverters. NMOS varactors are used at each core for fine tuning. Coarse frequency tuning is accomplished by changing core. The reason for using multiple cores is the limited performance of varactors at 60 GHz, preventing high phase noise performance and tuning range from being achievable with a single core. The inductors are modeled using [4] and have a Q of about 30 at 60 GHz.

The cores output from -7 to -4 dBm, with an average of -5 dBm output power over the frequency range, Fig. 1. The simulated phase noise is -110 dBc/Hz at 3 MHz offset frequency. The core

current consumption is 3.1 mA from a 1.2V supply.

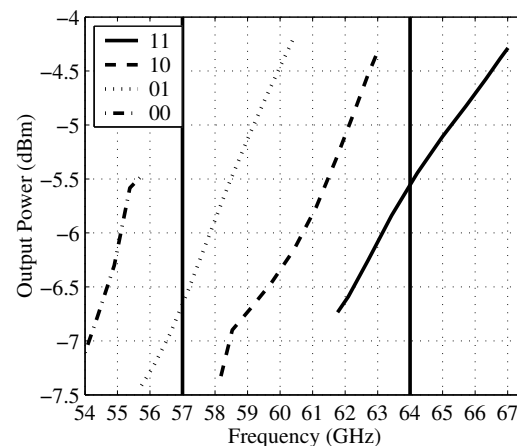


Fig. 1. Output power vs. frequency of the four oscillator cores. The legend shows the two bit control word

III. CONCLUSION

A quad-core 130-nm CMOS oscillator covering the 57-64 GHz frequency band is presented. It outputs -5 dBm and has -110 dBc/Hz phase noise at 3 MHz offset frequency.

REFERENCES

- [1] Federal Communications Commission, *Amendment of Parts 2, 15 and 97 of the Commissions Rules to Permit Use of Radio Frequencies Above 40 GHz for New Radio Applications*, FCC 95-499, ET Docket No. 94-124, RM-8308, Dec. 1995.
- [2] E. R. C. (ERC), *The European Table of Frequency Allocations and Utilisations Covering the Frequency Range 9 kHz TO 275 GHz*, ERC REPORT 25, <http://www.ero.dk/documentation/docs/doc98/official/pdf/ ERCREP025.PDF>, Copenhagen: 2004.
- [3] A. Kral, F. Behbahani, and A. Abidi, "RF-CMOS Oscillator with Switched Tuning," *Custom Integrated Circuits Conference*, pp. 555-557, May 1998.
- [4] N. Troedsson, <http://www.indentro.com>.

Session IV

1030-1210 Thursday 6 March 2008

GaN HEMT Development for Microwave Power Applications - Current Status and Trends -

Masaaki Kuzuhara

Department of Electrical and Electronics Engineering, University of Fukui

3-9-1 Bunkyo, Fukui 910-8507, Japan

Email: kuzuhara@fuee.fukui-u.ac.jp

GaN is a direct semiconductor with a bandgap energy of 3.4eV. Nevertheless it has an excellent high-field drift velocity of over 2×10^7 cm/s. making it suitable for high-voltage and high-frequency applications. Furthermore, GaN has a capability of constructing various heterojunctions for high-frequency operation using a modern epitaxial technology. Thus GaN and related heterojunctions are more flexible to adjust material properties to their specific device applications. For example, a properly designed AlGaIn/GaN HEMT is easy to scale its gate length down to less than 50nm without much sacrificing its breakdown behavior, indicating that ultra-short channel GaN HEMTs are particularly suited for transmitter applications at millimeter-wave frequencies and for post-CMOS n-channel FETs [1].

To achieve outstanding microwave performance, several improvements have been thus far made in the basic device structure, including passivation, epi-layer design, metallization, and field plates. Wu et al. employed a gate field-plate technology to achieve a record output power density of 32.2W/mm operated at 4GHz with a drain bias (V_{dd}) of 120V using an AlGaIn/GaN HEMT fabricated on a SiC substrate [2]. Okamoto et al. reported a record one-chip microwave output power of 230W (CW) at 2GHz with $V_{dd}=53$ V using a GaN HEMT with a gate width (W_g) of 48mm [3]. At C-band (5GHz), a record one-chip output power of 167W was reported with $W_g=24$ mm operated at $V_{dd}=65$ V [4]. As a microwave amplifier, Mitani et al. reported a pulsed output power of 1kW at S-band (3.2GHz) operated at $V_{dd}=80$ V using 4-dies of an internally partial-matched GaN HEMT chip with $W_g=36$ mm fabricated on a SiC substrate [5]. At millimeter-wave frequencies, Murase et al. achieved a record CW output power using a 0.2 μ m recessed-gate GaN HEMT chip with a newly-designed source via-hole structure. The fabricated one-chip FET amplifier with $W_g=6.3$ mm operated at $V_{dd}=25$ V delivered an output power of 20.7W with a linear gain of 5.4dB at 26GHz [6].

At the moment, device-quality heterojunctions other than AlGaIn/GaN are still not easy to prepare because of the difficulty in epitaxial growth. With the development of high-quality bulk nitride substrates, this problem would be considerably solved. One such promising example is the use of InGaIn with high In composition as a channel material. Simulation results for THz operation using an AlInN/InN material system will be presented at the symposium.

References

- [1] Y. Ohno and M. Kuzuhara, IEEE Trans. Electron Devices, vol.48, pp.517-523 (2001).
- [2] Y.-F. Wu et al., IEEE Electron Device Lett., vol.25, pp.117-119, (2004).
- [3] Y. Okamoto et al., IEEE Trans. Microwave Theory Tech., vol.52, pp.2536-2540 (2004).
- [4] K. Yamanaka et al., IEICE Tech. Report, ED2007-210, pp.23-28 (2008) (in Japanese).
- [5] E. Mitani et al., Proc. EuMIC Conf., pp.176-179 (2007).
- [6] Y. Murase et al., IEICE Tech. Report, ED2007-212, pp.33-38 (2008) (in Japanese).

Paving the road for integrated gallium nitride transceivers

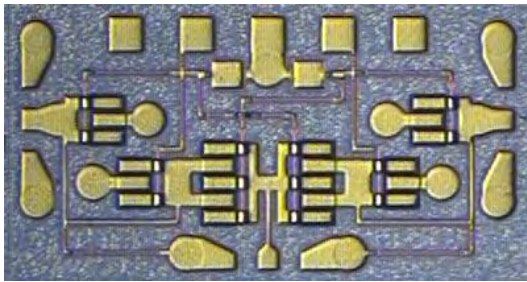
Kristoffer Andersson, Mattias Thorsell, Niklas Billström, Joakim Nilsson*, Jonas Holmkvist*, Ann-Marie Andersson*, Mattias Södow, Martin Fagerlind, Per-Åke Nilsson, Anna Malmros, Hans Hjelmgren, Niklas Rorsman*

GigaHertz Centre, Microwave Electronics Laboratory, Department of Microtechnology and Nanoscience, Chalmers University of Technology, Göteborg, SE-41296, Sweden

** Saab AB (incl. Saab Microwave Systems, Saab Avionics and Saab Bofors Dynamics)*

Gallium nitride is a very attractive material for manufacturing high-frequency microwave transistors. The high saturated electron velocity, high breakdown field combined with the good thermal conductivity of the silicon carbide substrate makes it almost ideal for high-power transistors. The output density of GaN is at least 5 W/mm with reported hero numbers of 40 W/mm at GHz frequencies. Also at millimeter wave frequencies there are reports of power densities of 2 W/mm. Besides the excellent power properties of GaN recent results indicates noise performance close to what was achieved in GaAs a few years ago. Typically F_{min} values of 1 dB at X-band are reported. There are preliminary results showing that GaN HEMTs are capable of withstanding significant input powers; up to 36 dBm. If these results hold, it will be possible to eliminate the input protection circuitry and thus remedy the higher noise figure of GaN. Thus GaN seems to be a very capable candidate for future integrated transceivers for radar/communication and electronic warfare applications. This work reports on the first design steps towards such integrated transceivers.

During the last year several integrated gallium nitride circuits have been fabricated at Chalmers. Below are a SPDT-switch and a resistive feedback amplifier. The SPDT switch is a broadband switch (DC-18 GHz) with an insertion loss less than 3 dB at the high-frequency end. The switch could handle at least 3W of input power. The resistive feedback amplifier provides more than 8 dB of gain in the 1 – 6 GHz frequency band with a noise figure of about 4 dB.



Acknowledgements

This research has been carried out in the GigaHertz Centre in a joint research project financed by Swedish Governmental Agency of Innovation Systems (VINNOVA), Chalmers University of Technology and Saab AB.

Demonstrator of Class-S Power Amplifier

Andrzej Samulak ⁺, Georg Fischer ^{*}, and Robert Weigel ⁺

⁺Lehrstuhl für Technische Elektronik, Friedrich-Alexander-Universität Erlangen-Nürnberg,
91058 Germany, E-mails: {Samulak, Weigel}@lfe.de

^{*}Alcatel-Lucent, Bell Labs Europe, 90411 Nürnberg, Germany,
E-mail: georgfischer@alcatel-lucent.com

Abstract—A realized demonstrator of a Class-S Power Amplifier based on GaN transistors is presented. An input signal is prepared externally in a simulative way (ADS, Matlab) and is based on a 4th order Bandpass Δ - Σ modulator definition. FPGA board is engaged as a signal generator. The demonstrator is based on a Current Switching Class D (CSCD) topology. The presented solution offers an output power of at least 37 dBm. Module efficiency is 20% (30% drain efficiency respectively) for full scale 3GPP Δ - Σ input signal. Center frequency is fixed at 225 MHz, but analyses and measurements require wider bandwidth.

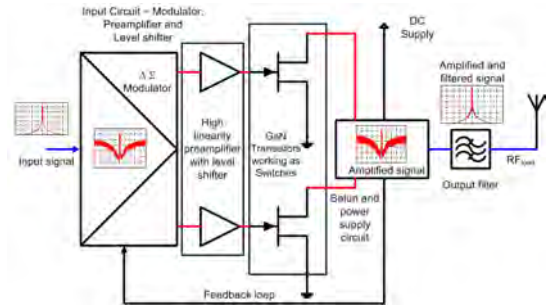


Fig. 1. General idea of Class - S Amplifier.

I. OVERVIEW

Linear classes of amplifiers offer high output power and low distortions, but efficiency is still unsatisfactory. Moreover, high power amplifiers dedicated for base stations occupy more than a half the form factor of a base station cabinet. These main limits and problems make the idea of Switch Mode Power Amplifiers (SMPA) more attractive. The presented Class-S amplifier is based on Current Switching Class D (CSCD) configuration, which despite supply problems, is more attractive with RF demonstrator solutions [1], [2]. A Class-S amplifier consists of 4 main parts. The first part is the Δ - Σ Modulator which converts the RF input signal to a delta sigma modulated "Digital RF" signal. This conversion is necessary, because the transistors operate as switches and a two-state input signal is required. The Δ - Σ Modulator is mainly dedicated to conversion of narrow band signals, but can be as well employed in 3GPP wideband signal conversion. The main problem of bandpass Δ - Σ Modulator is the operation on oversampled signals. The second part of a Class-S PA is the preamplifier with level shifter. The preamplifier provides Δ - Σ Modulated signal in two antiphase bit trains, amplifies to the proper level and shifts them to the appropriate gate voltage swing. The preamplifier's parameters depend on the transistor technology used as switches. The main part of

amplifier are the switching transistors, which are driven by the preamplifier. Devices work in antiphase, when the first one is in "ON" state (conducts current), the second one is in "OFF" state. In practice, active device imperfections limit maximum bandwidth and sampling rate. In addition, reactive parasitics (bond wires, C_{ds} , C_{gs}) and memory effects [3] contribute to the losses at higher frequencies, which decreases total efficiency of the SMPAs. The output signals from the switches are combined and filtered in the last part of the whole circuit. The transistor supply circuit is integrated with the output part of the amplifier. Finally, losses in the output circuit decide on the overall amplifier efficiency. The topology of a Class S amplifier assumes an existing feedback loop from SMPA output to Δ - Σ Modulator input, which assists in adopting modulation parameters to circuit non-idealities and output signal conditions. In addition, this can be seen as some sort of self linearization.

REFERENCES

- [1] Johnson, T.; Stapleton, S.; "Available Load Power in a RF Class D Amplifier with a Sigma-Delta Modulator Driver" *Radio and Wireless Conference*, Sept. 2004 Pages:439 - 442 .
- [2] Kobayashi, H.; Hinrichs, J. M.; "Current-mode class-D power amplifiers for high-efficiency RF applications", *Microwave Theory and Techniques*, IEEE Tran. on Vol. 49, Issue 12, Dec. 2001.
- [3] S. C. Binari, P. B. Klein "Trapping effects in GaN and SiC Microwave FETs", *Proceedings of the IEEE*, Vol. 90, June 2002.

30/20 GHz Balanced Sub-harmonic MMIC Mixer for Space Applications

Dennis Kleén dennis.kleen@space.se, Joakim Thelberg joakim.thelberg@space.se

Saab Space AB, Göteborg, Sweden

Summary: A sub-harmonic MMIC mixer with an integrated pre-amplifier has been developed. The RF input frequency range is 27-31 GHz and the IF output frequency range is 18-21 GHz. Due to the sub-harmonic mixing the LO frequency is in the range of 4.3-5.8 GHz. The mixer shows a conversion gain of 3 dB with a noise figure of 4.2 dB. The mixer is based on a zero bias diode implemented in an E-mode technology. The circuits were fabricated in the OMMIC ED02AH process.

I. Introduction

The telecommunication market in general is experiencing a rapidly increasing demand for broadband connections and interactive services. These services may include HDTV, interactive multimedia services, internet access etc. There is therefore a need for new components and MMICs for these Ka-band systems.

II. Pre-Amplifier

The pre-amplifier was designed to cover 27-31 GHz, realised as a two-stage design, based on a 6x25 μm and a 6x50 μm FET. The input stage utilizes an inductive series feed back in order to achieve a good input match as well as low noise figure. The amplifier also contains a voltage controlled 3 dB attenuator at the output. The overall maximum gain is 15 dB with a noise figure of 3.2 dB and an output third order intercept point of >20 dBm.

III. Mixer Core

The balanced sub-harmonic mixer was designed for an RF input frequency of 27-31 GHz and an IF output frequency of 18-21 GHz. The LO frequency range was 4.3-5.8 GHz. The mixer core is based on eight 4x60 μm zero bias diodes realised in an e-mode FET technology. For sub-harmonic mixing the diodes are connected as anti-parallel pairs, with two diodes in each pair for improved linearity. The LO is applied in anti-phase to each of the pair by a spiral Marchand balun. The termination of the LO harmonics is crucial for high IP3 performance. The RF signal is applied and the IF signal extracted via a distributed diplexer connected to the common point of the anti-parallel diode pairs. Typical conversion loss for the mixer core is 10 dB. The 4LO-to-IF isolation was 75 dBc.

IV. Results

The multi-function chip with the pre-amplifier and mixer core combined, showed a conversion gain of +3 dB with a noise figure of 4.2 dB. The 4LO-to-IF isolation was measured to 75 dBc. Chip size is 2.5x5 mm², shown in figure 1.

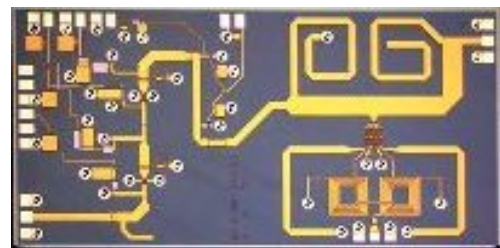


Figure 1 MMIC Chip

V. Conclusion

A balanced sub-harmonic mixer with an integrated pre-amplifier has been described. Demonstrated performance is good and makes it an interesting candidate for future broadband space applications.

References

- [1] Andreas Ådahl, Herbert Zirath, "A Reliable Ka-Band Sub-harmonic Mixer for Satellite Converters", Compound Semiconductor IC Symposium 2006
- [2] Paul Blount & Charles Trantanella, "A high IP3, Subharmonically Pumped Mixer for LMDS Applications", IEEE GaAs IC Symposium 2000
- [3] C.A. Zelle, A.R. Barnes and R.W. Ashcroft, "A 60 GHz double balanced sub-harmonic mixer MMIC", Gallium Arsenide Applications Symposium. Gaas 2001
- [4] M van der Merwe, JB de Swardt, "The Design and Evaluation of a Harmonic Mixer Using an Anti-Parallel Diode Pair"

ABSTRACT

ALMA, the Atacama Large Millimeter/ submillimeter Array, will be a single research instrument composed of 50 (or more) high-precision antennas, located on the Chajnantor plain of the Chilean Andes in the District of San Pedro de Atacama, 5000 m above sea level. ALMA will operate at wavelengths of 0.3 to 9.6 millimetres, where the Earth's atmosphere above a high, dry site is largely transparent, and will provide astronomers unprecedented sensitivity and resolution. The 50 antennas of the 12 m Array will have reconfigurable baselines ranging from 150 m to 18 km forming a big interferometer.



The water vapour radiometer is a support equipment used to compensate for the differences in phase due to different amount of water vapour in the atmosphere above each antenna. Other interferometers have been built without this compensation, but the availability of the instruments has then been very low.

The water vapour radiometer is measuring the energy on one of the spectral lines of water, 183.31GHz (1.6 mm). Since the measured signal is very weak, the measurement is calibrated by alternately measure on well defined hot or cold loads, so called Dicke-Switch radiometer. The overall accuracy of the WVR is 2K brightness temperature over the range from 50K to 370K To be able to reach this accuracy, the front end and parts of the back end is temperature controlled to better than 0.1K.

Omnisys will build up to 58 radiometers, including spares and option of 5 extra. The expected lifetime will be at least 15 years. This implies that high effort must be taken to design in a way that makes the WVR cost effective by means of MAIT.

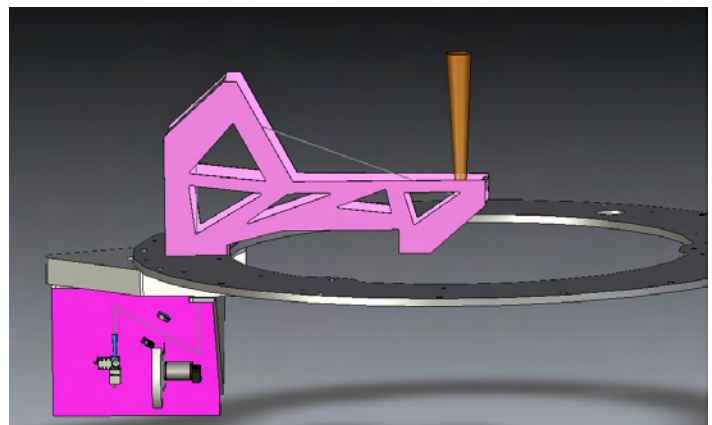
Subsystems of the WVR:

Quasi optics, one flat mirror and three active mirrors, chopper wheel with mirrors for hot and cold loads.

Front End, corrugated horn antenna, low noise (NF=7.5 dB) integrated schottky mixer and LNA (30 dB), local oscillator system based on a DDS controlled 15 GHz VCO and active multiplier chain.

Back End, four channel filter bank with diode detectors and 50 dB of distributed stable amplification.

Control and power, thermal control, motor control, computing and communication.



European Radio & Microwave Interest Group - EuRaMIG
An initiative from GigaHertz Centre
Status and coming activities

Peter Olanders, Ericsson AB, Steering Board Chairman GigaHertz Centre
peter.oland@ericsson.com

Jan Grahn, Chalmers University of Technology, Director, GigaHertz Centre
jan.grahn@chalmers.se

The European industry depending upon RF/microwave technologies is scattered. As a result, it has been difficult to gather and coordinate European microwave stakeholders for creating impact on the formulation of European Framework Programs. In order to meet this challenge, GigaHertz Centre took the initiative to organise a meeting in Brussels on 10 January 2008 between representatives for the European Commission, a broad range of European industrial stakeholders, institutes and universities active in the RF/microwave field. The meeting resulted in the formation of European Radio & Microwave Interest Group (EuRaMIG). This is an industrial-academic-public network open to anyone who wants to contribute and support the development of European RF/microwave technologies. All viewgraphs from the meeting in Brussels including comments and current status can be found on www.chalmers.se/ghz

EuRaMIG is setting up working groups among European stakeholders to describe the future of European microwave industry and its position and impact on European growth, and the necessary research priorities and academic education to be carried out. The vision is a Europe taking the global lead in RF/microwave. The output from the EuRaMIG working groups will be addressed to the European Commission.

In GigaHertz Centre, Chalmers University of Technology and seven companies (Ericsson, Infineon Technologies, Saab, NXP Semiconductors, Sivers IMA, Omnisys Instruments, Comheat Microwave) conduct joint research and innovation in microwave power (RF amplifiers and GaN circuits), system-on-chip mm-wave solutions and low phase-noise circuit based oscillators. The research is partly supported by the Swedish Governmental Agency for Innovation Systems (VINNOVA) in the VINN Excellence program. Web page: www.chalmers.se/ghz

Workshop

Antennas

1300-1430 Thursday 6 March 2008

Integrated Antennas for RF MEMS Routers

A. Rydberg[#], S. Cheng[#], Paul Hallbjörner*, S. Ogden**, and K. Hjort**

[#] Signals and Systems Group and **Microsystems Group, Department of Engineering Sciences, Uppsala University. *SP Technical Research Institute of Sweden, Borås, Sweden
anders.rydberg@angstrom.uu.se

Summary:

Three antenna designs for flip-chip bonding with RF MEMS based switching routers at 20 GHz will be presented. The prototypes are fabricated on 100 μm thick Pyralux AP polyimide flexible laminates [1]. Measured results show very good agreements with the full wave simulations.

Introduction:

A microwave router based on RF MEMS switching is a novel application driven component for wireless communications (e.g. in microwave links or sensor networks). Integrating MEMS switches and transmission lines on a single router chip will enable a cost-effective and higher level of integration to be achieved.

A dipole, uniplanar Yagi antenna and four element Yagi antenna array are investigated in this report. As shown in Fig. 1, the dipole is placed in front of a ground plane which represents the effects of the RF MEMS router on the antenna performance and acts as a reflector. The uniplanar Yagi antenna is proposed to achieve higher gain and better front-to-back ratio than the dipole. Both the dipole and the uniplanar Yagi antenna are designed for 50 Ω differential feed. A 1:1 balun transformer on the same substrate as the RF MEMS router is required in order to match each antenna to a 50 Ω CPW of the router.

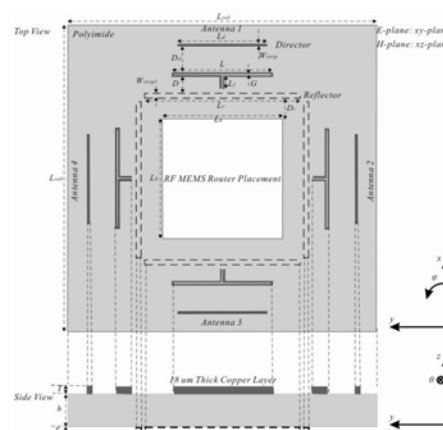


Fig. 1. Geometries of the four element Yagi antenna array: $L_{\text{sub}}=18 \text{ mm}$, $L_h=7 \text{ mm}$, $L=5.9 \text{ mm}$, $L_d=5.2 \text{ mm}$, $L_r=9 \text{ mm}$, $L_f=0.73 \text{ mm}$, $D=0.98 \text{ mm}$, $D_d=1.55 \text{ mm}$, $D_r=1.25 \text{ mm}$, $G=50 \text{ um}$, $W_{\text{strip}}=100 \text{ um}$, $T=18 \text{ um}$ and $h=100 \text{ um}$.

Results:

The antennas are well matched to the desired input impedance at the operation frequency. The presented dipole and uniplanar Yagi antenna feature about 10 % 10 dB return loss bandwidth at 20 GHz. The maximum gain of 3.8, 4.8 and 6.8 dBi is achieved, respectively. Moreover, good front-to-back ratio and appropriate beam coverage of all the antennas are observed.

Conclusion:

This report presents three antenna designs for flip-chip bonding with RF MEMS switching routers at 20 GHz. The antennas are good candidates for electrically steerable antenna arrays.

References:

1. Shi Cheng, Erik Öjefors, Paul Hallbjörner, Sam Ogden, Joakim Margell, Klas Hjort, Anders Rydberg, "Body Surface Backed Flexible Antennas for 17 GHz Wireless Body Area Networks Sensor Applications," published in the 10th European Conference on Wireless Technology, Oct. 2007.

Microstrip patch antennas for wireless applications

Naima Amar Touhami, Beatriz Aja, Antonio Tazón, Eduardo Artal
(naima@dicom.unican.es)

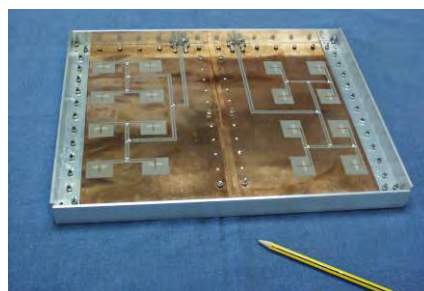
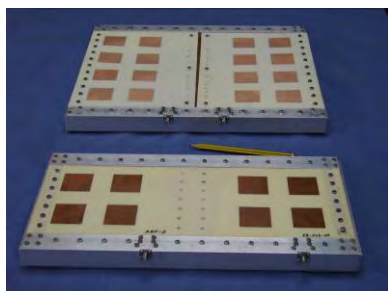
Departamento de Ingeniería de Comunicaciones. ETSIIT. Avenida de los Castros, s.n.
Universidad de Cantabria. Santander (Spain)

Summary

A 3.5 GHz planar antenna system has been developed for wireless applications [1]. The antenna structure is based on microstrip patch arrays [2]. Each patch is excited by a slot antenna coupled to a microstrip line. The antenna system has two arrays, one for the transmitter the other for the receiver, and meets the high isolation required between both. Antenna manufacturing is based in the combination of different substrates for microstrip lines and radiation elements.

Introduction

Planar antennas are well suited for wireless applications when space saving and compact terminals is a must. For short and medium range applications at 3.5 GHz the antenna gain requirements are about 14 dB. To achieve these gain values an array of printed patch radiators was designed, simulated with an Electro-Magnetic software tool and experimentally tested. Next Figure shows two pictures, first one with two antenna prototypes (four or eight patches), the second one shows the bottom side with microstrip power dividers and slot excitation (eight patches version).



Results

Different versions of such array antennas have been used to compare their performances according to the dielectric substrates used and their mechanical arrangement. Typical achieved values in a 3.5% bandwidth centred at 3.52 GHz are: input return losses better than 12 dB, isolation between coaxial ports better than 60 dB and antenna gain around 14 dB.

Conclusion

Planar antennas based on microstrip patches are well suited for wireless terminals working at 3.5 GHz. It is possible the operation of a complete transceiver with separate antennas given the high isolation achieved between them.

References

- [1] Satish K. Sharma and L. Shafai "Performance of a Microstrip Planar Array Antenna at Millimeter Wave Frequencies Using a Series Parallel Feed Network" IEEE Antennas and Propagation Society International Symposium, 2001, vol.3, pp. 594-597
- [2] L. Cabria, J. A. García, A. Tazón, J. Vassal'lo, "Active reflectarray with beamsteering capabilities", Microwave and Optical Technology Letters, 2005, Vol. 48 , pp. 101 - 105

Small Microstrip Fractal Antenna for RFID tag

P. Enoksson¹, M. Rusu^{1,2}, A. Curutiu^{1,3}, H. Rahimi¹, C. Rusu⁴

¹Chalmers University of Technology, Micro and Nanosystems group, Göteborg, Sweden

²Faculty of Physics, Bucharest University, Bucharest-Magurele, Romania, mvrusu@yahoo.com

³Bonn University, Bonn, Germany

⁴Imego AB, Göteborg, Sweden

Feasibility study of using fractal-based multi-band antenna for RFID tag is presented. The requirements are: one antenna layout for two bands (868MHz, 2.45GHz), small size (3x3cm), and reading distance of at least 10cm and 30cm for 868MHz and 2.45GHz, respectively. The simulations show that fractal antenna can be useful for RFID tags.

The RFID antenna requirements are at the limit of conventional antenna [1], so we propose to use fractal-shape antenna. Fractals have long perimeter packed in a small area and an intricate (tortuous) structure allowing for many possible bands of resonances which are not necessarily harmonics [2]. This type of antenna has gained interest only in the last decade [3-5].

A number of fractal curves have been simulated by ADS Momentum (Agilent Technologies) and Minkowski is the most promising one (Figure 1).

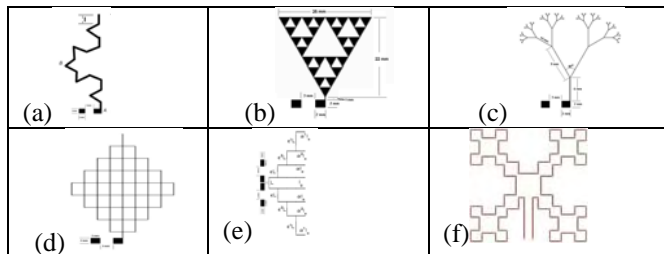


Figure 1. The six fractal shapes tested for antenna layout: (a)Koch, (b)Sierpinski, (c)'tree', (d)'cuboid', (e)'log-periodic', (f)Minkowski

Design a small antenna (physical length \ll wavelength of operation) satisfying simultaneously all the requirements asks for a compromise among parameters such as different resonance frequencies with reasonable high $|S_{11}|$ values, desired impedance and the highest possible antenna efficiency. Statistical correlation between S_{11} and the resonance frequency (Figure 2) for our Minkowski-based fractal antenna shows that the desired requirements could be obtained.

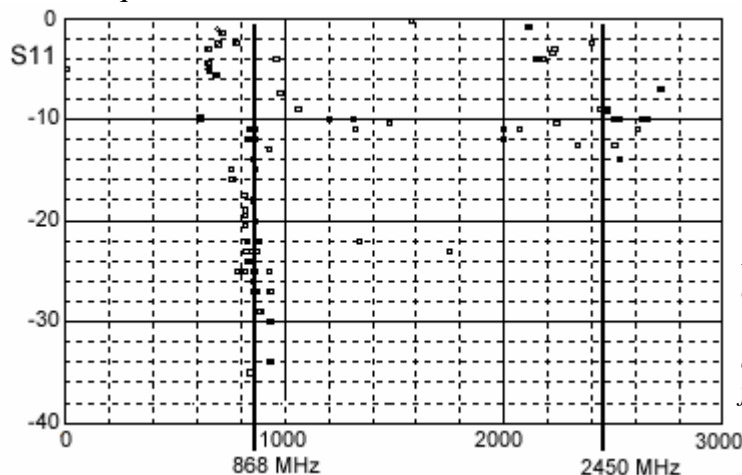


Figure 2. Statistical correlation between S_{11} and resonance frequency for simulated Minkowski-based fractal antenna.

References:

1. Wheeler H., Small Antennas, *IEEE Transactions on Antennas and Propagation*, **23**(4), 1975.
2. Cohen N., Fractal and Shaped Dipoles, *Communications Quarterly*, p.25-36, Spring 1996.
3. Puente C., "Fractal Antennas", Ph.D. Dissertation at the Dept. of Signal Theory and Communications, Universitat Politècnica de Catalunya, June 1997.
4. M. Rusu, R. Baican, Adam Opel AG, Patent 01P09679, "Antenne mit einer fraktalen Struktur", die auf der Erfindungsmeldung 01M-4890 "Fractal Antenna for Automotive Applications" basiert, 18 Okt. 2001.
5. Rahimi H., Rusu M., Enoksson P, Sandström D., Rusu C., Small Patch Antenna Based on Fractal Design for Wireless Sensors, *MME07, 18th Workshop on Micromachining, Micromechanics, and Microsystems*, 16-18 Sept. 2007, Portugal.

Dual-band choke horn Eleven Feed

Adeel Yasin¹, Jian Yang¹, Tomas Östling²
¹Chalmers University of Technology, ² Arkivator AB
E-mail: yasin@student.chalmers.se

Short Summary

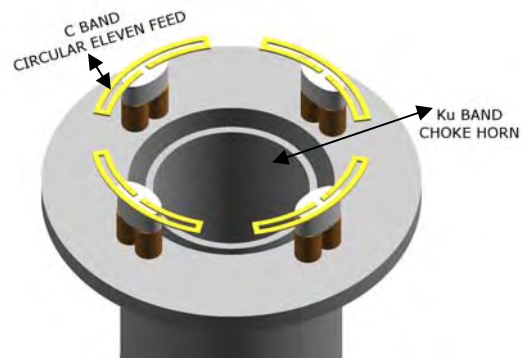
The aim of this research is to propose a compact solution of combining Eleven antenna and choke horn as a feed for dual band reflector antenna. A novel circular geometry of Eleven antenna has been investigated for improving system performance. The combined solution is a low-cost, low-profile wide-band solution for satellite terminals. The simulated and measured performance of the prototype is presented in the paper.

Introduction

Multiband antennas are of interest for many applications, for example, in satellite communications. Some of the benefits are simultaneous operation at several frequency bands, independent tracking control and different polarization schemes. In this research, frequency bands of interest are C and Ku bands for satellite communication applications. Analysis studies have been done for best performance of combined feed parameters. The novel circular geometry of Eleven feed (Fig.1) has better BOR₁ efficiency as compared to conventional linear Eleven feed configuration [1]. Choke horn [3] design has been modified to adjust circular Eleven feed for required operational bands (Fig.1). The combined feed has been characterized in terms of aperture efficiency of reflector and coupling efficiency due to mutual coupling between the two feeds. The mono-pulse tracking capability has also been verified for multi-port model of circular Eleven feed.

Results

Frequency Bands: [5.5-6.5, 10.5-14.5]GHz
Directivity ~10dBi
Peak XP sidelobe Level < -15dB
Aperture Efficiency > -2.5dB @ 50°
Coupling Efficiency > -0.5dB
Input Reflection co-efficient < -10dB



Conclusions

1. Dual-band and dual polarized.
2. Wideband with capabilities for tri-bands as (C/Ku/Ka)

Fig1. Dual Band choke horn Eleven feed

References

- [1] R. Olsson, P.-S. Kildal and S. Weinreb, "The Eleven antenna: a compact low-profile decade bandwidth dual polarized feed for reflector antennas," IEEE Trans. Antennas Propag., vol. 54, No. 2, Feb. 2006.
- [2] P.-S. Kildal, R. Olsson and Jian Yang, "Development of three models of the Eleven antenna: a new decade bandwidth high performance feed for reflectors," Proceedings of EuCAP 2006, Nice, November 2006.
- [3] Z. Ying, P.-S. Kildal, and A. Kishk, "A broadband compact horn feed for prime-focus reflectors", Electronics Letters, vol. 31, 14, pp.1114,1115, 6th July, 1995.

OPTIMIZATION OF 200-800MHZ ELEVEN FEED FOR USE IN REFLECTOR ANTENNAS OF GMRT

*Y.B. Karandikar**, *P.S. Kildal*[†]

**PhD student, Chalmers Univ. of Technology, Sweden*

†Prof., Chalmers Univ. of Technology, Sweden.

yagesh@student.chalmers.se

per-simon.kildal@chalmers.se

This paper discusses in brief the electrical design of the Eleven Feed for the parabolic reflector antennas of Giant Meterwave Radio Telescope (GMRT-India) optimized for 200 to 800 MHz bandwidth. Paper also gives the comparison between the simulated and measured antenna input reflection coefficient and radiation patterns. The measured S11 of the feed is less than -8dB and the computed total efficiency including the mismatch losses, is better than -3dB over desired bandwidth for the reflector antennas of GMRT having 62.5° of half subtended angle.

The S11 of the current design shows 2-3dB improvement as compared to previous designs of Eleven Feed [1][2][3]. To achieve this, efforts are taken to first understand conventional log-periodic arrays of folded dipoles defined by set of optimization parameters like scaling constants, spacing constants, folded dipole lengths, wire diameters etc. This understanding is then further extended to match folded dipole log-periodic arrays made up of metal plate of constant thickness to 200ohm in free space. Different matching techniques like shorting stub on longest dipole, truncation of array by shortening the lengths of first and last folded dipole, are applied to get simulated S11<-10dB. Finally the folded dipole log-periodic arrays made up of plates designed in free space are used in Eleven Feed configuration and designed is further optimized to get simulated S11<-10dB for Eleven Feed.

The difference between the measured and simulated S11 is due to mechanical tolerances in the manufacturing process. And reason of low aperture efficiency is the deep dish of GMRT having 62.5° of half subtended angle where the pattern of the Eleven Feed is more suitable for half subtended angles of 50-55°. This means the GMRT reflector is somewhat under illuminated.



Figure 1: Manufactured Eleven Feed

- [1] R. Olsson., P. S. Kildal, S. Weinreb. "A novel low profile log-periodic ultra wideband feed for dual reflector antenna of US-SKA", *IEEE Symposium Antennas & Propagation*, pp. 3035-3038, (2004).
- [2] R. Olsson., P. S. Kildal, S. Weinreb. "Measurements of a 1 to 13 GHz lab model of dual polarized low profile log-periodic feed for US-SKA", *IEEE Symposium. Antennas & Propagation*, pp. 700-703, (2005).
- [3] R. Olsson., P. S. Kildal, S. Weinreb. "The Eleven Antenna: A compact low profile decade bandwidth dual polarized feed for reflector antennas", *IEEE Trans. Antennas & Propagation*, volume 54, pp. 368-375, (2006).

METHOD FOR CIRCUIT BASED OPTIMIZATIONS OF RADIATION CHARACTERISTICS OF MULTI-PORT ANTENNAS

Kristian Karlsson^(I) Jan Carlsson^{(I)(II)}

^(I) Email: {kristian.karlsson, jan.carlsson}@sp.se ^(II) Chalmers University of Technology
SP Technical Research Institute of Sweden 412 96 Gothenburg, Sweden
501 15 Borås, Sweden

Summary This contribution presents a method for using data from full-wave EM simulations in combination with a circuit simulator to simplify antenna integration and antenna parameter evaluation.

Introduction Today's compact multi functioning mobile terminals offers complex problems to the antenna and system engineer. Several antennas have to be located within a limited space and will of course couple to each other as well as to other units within the terminal (EMC problems). The presented method [1,2] can be applied on multi-port antennas including arbitrary circuits and feeding networks connected to their ports. Studies can be performed on far field antenna parameters (e.g. efficiency, diversity gain, and correlation) as well as near field properties (EMC, SAR). The contribution also describes how the method is used in combination with a global optimization scheme.

Result The method is implemented in a software named MPA (Multi Port Antenna evaluator) which can compute antenna parameters such as: total radiated power, radiation efficiency, total radiation efficiency, radiation pattern, near field, user defined transfer functions (mutual coupling, isolation, impedance), correlation and apparent diversity gain. The MPA software handles input data from several commercial full-wave EM simulators (CST, EMDS, MicroStripes and IE3D) and has been used in several studies concerning diversity antennas and EMC characteristics.

Conclusion A method for computation of radiation patterns and near fields using full-wave EM simulator data in combination with a circuit simulator is described. The method will help to reduce the number of full wave simulations needed during the integration process of e.g. a multi port antenna in a terminal. It can also be used in combination with a global optimization scheme to improve e.g. radiation efficiency, diversity gain or near field characteristics.

Acknowledgement This research has been carried out in the Chase VINN Excellence Centre at Chalmers.

References

- [1] K. Karlsson, J. Carlsson, I. Belov, G. Nilsson and P.-S. Kildal, "Optimization of antenna diversity gain by combining full-wave and circuit simulations", Proceedings of EuCAP 2007, UK, 11-16 Nov. 2007, MoPA.36.
- [2] D.F. Kelley, "Embedded element patterns and mutual impedance matrices in the terminated phased array environment", Proceedings of IEEE AP-S International Symposium, USA, 3-8 July 2005, vol. 3A, pp. 659-662.

Circular Monopole and Dipole Antennas for UWB Radio Utilizing a Flex-rigid Structure

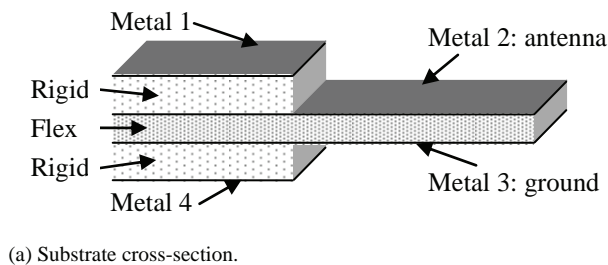
Magnus Karlsson, and Shaofang Gong, *Member, IEEE*

Department of Science and Technology, Linköping University, SE-601 74 Norrköping, Sweden

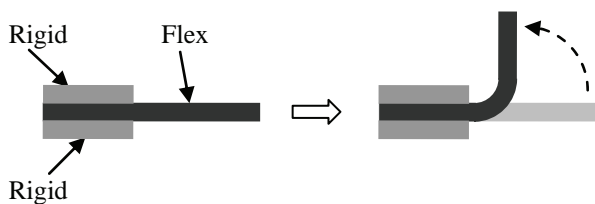
Phone: +46 11 363491, E-mail: magka@itn.liu.se

The general focus during the era of UWB antenna development has so far been on the antenna element but not so much on how the antenna can be integrated and used in a UWB system. In this paper the concept of utilizing a flexible and rigid (flex-rigid) substrate is presented. Using this flex-rigid concept the antenna is made on the flexible part of the flex-rigid structure, and other circuits, e.g., a balun can be integrated in the rigid part.

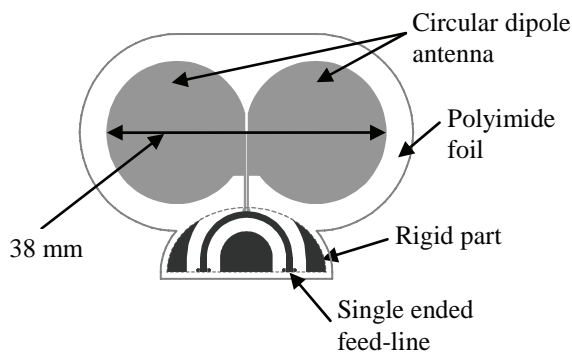
Figs. 1a and 1b show the substrate structure in which two dual-layer NH9326 laminates are bonded together with a polyimide-based flexible substrate. Fig. 1c shows a circular dipole antenna integrated in the flex-rigid substrate. The balun (in the rigid part) utilizes broadside-coupled microstrips.



(a) Substrate cross-section.



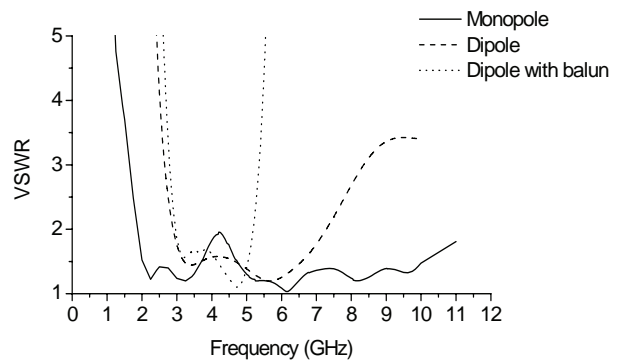
(b) Bendable property.



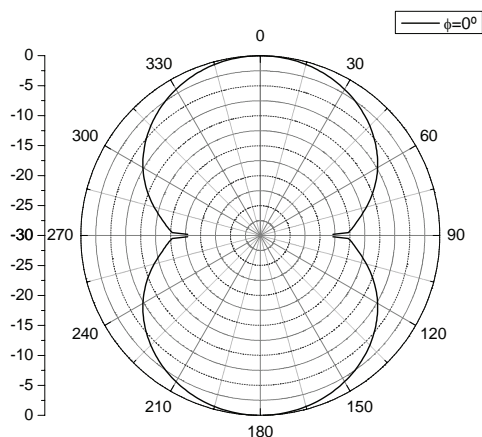
(c) Circular dipole antenna.

Fig. 1. Antenna design: (a) detailed cross-section, (b) bendable property, and (c) circular dipole antenna.

Fig. 2a shows voltage standing wave ratio (VSWR) simulation of a circular monopole, and a dipole antenna on the flex-rigid substrate. It is seen that the designed circular monopole antenna has a wide impedance bandwidth using the proposed flex-rigid structure. It covers the entire UWB frequency band 3.1-10.6 GHz at $VSWR < 2$. Moreover, Fig. 2a shows also VSWR simulation of the dipole antennas. It is seen that the circular dipole antenna has a wide impedance bandwidth using the suggested flex-rigid structure and the balun is the component limiting the bandwidth. More precisely, the circular dipole antenna implemented using the flex-rigid substrate can cover the Mode 1 UWB frequency-bandwidth (3.1-4.8) at $VSWR < 1.54$ without a balun and $VSWR < 1.68$ with a balun. The circular dipole antenna radiation simulation shown in Fig. 2b indicates that the antenna has a typical dipole-antenna radiation pattern.



(a) VSWR simulation.



(b) Normalized E_0 radiation pattern at 3.960 GHz, $\phi=0^\circ$.

Fig. 2. Simulation of the monopole and dipole antennas: (a) VSWR simulation, and (b) normalized radiation pattern.

Design, Manufacture and Test of Eleven Feed for 1-13 GHz

Jian Yang, Ingmar Karlson, Xiaoming Chen and Per-Simon Kildal
Department of Signals and Systems
Chalmers University of Technology
S-412 96 Gothenburg, Sweden
E-mail: jian.yang@chalmers.se

Short Summary: A simple one-by-one parameter optimization scheme has been applied to design the Eleven feed for 1-13GHz. The dipoles have been printed on a thin dielectric film printed circuit board (PCB) technology is used to manufacture the Eleven feed (Fig.1). A new method of combining several commercial software tools (WILP-D – CST – ADS) has also been investigated in order to more efficiently compute the performance of the Eleven feed with the center puck included.

Introduction: Wide frequency band systems are required for many applications, such as in radio astronomy and ultra-wideband (UWB) technology. Chalmers University of Technology has during the last years been developing a new ultra wideband antenna – the Eleven antenna. It has very good features such as nearly constant beamwidth, 10-11 dBi directivity and almost fixed phase centre location over the whole bandwidth, low profile and simple geometry. The Eleven antenna is very suitable for use as a feed in reflector antennas. Previously, we have reported three Eleven feeds designed for use in different radio telescopes; Green Bank, GMRT and RATAN. The purpose of the present project is to report the development of an Eleven feed for 1 – 13 GHz. One critical performance of a feed for a reflector antenna used in radio telescope is impedance mismatch, because strong reflection at the antenna input port will increase the system noise level. Previously, a measured reflection coefficient of -8 dB up to 3 GHz was reported, whereas attempts to make feeds at higher frequencies were unsuccessful so far due to problems in manufacturing the small dipoles at the higher part of the frequency range. A new 1-13 GHz Eleven feed has been designed by using a one-parameter at the time optimization technique, manufactured and tested. The present paper reports the results of the testing and compares with simulations.

Results: The measured reflection coefficient of the Feed is below -10 dB from 1 – 8GHz (agreed with calculation) and -5dB up to 13 GHz due to the effect of the center puck. A new method of accounting for the center puck in the design has been developed, based on using different software tools for the center puck and the dipole panels and combining the results. With the new method we show that we are able to predict the effect of the center puck. The effect of the crossing of the feed lines of the two polarizations at center puck has been investigated and shown to be essential for a successful design.

Conclusion: The reported design and manufacture method have improved the performance of the Eleven feed up to 8GHz. The effects of overlapping and center puck have been investigated numerically, and new solutions based on this work are proposed and will certainly cause further improvements and enable Eleven feeds at even higher frequencies.

References:

- [1] R. Olsson, P.-S. Kildal and S. Weinreb, “The Eleven antenna: a compact low-profile decade bandwidth dual polarized feed for reflector antennas,” *IEEE Trans. Antennas Propas.*, vol. 54, No. 2, Feb. 2006.
- P.-S. Kildal, R. Olsson and Jian Yang, “Development of three models of the Eleven antenna: a new decade bandwidth high performance feed for reflectors,” *Proceedings of EuCAP 2006*, Nice, November 2006.

Workshop

RF Power Amplifiers (2)

1300-1430 Thursday 6 March 2008

Output Power Density and Breakdown Voltage in Field-Plated Buried Gate Microwave SiC MESFETs

P.Å. Nilsson, F. Allerstam, K. Andersson, M. Fagerlind, H. Hjelmgren, A. Malmros, M. Südow, E. Ö. Sveinbjörnsson, H. Zirath, and N. Rorsman.

Microwave Electronics Laboratory, Microtechnology and Nanoscience, Chalmers University of Technology, SE-412 96 Goteborg, Sweden. per-ake.nilsson@mc2.chalmers.se

Silicon Carbide MESFETs, with field plates, were simulated, fabricated, and characterized. Using filed plates, it was possible to reach a breakdown voltage for a microwave power device of 170 V, and an output power density at 3 GHz of 8W / mm.

MESFETs made of Silicon Carbide (SiC) have long been a good candidate for microwave power applications, and are now commercially available. Their suitability for radar and communication applications is due to the high thermal conductivity, the high breakdown field, and the high saturation velocity of SiC.

The maximum output power of the devices depends on the drain voltage. The drain voltage can be increased by increasing the breakdown voltage of the device. In this work, we study the effect of field plates on the breakdown voltage of SiC MESFETs.

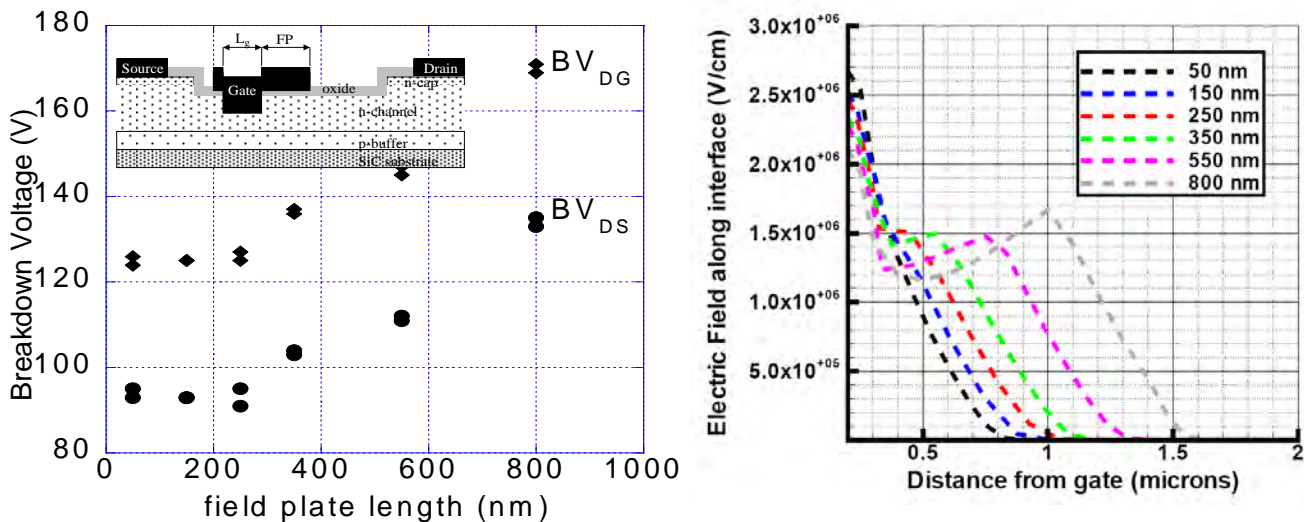


Fig. 1.: Measured breakdown voltage vs. field plate length (left) and simulated electric field in the device close to breakdown (right). The inset shows the device cross section.

The devices made for this study were field-plated buried gate MESFETs [1] made at Chalmers University. The field plate overlap was varied from 50 nm to 800 nm. A clear increase of breakdown voltage was seen for longer field plates (fig. 1.) This is in accordance with physical simulations. The output power at 3 GHz was measured for the devices and values up to 8 W/mm were achieved.

We have shown that the use of field plates is a useful way to increase the breakdown voltage, and thus the output power, of silicon carbide MESFETs.

This research has been carried out in the Microwave Wide Bandgap Technology project financed by Swedish Governmental Agency of Innovation Systems (VINNOVA), Swedish Energy Agency (STEM) Chalmers University of Technology, and Ericsson AB, Saab AB, Norstel AB, Infineon, NXP, Furuno, and Norse Semiconductor Laboratories AB.

References

[1] K. Andersson, M. Sudow, P. A. Nilsson, E. Sveinbjörnsson, H. Hjelmgren, J. Nilsson, J. Stahl, H. Zirath, and N. Rorsman, IEEE Electron Dev. Lett. **27**, 573, (2006).

Silicon-on-SiC hybrid substrate with low RF-losses and improved thermal performance

J. Olsson, Ö. Vallin, D. Martin, L. Vestling, U. Smith, and H. Norström*

Uppsala University, The Ångström Laboratory, Solid State Electronics, P. O. Box 534, SE-751 21 Uppsala, Sweden
*permanent address: Infineon Technologies AB, SE-164 81 Kista, Sweden
Email: jorgen.olsson@angstrom.uu.se, Tel: +46(0)18 471 3035

1. Abstract

A novel SOI hybrid substrate ("BaSiC") consisting of silicon-on-silicon carbide is presented. Compared to ordinary SOI-material, MOS transistors on the BaSiC substrate show no self-heating and RF-measurements up to 30 GHz show more than a factor of ten lower substrate losses.

2. Introduction

SOI-technology in general offers advantages at high-frequencies compared to ordinary silicon technology [1]. However, the low thermal conductivity of the buried silicon dioxide insulator may cause self-heating of devices and reduced performance. A new Si-on-SiC hybrid substrate for high performance SOI was recently presented and it addresses this problem [2]. The hybrid substrate uses polysilicon as an intermediate layer, see Fig. 1, thereby avoiding the thermally unfavorable SiO₂ [3]. Previous efforts to improve the SOI thermal properties include replacing the buried SiO₂ insulator by diamond [4], AlN [5], or Al₂O₃ [6].

3. Results

Manufactured MOSFET devices on BaSiC show well behaved subthreshold and I_d - V_d characteristics without any self-heating effects, whereas the SOI reference devices show self-heating. The effective thermal resistance of the different substrates was measured using heating resistors. A factor of two lower effective thermal resistance is observed for BaSiC compared to SOI, which is in good agreement with results for similar substrates [3]. As to RF performance, Fig. 2 illustrates the relative resistive substrate losses. The equivalent parallel resistance, measured on an open-pad structure for a wide frequency range

up to 30 GHz, is significantly higher for BaSiC compared to the reference substrates.

4. Conclusions

A recently presented Si-on-SiC hybrid substrate, called BaSiC, has been investigated. The high thermal conductivity of SiC results in an effective thermal resistance about a factor of two lower than the SOI reference. Due to the semi-insulating properties of the SiC, the BaSiC substrate has very low losses at high frequency as compared to SOI-substrates.

References

- [1] F. Gianesello et al. IEEE SOI Conf. p. 119, 2007
- [2] J. Olsson et al. IEEE SOI Conf. p. 115, 2007
- [3] S. Whipple et al. MRS Proc. v.911, p.383, 2006
- [4] B. Edholm et al. IEEE SOI Conf., p. 30,1997
- [5] D. M. Martin et al. EUROSIOI, p. 67, 2007
- [6] C. de Beaumont et al. EUROSIOI, p. 123, 2006

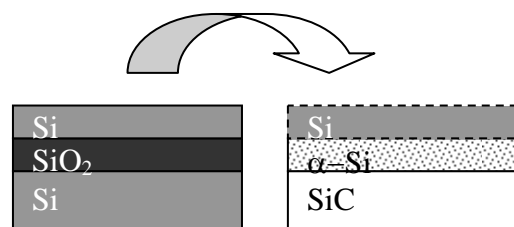


Fig.1: Bonding process of the BaSiC hybrid wafer.

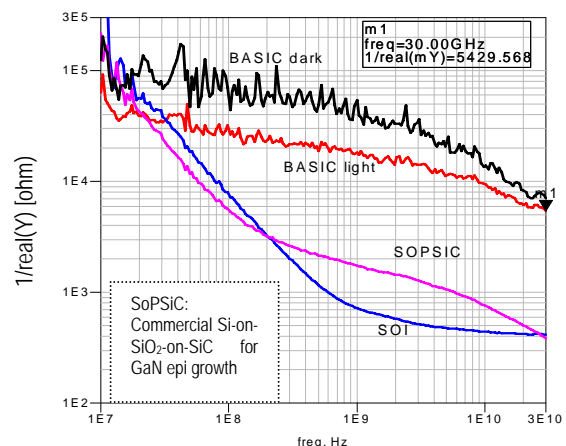


Fig.2: NVA measurements of the substrate losses

A review of validation criteria for behavioral power amplifier models

P. Landin and M. Isaksson

University of Gävle, Dept. of Electronics, SE-80176 Gävle, Sweden.
email: min@hig.se

Abstract

The radio frequency power amplifier is still one of the most interesting components in a telecommunication system; its power consumption dominates the other parts in the system. The purpose of the radio frequency power amplifier is to amplify the radio signal to a necessary power level for transmission to the receiver. The transmission is performed through the air. It is important to handle the power amplifier's conflicting behaviors of efficiency and linearity in this process. The design of linear and efficient radio frequency power amplifiers in modern radio telecommunication systems has been described in the literature as one of the most challenging design problems.

One of the most promising techniques to overcome the interference problem due to the nonlinear behavior of the power amplifier is the technique of digital predistortion. In order to work, digital predistortion requires knowledge of the nonlinear characteristics of the amplifier since it, in principle, applies the inverse of the raw amplifier to the signal prior to amplification. Accurate nonlinear characterization of the amplifiers is necessary for several of these techniques and for optimizing the amplifier design. Behavioral models, also denoted as black-box models, have attracted interest as a means for characterizing power amplifiers.

Hence, the accuracy of the nonlinear behavior model is central and must be evaluated in some way so that strong candidates for e.g. digital predistortion can be found among a variety of behavioral models. An attractive way of comparing two models is to evaluate their performance on *validation data*. A validation data set is one that has not been used to help construct any of the models that we would like to evaluate. This procedure is often called *cross-validation*. The cross-validation technique is attractive because it makes sense without any probabilistic arguments and assumptions about the true system. The quality of the validation data is of great importance; the accuracy of the model can not be shown better than the accuracy of the measurements. A challenge is therefore to create a measurements system that can measure and deliver validation data with extra ordinary properties with respect to e.g. bandwidth and dynamic range.

An obvious choice of a validation criteria is to calculate the total error of the model, i.e. the difference between the measured output and the output of the model using validation data. Often it is calculated as the *normalized mean-square error* (NMSE). A strong drawback with the NMSE is that it mainly measures the *in-band* error while it is mainly the *out-of-band* error that is of interest.

In this paper we go through a number of validation criteria for radio frequency power amplifier behavioral models, showing their pros and cons in a comparative way. Examples of measures that will be considered is the NMSE, the *adjacent channel power ratio*, the *power spectrum comparative method*, the *adjacent channel error power ratio*, the *weighted error-to-signal power ratio*, and the complementary memory measures, the *memory effect ratio* and the *memory effect modeling ratio*.

- [1] S. C. Cripps, *Advanced Techniques in RF Power Amplifier Design*. Boston, MA: Artech House, 2002.
- [2] M. Isaksson, D. Wisell, and D. Rönnöw, "A Comparative Analysis of Behavioral Models for RF Power Amplifiers," *IEEE Trans. Microwave Theory Tech.*, vol. 54, pp. 348-359, Jan. 2006.
- [3] H. Ku and J. S. Kenney, "Behavioral Modeling of Nonlinear RF Power Amplifiers Considering Memory Effects," *IEEE Trans. Microwave Theory Tech.*, vol. 51, pp. 2495-2504, 2003.
- [4] D. Wisell, M. Isaksson, and N. Keskitalo, "A General Evaluation Criteria for Behavioral PA Models," in *69th ARFTG Conf. Dig.*, Honolulu, HI, USA, 2007, pp. 251-255.

CMOS for micro- and millimeter wave power applications

Mattias Ferndahl¹, Hossein Nemati¹, Herbert Zirath¹.

¹ Microwave Electronics Laboratory, Chalmers University of Technology, SE-41296 Göteborg, Sweden

SUMMARY

This abstract presents an empirical study of the large signal behavior of CMOS devices from two different nodes, 130 nm and sub 65 nm ($L_{phys} \leq 45nm$) using a load pull system at micro and millimeter wave frequencies to evaluate their use for millimeter wave power amplifiers.

I. INTRODUCTION

THE down scaling of CMOS technology has led to very high transit frequencies and is becoming a realistic alternative to III-V technologies for millimeter wave applications with several successful design examples [1]–[3]. Not much has however been reported regarding this issue. Above 15 GHz Vasylyev et al [4] with 17.8 dBm output at 17 GHz represent highest power and Yao et al [5] with 6.4 dBm at 60 GHz highest power combined with high frequency. Previous work by the authors [6] was limited to lower frequencies and relatively small devices.

II. RESULTS

Load pull measurements on different CMOS devices with different gate lengths and widths have been carried out to evaluate their power performance. At 23 GHz output power levels of 22 dBm with 5 dB gain was obtained for 1 mm devices using 130 nm CMOS. At 35 GHz the gain of these was found too low to be of practical use. 40 nm gate length devices however showed very promising performance with 12 dBm output power, 7 dB gain and a maximum power added efficiency (PAE) of 33 %, for 192 μ m devices. In the extensive work by Scholvin et al [7], extending up to 20 GHz, they state a maximum operating frequency of 20-25 GHz for the 65 nm node. The results presented here however shows that this limit could be extended to 35 GHz, at least, for sub 65 nm nodes.

We also argue that the approach of using non-minimum dimensions in the transistor layout to increase

the breakdown voltage cannot be used higher up in frequency. This due to that the f_{max} , f_t of the non-minimum dimension transistors are too low.

III. CONCLUSION

Through load pull measurements it is shown that CMOS power amplifiers with acceptable gain and output power can be made well up into the millimeter wave region. It is also shown that, for these high frequencies, the short gate length technologies surpass the longer gate length technologies in terms of power added efficiency while output power density stays fairly constant at 100 mW/mm. This is in contrast to lower frequencies, *i.e.* below 5 GHz, there non-minimum gate length devices with thicker gate oxide are used for power amplification.

REFERENCES

- [1] C.H. Doan, S. Emami, A.M. Niknejad, and R.W. Brodersen, "Millimeter-Wave CMOS Design," *Solid-State Circuits, IEEE Journal of*, vol. 40, no. 1, pp. 144–155, 2005.
- [2] M. Ferndahl, B. M. Motlagh, A. Masud, I. Angelov, H. O. Vikes, and H. Zirath, "CMOS Devices and Circuits for Microwave and Millimetre Wave Applications," in *European Gallium Arsenide and Other Semiconductor Application Symposium, GAAS 2005*, Paris, 2005, p. 105.
- [3] H. Shigematsu, T. Hirose, F. Brewer, and M. Rodwell, "Millimeter-Wave CMOS Circuit Design," *Microwave Theory and Techniques, IEEE Transactions on*, vol. 53, no. 2, pp. 472–477, 2005.
- [4] A. V. Vasylyev, P. Weger, W. Bakalski, and W. Simbuerger, "17-GHz 50-60 mW power amplifiers in 0.13 μ m standard CMOS," *Microwave and Wireless Components Letters, IEEE*, vol. 16, no. 1, pp. 37, 2006.
- [5] T. Yao, M. Q. Gordon, K. K. W. Tang, K. H. K. Yau, M. T. Yang, P. Schvan, and S. P. Voinigescu, "Algorithmic Design of CMOS LNAs and PAs for 60-GHz Radio," *Solid-State Circuits, IEEE Journal of*, vol. 42, no. 5, pp. 1044–1057, 2007.
- [6] M. Ferndahl, H. O. Vikes, H. Zirath, I. Angelov, F. Ingvarson, and A. Litwin, "90-nm CMOS for microwave power applications," *IEEE Microwave and Wireless Components Letters*, vol. 13, no. 12, pp. 523, 2003.
- [7] Jorg Scholvin, David R. Greenberg, and Jesus A. del Alamo, "Fundamental Power and Frequency Limits of Deeply-Scaled CMOS for RF Power Applications," in *Electron Devices Meeting, 2006. IEDM '06. International*, 2006, pp. 1–4.

Comparative analysis of the complexity/accuracy tradeoff for power amplifier behavior models

Ali Soltani Tehrani[†], Haiying Cao, Thomas Eriksson[†], Christian Fager

[†]Department of Signals and Systems Department of Microtechnology and Nanoscience
Chalmers University of Technology, Göteborg, Sweden
asoltani@chalmers.se

Summary – A comparative study of state-of-art nonlinear amplifier models are presented in this document. The main focus is on the modeling accuracy as a function of the computational complexity.

Introduction – Due to electrical consumption requirements, power amplifiers are driven to high efficiency regions, which have nonlinear characteristics. Nonlinear dispersive effects also exist, which are typically due to RF mismatching and thermal effects. These impairments cause the amplifier to distort the communication signal and introduce spectral regrowth. Linearization of the amplifiers is needed among many reasons in order to avoid interfering with applications at neighboring frequencies. Digital predistortion of the input data to the amplifier can help us achieve this. In order to utilize this technique, behavior models for power amplifiers have to be established.

Model Definitions – In literature many behavior models have been proposed to model the amplifier characteristics. In this project some of the more well-known models are characterized in terms of their accuracy and computational complexity. Some of these models include the Volterra model, memory polynomial model, generalized memory polynomial model and the Kautz Volterra model [2]. The Volterra series is the most general model, but due to high complexity is seldom used in practice. The other models can be viewed as reduced Volterra series models. The model parameters are identified from data from a 3.5 GHz WiMAX amplifier.

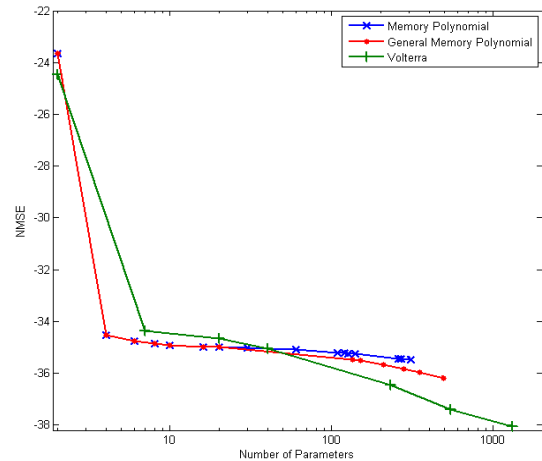
Results – The modeling accuracy is defined by two measures; the normalized mean square error (NMSE) and the adjacent channel error power ratio (ACEPR). The NMSE is defined as

$$NMSE = 10 \log_{10} \left(\frac{\text{var}(Model - Meas)}{\text{var}(Meas)} \right)$$

and the ACEPR as

$$ACEPR = \frac{\int_{\text{out of band of the signal}} |Meas(f) - Model(f)|^2 df}{\int_{\text{inband of the signal}} |Meas(f)|^2 df}$$

The models are compared in terms of NMSE and ACEPR vs. the computational complexity. At this stage, the number of parameters required to construct the model is used as a measure of the complexity. The Volterra was shown to reach low NMSE values albeit at the cost of high complexity. The memory polynomial model on the other hand was shown to reach a limit in NMSE but at a fairly low complexity. The models are arranged in the figure below:



Conclusion – Depending on the amount of complexity available for the transmitter, a model can be chosen from the models characterized. The behavior models are arranged according to their performance in terms of complexity and accuracy. Inverse modeling is also analyzed and characterized for the different models.

- [1] J. C. Pedro and S. A. Maas, "A comparative overview of microwave and wireless power-amplifier behavioral modeling approaches," *Microwave Theory and Techniques, IEEE Tran.*, vol. 53, pp. 1150-1163, 2005.
- [2] M. Isaksson, D. Wisell, and D. Ronnow, "A comparative analysis of behavioral models for RF power amplifiers," *Microwave Theory and Techniques, IEEE Tran.*, vol. 54, pp. 348-359, 2006.

A Computational Load-Pull Investigation of Harmonic Loading effects on AM-PM conversion

¹O. Bengtsson, ²L. Vestling, and ²J. Olsson

¹University of Gävle, SE-801 76 Gävle, Sweden, phone: +46 26 648904, fax: +46 26 648828, e-mail: bob@hig.se, ²Uppsala University, The Ångström Laboratory, Solid State Electronics, P.O. Box 534, SE-751 21 Uppsala, Sweden

Summary— In this work computational harmonic load-pull have been used to study the effect of harmonic loading on AM-PM conversion for an RF-Power LDMOS transistor. It is found that especially the load impedance seen at the 2nd harmonic has a large impact (up to 2° or 15% difference) on the phase distortion at P_{1dB} in this investigation conducted at chip level.

I. INTRODUCTION

In computational load-pull transient simulations are conducted for different load settings [1]-[2]. The effects of harmonic loading can be investigated using a combination of passive and active loads, Fig. 1, [3]. From the phase shift of i_d versus v_g at different power (voltage) levels the voltage dependent phase shift (AM-PM conversion) can be investigated by comparison to the ideal phase shift.

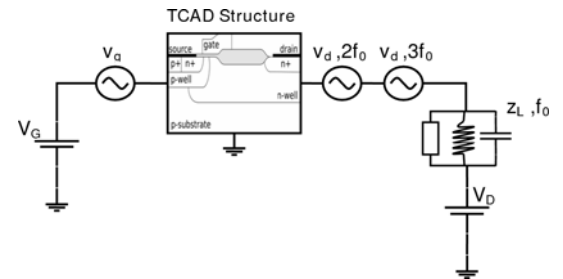


Fig. 1. Computational load-pull setup

II. RESULTS

The harmonic loads have been swept with the fundamental load in the primary optimum position for maximum output power. Non optimum 2nd harmonic loading is shown to create up to 2° (15%) increase in AM-PM conversion at P_{1dB} , Figs . 2-5. 3rd harmonic has less impact.

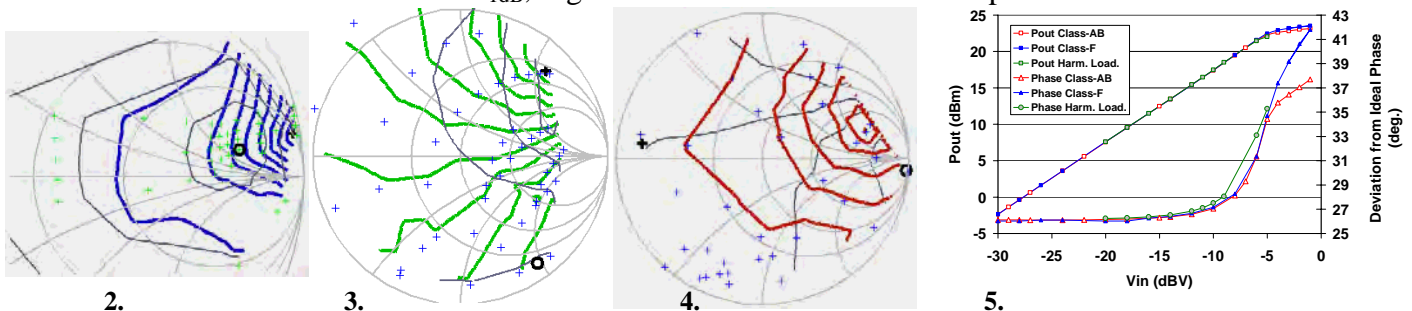


Fig. 2-5. Fundamental, 2nd and 3rd harmonic load-pull at -5 dBV input voltage (about P_{1dB}) and for swept input voltage. Output power contours are shown in grey with maximum at black (o). Absolute phase is shown in colors with maximum at black (+). Contours show levels of 10° for f_0 , 0.5° for $2f_0$ and 0.25° for $3f_0$.

III. CONCLUSION

An AM-PM investigation using computational harmonic load-pull has been conducted for an RF-Power LDMOS transistor. A large impact of the 2nd harmonic loading on phase distortion at chip level is observed.

IV. REFERENCES

- [1] Loechelt GH, Blakey PA. A Computational Load-Pull System for Evaluating RF and Microwave Power Amplifier Technologies. IEEE MTT-S Digest 2000;465-8
- [2] Jonsson R, Wahab Q, Rudner S, Svensson C. Computational load pull simulations os SiC microwave power transistors. Solid-State Electronics 2003;47:1921-6.
- [3] Bengtsson O, Vestling , Olsson J. A Computational Load-Pull Method with Harmonic Loading for High-Efficiency Investigations. Submitted to Solid-State Electronics

Identification of Distortions in a RF Measurement System

Haiying Cao*, Ali Soltani, Christian Fager*, Thomas Eriksson

* Department of Microtechnology and Nanoscience, Department of Signals and Systems
Chalmers University of Technology, Gothenburg, Sweden
{haiying, asoltani, christian.fager, thomase}@chalmers.se

Summary: Distortions in a RF measurement system can adversely impact the characteristics of the measured signal. In this paper, signal processing techniques are used to identify the sources for distortions. Promising measurement results are shown.

Introduction: The measurement system setup in Fig. 1 is used for characterization of power amplifiers. Since high measurement accuracy is needed, it is necessary to compensate for the system impairments. Models for the measurement system have therefore been evaluated. In Fig. 1 a computer is used to generate a baseband signal, a vector signal generator (VSG, Agilent E4438C) acts as the modulator and transmitter, and a digital storage oscilloscope (DSO, Agilent Infiniium 54854A) acts as the receiver. The described system has inherent linear and nonlinear distortions. Therefore, a Wiener filter is proposed to model the linear distortion, and the well-known Parallel Hammerstein (PH) model is used to model the nonlinear distortion. Here, we use two measurement setups to identify the distortion. First, the computer is used to download the baseband signal to the VSG, and the RF signal is recorded from one channel in the DSO. Second, the computer is used to download the baseband signal to the VSG, and the DSO records the same RF signal in two separate channels.

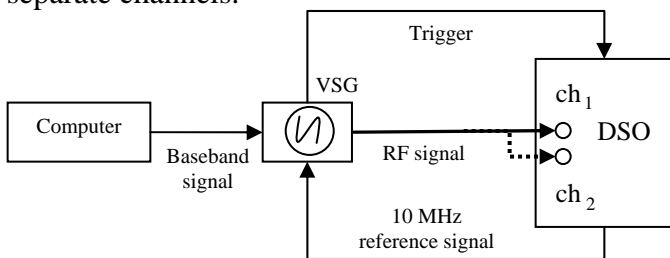


Fig. 1 Measurement system setup

Result: Pre-processing the signal is necessary before the identification, which includes delay elimination, normalization and statistical averaging. Since a measurement noise floor exists in the devices, statistical averaging is used to lower the noise variance which enhances the dynamic range [1, 2]. Signal to noise ratio (SNR) is used to evaluate the agreement between the measurement system and its model. It is defined here as the difference between

the baseband and the measured signals. In Fig. 2, SNRs versus the number of measurements is shown. The SNR with the linear and nonlinear models is higher compared to the SNR with just linear model or with no model. We note that they get saturated after a certain number of measurements since they are limited by the inherent nonlinearities of the VSG and DSO. In order to isolate the distortions from the VSG and DSO, we feed the same signal using two channels of the DSO to remove the nonlinearity effect of the VSG, and we are able to see the nonlinearity effect of the DSO. In this case, we define the SNR between the two channels as: $10\log_{10}(\text{var}(ch_1)/\text{var}(ch_1 - ch_2))$, and we get higher SNR. This implies that the performance of the measurement system is limited by the nonlinearity of the VSG, and further research on modeling this nonlinearity will be investigated.

Conclusion: A Wiener filter and PH model are used to model the linear and nonlinear distortions of the measurement system respectively, and the SNR of the system is improved. Two channel measurements are used to isolate the nonlinearity effects of the VSG and DSO.

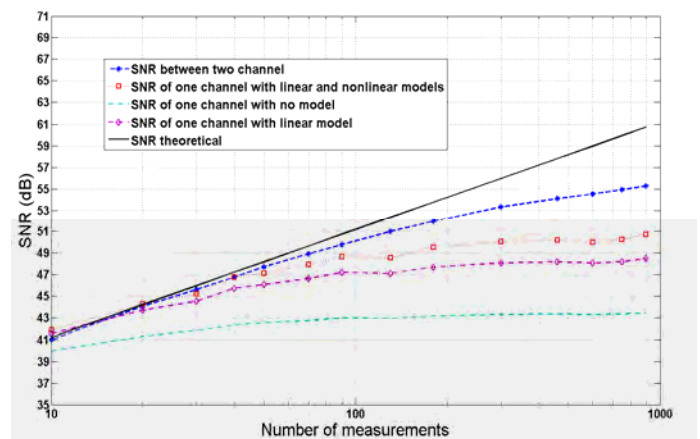


Fig. 2 SNR versus number of measurements

Reference:

- [1] Fager, C.; Andersson, K.; "Improvement of Oscilloscope Based RF Measurements by Statistical Averaging Techniques" Proc. of IEEE MTT-S, June 2006 pp. 1460 – 1463
- [2] D. Wisell; "A baseband time domain measurement system for dynamic characterization of power amplifiers with high dynamic range over large bandwidths" Proc. of IMTC' 03, May 2003, vol. 2, pp. 1177-1180.

Further enhancement of Load pull simulation technique to study non linear effects of LDMOS in TCAD

A. Kashif^a, T. Johansson^b, C. Svensson^c, T. Arnborg^d and Q. Wahab^{a,e}

^a Department of Physics, Chemistry and Biology (IFM), Linköping University, SE-581 83 Linköping, Sweden

^b Infineon Technologies Nordic AB, SE-164 81 Kista, Sweden

^c Department of Electrical Engineering (ISY), Linköping University, SE-581 83 Linköping, Sweden

^d Ericsson AB, SE-221 83 Lund, Sweden

^e Swedish Defense Research Agency (FOI), SE-581 11 Linköping, Sweden

E-mail: ahska@ifm.liu.se

High linearity and efficiency in power amplifiers (PAs) are always demanding. In PAs, the *RF* transistor is major component and should have high performance. The accurate large signal transistor's model is important to attain high performance in terms of *RF* output power, gain, efficiency and linearity at desired bandwidth [1]. Computational load pull simulation technique is found a suitable solution to study the transistor's performance in real circuit context [2]. The technique has been further extended to study the intermodulation distortion (IMD) of the intrinsic transistor exclusively [3].

The LDMOS transistor is cost effective technology and used in communication system due to reasonable linearity at medium power density [4]. We studied LDMOS transistor's structure provided by Infineon Technologies. The structure was optimized by observing the effects of interface charges at the RESURF region. The optimized structure showed lower on-resistance, which in turn increases the drain current. This enhances the *RF* output power as well as frequency of operation. This optimized transistor delivered 1.3 W/mm *RF* output power upto 4 GHz in class AB operation.

The optimum performance in PAs can be achieved by understanding the non-linear behaviour at device level under large signal operation. We studied intermodulation distortion by two tone test in TCAD. The carrier frequency (f_1) was selected at 1 GHz with 200 MHz tone spacing to reduce the computational resources. A complete harmonic current and voltage signals were evaluated with 5 cycles of 1 GHz signal in time domain. At input, two *ac* voltage signal sources (Carrier (f_1) and 2nd tone (f_2)) were applied in series while at the output these *ac* voltage signals sources were used with 180° phase difference with respect to the input signal. The time domain current and voltage signals were transformed into frequency domain by Fast Fourier Transformation (FFT) using Matlab. The IMD_3 were observed at $2f_2 - f_1$ and $2f_1 - f_2$. In this technique the higher order harmonics are shorted. To estimate the power of IMD_3 , we calculated the power by current flowing into the real part of impedance of the carrier frequency. By optimization of LDMOS structure, the value at the power level 10 dB back-off from P_{1dB} enhances from -17 to -36 dBc.

The TCAD load pull simulation technique is now able to predict the large signal parameters such as *RF* output power, efficiency, gain, impedances and non-linear effects of the transistor in real context for the designing of power amplifiers.

References

- [1] Frederick H. Raab, Peter Asbeck, Steve Cripps, Peter B. Kenington, Zoya B. Popovic et al, "Power Amplifiers and Transmitters for RF and Microwave", *IEEE Transactions on Microwave Theory and Techniques*, vol. 50, no. 3, March 2002: pp. 814-26.
- [2] R. Jonsson, Q. Wahab, S. Rudner, and C. Svensson, "Computational load pull simulations of SiC microwave power transistors," in *Solid State Electronics*, vol. 47, pp. 1921-1926, 2003.
- [3] A. Kashif, C. Svensson, T. Johansson, S. Azam, T. Arnborg and Q. Wahab, "A non-Linear TCAD large signal method to enhance the linearity of transistor" in *International Semiconductor Device Research Symposium (ISDRS'07)*, 12-14 December 2007.
- [4] A. Wood, W. Brakensick, C. Dragon, and W. Burger, "120 Watt, 2 GHz, Si LDMOS RF power transistor for PCS base station applications" in *IEEE MTT-S*, vol. 2, 7-12 June 1998: pp. 707-710

GaN device and MMIC development at Chalmers University of Technology

M. Fagerlind, M. Südow, K. Andersson, M. Thorsell, A. Malmros, P.Å. Nilsson, H. Zirath, and N. Rorsman

Microwave Electronics Laboratory, Microtechnology and Nanoscience, Chalmers University of Technology, SE-41296 Göteborg, Sweden. martin.fagerlind@chalmers.se

Introduction

At Chalmers we are working with the development of GaN based HEMT (High Electron Mobility Transistor) devices and MMICs (Monolithic Microwave Integrated Circuits). GaN and its III-nitride alloys are interesting in microwave power applications, where properties like high breakdown field and high saturation velocity are required.

Device

In the device area we are working towards an optimization of device characteristics like maximization of transconductance and power handling capabilities i.e. maximization of breakdown fields and source to drain current densities. This is done in-house by process and device layout optimization, as well as physical simulations. Feedback to external suppliers of GaN epitaxial wafers is also part of the optimization process.

Typical DC device performance is, drain saturation current (at zero gate voltage) around 1 A/mm. Maximum transconductance in the range of 250 mS/mm. Typical small signal measurements for similar devices are extracted to a maximum of $f_T=40$ GHz and a maximum of $f_{max}=70$ GHz.

MMIC

There is a strong consensus about the benefits of power amplifiers in GaN. These devices are however, also well fit for receiver electronics. Characterization of receiver blocks for robustness and low noise, with the ultimate goal of realizing transceiver modules monolithically integrated on one chip is therefore one of our major areas of research.

As an example of this effort, a high linearity X-band mixer based on a single $4 \times 100 \mu\text{m}$ GaN HEMT is presented, Fig1a. The mixer has an RF bandwidth of 7-16GHz, an IF bandwidth of 2GHz and exhibits a conversion loss of $<8\text{dB}$ across the entire RF band, Fig1b. This mixer has very good intermodulation properties seen in an IIP3 of 30dBm at 10.2GHz.

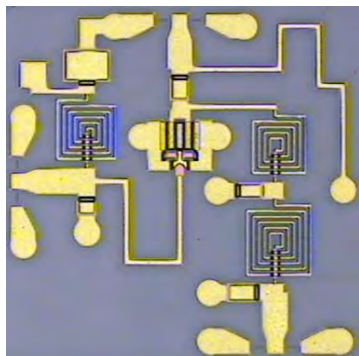


Fig1a. Photograph of X-band mixer MMIC

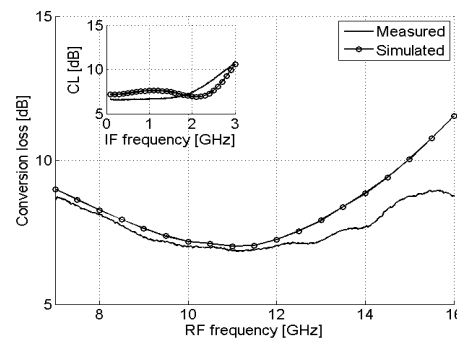


Fig1b. Conversion loss vs. IF and RF.

Acknowledgement

This research has been carried out in the Microwave Wide Bandgap Technology project financed by Swedish Governmental Agency of Innovation Systems (VINNOVA), Swedish Energy Agency (STEM) Chalmers University of Technology, and Ericsson AB, Saab AB, Norstel AB, Infineon, NXP, Furuno, and Norse Semiconductor Laboratories AB.

Workshop

Measurement - Modeling

1300-1430 Thursday 6 March 2008

Model-Based Pre-distortion for Signal Generators

Carolina Luque and Niclas Björsell

University of Gävle, ITB/Electronics, SE-801 76 Gävle, Sweden

e-mail: caalue@hig.se, Phone: +46739823405

Currently, devices such as power amplifiers (PA) and analog to digital converters (ADC) targeted to achieve the demanding WiMax and 3G wireless communications applications must have performances high enough to support the current wireless standards and ensure an appropriate response of the whole system.

To fulfill the requirements on spurious free dynamic range (SFDR) and signal to noise and distortion ratio (SINAD) in ADCs [1] and to have exceptional linearity and efficiency at high output power for PAs [2], high measuring performance of these high-quality components are required. One must ensure that the test setup has superior performance compared to the device under test (DUT) [3].

Even state-of-the-art signal generators (SG) can have problem to generate spectrally pure signals. Due to imperfections in the SG such as nonlinearities, the generated signal will contain unwanted intermodulation products (IMD). This work approaches the problem by modeling the SG and using model-based digital pre-distortion (DPD), to reduce the 3rd-order IMD products. Modeling and DPD are applied for a three tones input signal; initially for a polynomial memory-less model, and in the near future to a grey-box with memory that also takes the internal architecture of the SG into account.

The results from the memory-less model shows that the accuracy of the model and the effectiveness of the DPD to some extent depend on the amplitude of the input signal. We have shown that DPD, for certainly range of frequencies and using polynomials of 9th order, can reduce the 3rd order IMD product up to 15dB.

The extension of the memory-less model to also include dynamic behavior, may improve the performance in the DPD, and decrease the distortion even more due to the memory effects in the system.

References

- [1] D. Brandenburg, "High-Speed ADC Specs for Wireless Applications" Department of technology, Signal Conditioning Group, Fairchild Semiconductor Article, 2007.
- [2] P.M. Asbeck, L.E. Larson, I.G. Galton, "Synergistic design of DSP and power amplifiers for wireless communications " IEEE Transactions on Microwave Theory and Techniques, Volume 49, Issue 11, Nov 2001.
- [3] N. Björsell, O. Andersen, P. Händel, "High dynamic range test-bed for characterization of analog-to-digital converters up to 500 MSPS," 14th IMEKO Symposium on New Technologies in Measurement and Instrumentation & 10th Workshop on ADC modeling and testing, September 12-15, 2005, Gdynia, Poland , pp. 601-604.

A COMPARISON OF ANTENNA DIVERSITY CHARACTERIZATION METHODS USING REVERBERATION CHAMBERS AND DRIVE TESTS

D. Nyberg*, M. Franzén‡ and P.-S. Kildal†

*Chalmers University of Technology, Sweden, daniel.nyberg@chalmers.se

‡Bluetest AB, Sweden, magnus.franzen@bluetest.se

†Chalmers University of Technology, Sweden, per-simon.kildal@chalmers.se

The aim of this paper is to compare two ways of characterizing diversity antennas; by using conventional drive tests and using the high performance reverberation chamber available from Bluetest AB. This work is collaboration between Chalmers, Bluetest AB and Rayspan Corporation and it is done within the Chase research center at Chalmers.

Three different antennas are used throughout the comparison and they are of two types. The first antenna is a circular array consisting of 6 conventional monopole elements. Those are mounted on a circular metallic ground plane of 140 mm radius. Furthermore 3 different sets of holes have been drilled in the ground plane allowing three different configurations of the array. The spacing between the elements in the different configurations is 0.24λ , 0.14λ , 0.06λ at 900 MHz. This antenna is a new version of a similar antenna that has been used extensively as an example antenna at Chalmers when the measurement technique in the reverberation chamber was developed [1]. The previous antenna was measured in the standard Bluetest chamber, whereas the present measurements are done in the new high performance chamber.

The purpose of the present paper is to compare performance obtained in the standard and high performance Bluetest reverberation chambers. We will also include results of the planned drive test measurements of the antenna. We will not expect very good agreement between the drive tests and the measurements in the reverberation chamber. In that sense, the reverberation chamber is superior, since all chambers creates the same statistical isotropic environment which also is repeatable, where as for drive test different values will be obtained for different test locations and even different individual measurements, thus making comparisons between different antennas very difficult. We also hope to report the results of similar measurements of antennas manufactured and designed by Rayspan Corporation. One of them is a 3-element array working at 2.5 GHz. The other is a 4-port dual-band antenna at 2.5 & 5.2 GHz.

References:

- [1] K. Rosengren & P.-S. Kildal, "Radiation efficiency, correlation, diversity gain and capacity of a six-monopole antenna array for a MIMO system: theory, simulation and measurement in reverberation chamber", *Proceedings IEE Microwaves, Optics and Antennas*, pp.7-16. vol. 152, no. 1, Feb 2005. See also Erratum published in *Proceedings IEE, Microw. Antennas Propag.*, Vol. 153, No. 4, August 2006

Measuring Relative Receiver Sensitivity of Wireless Terminals in One Minute in a Reverberation Chamber

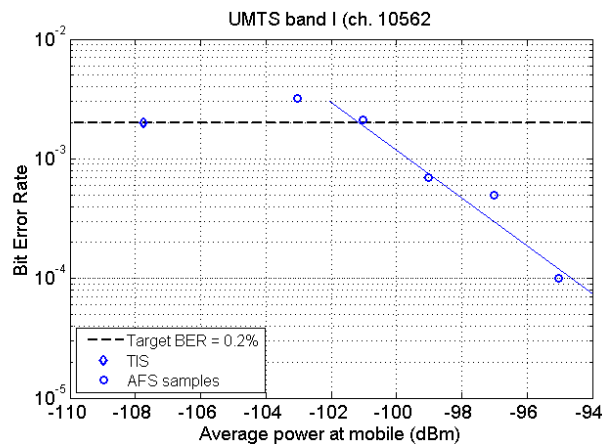
*M. Andersson**, C. Orlenius, M. Franzén

**Bluetest AB, Götaverksgatan 1, SE-417 55 Gothenburg, Sweden,
mats.andersson@bluetest.se*

Summary: The traditional way of measuring receiver sensitivity of wireless terminals is the Total Isotropic Sensitivity (TIS) measured in an anechoic chamber. This paper describes an alternative, up to 60 times faster, method to optimize receiver sensitivity during the design process.

Introduction: The downlink speed of mobile broadband services is directly affected by the receiver sensitivity of the terminal. The traditional way of evaluating receiver sensitivity during design to optimize performance is to measure the Total Isotropic Sensitivity (TIS) in an anechoic environment [1]. An alternative method is to measure the Average Fading Sensitivity (AFS) in a reverberation chamber with continuous Rayleigh fading [2].

Results: The AFS value can be found from fitting a line to a number of one minute relative receiver sensitivity values where the average bit error rate corresponding to a given output power from a base station simulator is measured, see fig. 1.



Conclusions: For many measurements, especially during antenna design, it is not the absolute receiver sensitivity of the terminal which is of most importance but the ability to quickly optimize the design, i.e. to be able to say if a new antenna or antenna configuration is better than another. By using the same average transmit power and to see if the average bit error rate has changed up or down it is possible in only one minutes time to see if the relative receiver sensitivity has improved or not by a design change. This offers a tremendous saving in time during development to find the optimum receiver sensitivity configuration.

References:

- [1] "Test Plan for Mobile Station Over The Air Performance" CTIA Certification, rev. 2.2, November 2006.
- [2] C. Orlenius, P-S. Kildal, and G. Poilasne, "Measurements of total isotropic sensitivity and average fading sensitivity of CDMA phones in reverberation chamber", *IEEE AP-S International Symposium*, Washington DC, July 2005.

Modeling of SiGe HBT Operation in Extreme Temperature Environment

P.Sakalas^{1,2}, M.Ramonas^{2,4}, M.Schroter^{1,5}, A.Kittlaus³, H.Geissler³, C.Jungemann⁴, A.Shimukovitch²

¹Chair for Electron Devices and Integrated Circuits, Dresden University of Technology, 01062 Dresden, Germany,

²Fluctuation Phenomena Laboratory, Semiconductor Physics Institute, 01108 Vilnius, Lithuania,

³SUSS MicroTec Test Systems, 01561 Sacka, Germany,

⁴EIT4, Bundeswehr University 85577 Neubiberg, Germany

⁵University of California San Diego, ECE, La Jolla, CA 92093-0407, USA.

Abstract - DC, RF and noise characteristics of SiGe HBTs, featuring peak f_T of 80 GHz, were measured and modeled in different ambient temperatures. Forward Gummel, output characteristics and S-parameters were measured in the range $T_0=4-473K$. Very good agreement of simulated DC data with experimental enabled analysis of temperature dependent RF performance and noise sources of investigated SiGe HBTs.

I. INTRODUCTION

Automotive radar and cryogenic amplifier [1][2] satellite communication [3] applications require transistors capable of operating in extreme environments. Recently, it was shown that SiGe HBT BiCMOS technology can be successfully used for cryogenic environment applications [4][5][6][7][8], including extremely low ambient temperatures ($T_0=4K$) [9][10]. Though resulting in degradation of DC and RF performance, SiGe HBTs - opposite to conventional Si BJTs - can operate at high ambient temperatures, reaching $T_0=573K$ [11]. Due to the demonstrated reasonable performance of SiGe HBTs over a wide T_0 range, compact modeling becomes increasingly important for designing circuits operating at extreme conditions. This work presents a comparison of TCAD simulation, compact modeling (using HICUM) with measured data for temperature dependent DC, RF and noise characteristics.

II. EXPERIMENTAL AND RESULTS

Noise parameters were measured with an automated tuner system from Maury in the 1-26 GHz frequency range at lattice temperatures of $T_0=293-423K$. The temperatures of the chuck, probes and shield were measured and controlled. Very good agreement of forward Gummel characteristics was obtained with the hydrodynamic (HD) device simulator GALENE [12] and with the compact model HICUM [13] (cf. Fig. 1). A fair agreement was obtained for the base current as well. Since at $T_0<78K$ base current changes its origin from diffusion to tunneling [4] modeling was performed for a limited T_0 range since

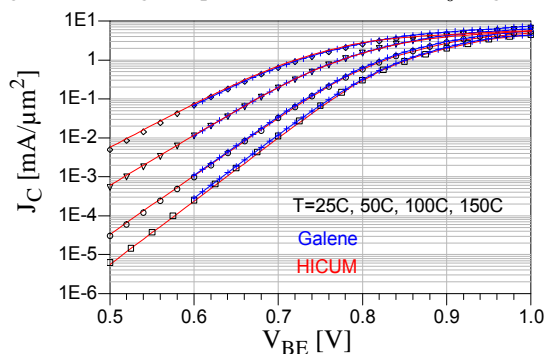


Fig. 1. Measured (symbols) and HD (blue lines with crosses) and HICUM (red solid lines) J_C versus V_{BE} .

this effect is taken into account neither in [12] nor the compact model. Cut-off frequency f_T (cf. Fig.2) increases with a drop in T_0 due to reduced electron scattering and bandgap narrowing, while it degrades with heating. Measured noise parameters are in Fig.3 compared to GALENE as well as to HICUM. The respective HICUM modeling and noise source analysis will be presented at the conference.

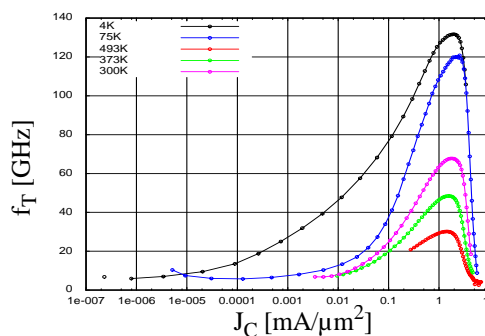


Fig. 2. Measured f_T versus J_C for a wide temperature range

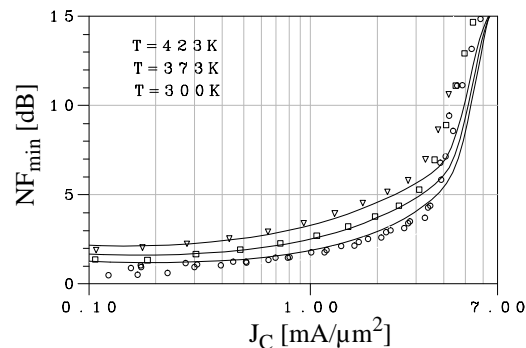


Fig. 3. Measured NF_{min} (symbols) and HD simulation (lines) vs. J_C .

III. REFERENCES

- [1] D.Gupta et al., *IEEE Trans.on Applied Superconductivity*, V. 13, pp. 477-483, 2003.
- [2] M.R.Murti et al., *IEEE TED*, V. 48, No. 12, pp. 2579-2587, 2000.
- [3] E.R.Soaes et al., *IEEE TED*, V. 48, No. 7, pp. 1190-1198, 2000.
- [4] J.D.Cressler: *Silicon Heterostructure Handbook*, Boca Raton, Taylor&Francis, 2005.
- [5] J.D.Cressler, *Proc. of the IEEE*, V. 93, Issue 9, pp. 1159-1582, 2005.
- [6] B.Banerjee et al., *IEEE BCTM*, pp.171-173, 2003.
- [7] S.Pruvost et al., *IEEE EDL*, V.26, No.2, pp.105-108, 2000.
- [8] N.Zerounian et al., *Electronic Letters*, V.36, No.12, pp.1076-1077, 2000.
- [9] Geissler et al., *Proc. ARTFG Microwave Meas. Conf.*, pp.137-140, 2006.
- [10] P.Chevalier et al., *IEEE BCTM*, pp. 26-29, 2007.
- [11] T.C.Wei-Min et al., *IEEE TED*, V. 51, No. 11, pp. 1825-1832, 2005.
- [12] B.Neinhus et al., *VLSI Design* 8, pp.387-391, 1998.
- [13] M.Schroter, *IEICE Transactions on Electronics*, V. E88-C, No.6, pp.1098-1113, 2005.

On-wafer network analyser uncertainty estimation

J. Stenarson^{*}, K. Andersson[†], C. Fager[†] and K. Yhland^{*}

^{*} SP Technical Research Institute of Sweden, email: jorgen.stenarson@sp.se

[†] Chalmers University of Technology

Summary—This paper presents a simple method for the estimation of the most important uncertainty components/contributions for on-wafer Vector Network Analyser (VNA) measurements. The method is based on the estimation of residual errors, of a calibrated VNA, using transmission lines. Results are presented using two different models for the calibration standards.

I. INTRODUCTION

In VNA calibration, the residual errors are traditionally estimated by terminated one-port transmission line measurements using the one-port ripple technique [1]. I.e. the residual errors are related to the characteristic impedance of the transmission lines. This method is inconvenient for on-wafer work because it requires many terminated transmission lines.

This paper applies the two-port ripple method [2, 3] to on-wafer uncertainty estimation. The residual errors are obtained from transmission line and thru measurements using a SOLT/SOLR calibrated network analyser. The method compares the system impedance defined by the VNA calibration standards to that of the reference transmission lines giving the residual errors directivity, tracking and match.

II. RESULTS

The method was applied to 150 μm Ground-Signal-Ground (GSG) coplanar wafer probes and a standard alumina calibration substrate containing SOLT/SOLR standards. For comparison, two sets of data were used for the SOLT/SOLR kit, a manufacturer model and a table based model. The table based model was measured with a TRL calibration.

The resulting residual errors are shown in Fig. 1. Since the residual directivity is approximately equal between using the table based model and the manufacturer model we can conclude that the load is of good quality. This is because the manufacturer's model of the load is a perfect match.

The residual match when using the table based model is similar to the residual directivity, which together with the excellent residual tracking means that the table based model accurately predicts the

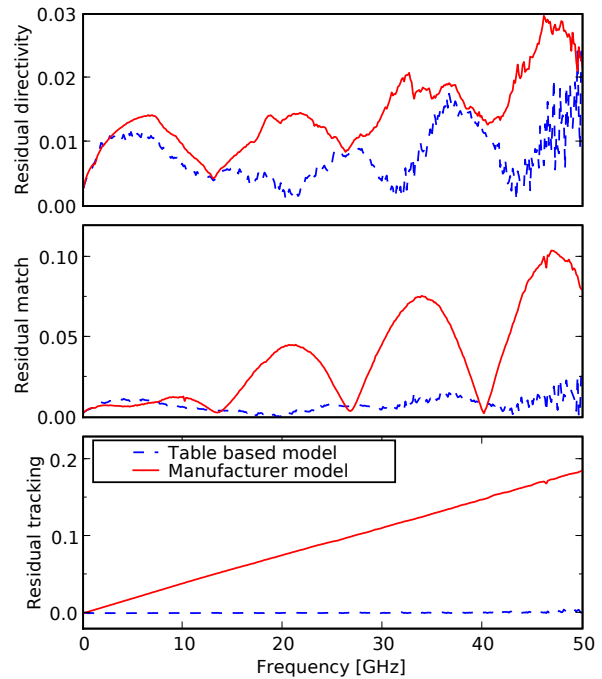


Fig. 1. Residual errors for calibrations using the table based model (blue) or the manufacturer model (red) of the same standards.

short and open. However, for the manufacturer model, the residual match and tracking show a substantial increase which indicates that the open and/or short standards were not accurately modeled.

III. CONCLUSION

We have shown how to use the two-port ripple method for estimating the residual errors of VNA measurements in the context of on-wafer measurements. The results show that the residual errors can be improved by modelling the calibration kit.

REFERENCES

- [1] EA, "Guidelines on the evaluation of vector network analysers (VNA)," Tech. Rep. EA-10/12 (rev.00), European co-operation for Accreditation, 2000.
- [2] J. Stenarson and K. Yhland, "Residual error models for the SOLT and SOLR VNA calibration algorithms," in *69th ARFTG Conference*, (Honolulu Hawaii), 2007.
- [3] J. Stenarson and K. Yhland, "A new assessment method for the residual errors in SOLT and SOLR calibrated VNAs," in *69th ARFTG Conference*, (Honolulu Hawaii), 2007.

mm-wave device testing using wideband coplanar transitions

Enrique Villa, Beatriz Aja, Luisa de la Fuente, Eduardo Artal (villae@unican.es)
Departamento de Ingenieria de Comunicaciones. ETSIIT. Avenida de los Castros, s.n.
Universidad de Cantabria. Santander (Spain)

Summary

A wideband coplanar to microstrip transition without via holes has been used for passive device testing at mm-wave frequencies (20 to 40 GHz). Testing circuits are built on 0.254 mm thick Alumina substrate. Test method, with a coplanar probe station, has been checked and validated with passive devices.

Introduction

At mm-wave frequencies coaxial test fixtures do not provide accurate characterisation of passive devices assembled in microstrip lines. A more repeatable method is to perform tests with coplanar probes through broadband coplanar to microstrip transitions. A coplanar transition has been designed to avoid metallized via holes in the dielectric substrate, using virtual grounds at the end of special shaped radial stubs [1], [2]. For calibration purposes a TRL kit has been included in the test set. Next Figure shows pictures of the TRL kit, a broadband pass filter at 30 GHz and two transitions to test beam lead diodes.



Results

Coplanar to microstrip transition design has been checked through electromagnetic simulations and S parameter tests. Band pass filter characterisation has been validated by comparison with tests based on a commercial coplanar to microstrip transition having via holes. Beam lead Schottky diodes and thin film resistors were tested and characterised from 20 to 40 GHz. Results showed a good repeatability and consistency.

Conclusion

A test method for S-parameters measurements of mm-wave passive devices based on broadband coplanar transitions has been developed. Transitions have a good performance from 20 to 40 GHz, and can be easily implemented on Alumina substrate without via holes.

References

- [1] K. Schmidt von Behren et al., "77 GHz Si-Schottky Diode Harmonic Mixer", Proceedings of 32nd European Microwave Conference, October 2002, pp. 1-4.
- [2] G. Zheng et al., "Wideband Coplanar Waveguide RF Probe Pad to Microstrip Transitions Without Via Holes", Microwave and Wireless Component Letters, IEEE, pp. 544-546, Vol. 12, Issue 13, December 2003.

This work has been supported by the Ministerio de Educación y Ciencia (Spain), grant references ESP2004-07067-C03-02 and AYA2007-68058-C03-03

High Efficiency using Optimized SOI-Substrates

Lars Vestling*, Olof Bengtsson†, Klas-Håkan Eklund* and Jörgen Olsson*

*Uppsala University, The Ångström Laboratory, Solid State Electronics,
Box 534, SE-751 21 Uppsala, Sweden. E-mail: lars.vestling@angstrom.uu.se

†University of Gävle, SE-801 76 Gävle, Sweden.

Abstract—The effect of the substrate resistivity on the efficiency for high-frequency SOI-LDMOS transistors is studied using computational load-pull simulations. It is shown that very low resistivity and high resistivity SOI-substrates both result in high efficiency. It is also shown that a normally doped, medium resistivity, substrate results in significantly lower efficiency.

I. INTRODUCTION

It is well known that high-resistivity (HR) SOI-substrates can improve the performance of high-frequency devices [1]. On the other hand, it has been shown that very low resistivity (LR) SOI-substrates may reduce substrate losses for RF-power devices [2].

In this paper the efficiency of an SOI-LDMOS transistor on three different substrate resistivities is studied. This is done using computational load-pull [3] in class AB at 1 GHz.

II. RESULTS AND CONCLUSION

The substrate losses may be represented by the off-state small-signal output resistance, $R_{OUT}=1/\text{Re}(Y_{22})$. Figure 1 shows the simulated output resistance for the three substrates, indicating that the HR and LR substrates are expected

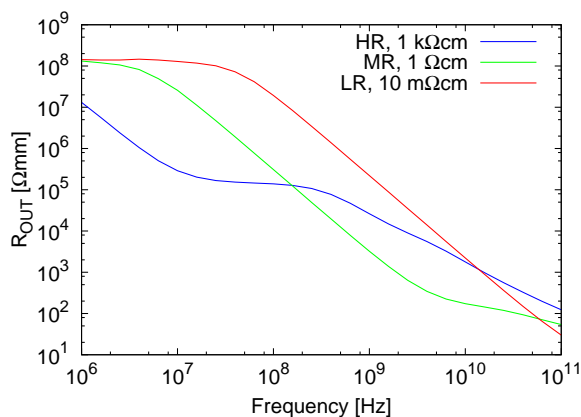


Fig. 1. The small-signal output resistance for the different substrates ($V_D=50\text{V}$, $V_G=0\text{V}$, $t_{SUB}=150\mu\text{m}$).

to have lower losses than the MR substrate at 1 GHz.

Figure 2 shows the results from the computational load-pull simulations. It is observed that all three devices have almost the same output power characteristics. However, there is a significant difference in the efficiency, where the MR substrate results in 10% lower efficiency than the LR and HR substrates. This is mainly explained by the low output resistance for the MR substrate, as was shown in Fig. 1.

The results show that devices on LR substrates would perform as good as devices on HR substrates from an efficiency point of view. However, when designing the transistors it is more difficult to do this using an HR substrate due to problems with depletion/accumulation in the region under the buried oxide [4].

The conclusion is that a LR substrate is the best choice for RF-power devices on SOI.

REFERENCES

- [1] F. Giancesello, et al., IEEE SOI Conf., pp. 119–120, 2007.
- [2] J. Ankarcrone, et al., EuroSOI2006, pp. 69–70, 2006.
- [3] G.H. Loechelt, et al., IEEE MTT-S Dig., pp. 465–468, 2000.
- [4] J. Scholvin et al., IEDM Tech. Dig., pp. 363–366, 2003.

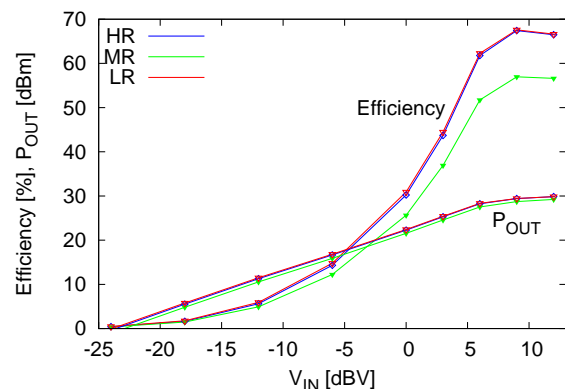


Fig. 2. The efficiency and output power from computational load-pull simulations (class AB, $V_{DD}=28\text{V}$, $V_{GS}=1.3\text{V}$, 1 GHz).

Spin Torque Oscillator Simulations and Circuit Designs

Yan Zhou*, Sandeep Srinivasan, Johan Persson, and Johan Åkerman
 Materials Physics, Department of Microelectronics and Applied Physics,
 Royal Institute of Technology, Electrum 229, 16440 Kista, Sweden
 *E-mail: zhouyan@kth.se

With the increasing integration and compactness of radio devices, the demand for further miniaturization of high-quality, highly tunable oscillators (over a large frequency range) continues to grow. To address this demand, we focus on the development of a novel, nanometer-sized, magneto-electronic device – the Spin Torque Oscillator (STO). The STO is compatible with the back-end flow of a standard Si process, and suitable for integration into high-frequency CMOS, SiGe, or ultrahigh-frequency InP, InGaP, and InGaAs. Because of its nano-scale dimensions (~50-100nm x 80-300nm), integration can be done without taking up large chip area. The small size, wide tuning range, low power consumption and compatibility with CMOS process make the STO an ideal candidate to replace traditional oscillator designs.

The Giant Magnetoresistance [1,2] based STO (Fig. 1.a) consists of one Cu layer sandwiched by two ferromagnetic layers. The electrons flowing through one of the layers get spin-polarized [3,4] and exert a torque on the localized magnetization of the other, creating a current-tunable oscillator (1-40 GHz) with a high quality factor (Q up to 18000) [5]. In this work we present numerical simulations of the STO in Matlab, Fortran, and Verilog-A. The magnetodynamics is found from the Landau-Lifshitz-Gilbert- Slonczewski (LLGS) equation,

$$\frac{d\hat{m}}{dt} = -\gamma\hat{m} \times \hat{H}_{\text{eff}} + \alpha\hat{m} \times \frac{d\hat{m}}{dt} + \gamma \frac{\eta\hbar I}{2\mu_0 M_s eV} \hat{m} \times (\hat{m} \times \hat{M}), \quad (1)$$

where γ is the gyromagnetic ratio, α is the damping parameter, η is the polarization ratio, μ_0 is the magnetic vacuum permeability, M_s is the saturation magnetization, and V the volume of the free layer. \hat{H}_{eff} is the effective magnetic field, which includes an applied magnetic field \hat{H}_{app} , the uniaxial magnetic anisotropy field \hat{H}_k , and the demagnetization field \hat{H}_d .

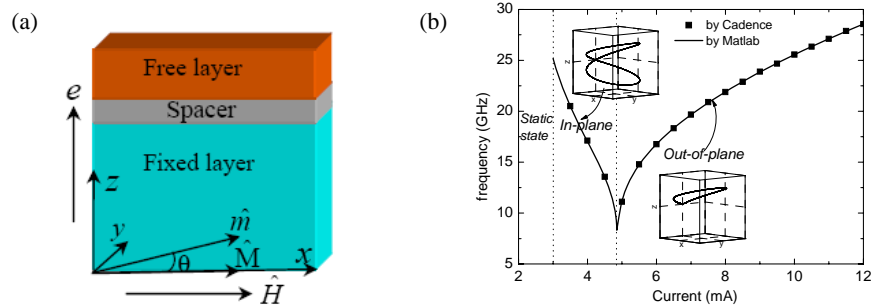


Fig. 1: (a) Schematic structure of the spintronics nano-oscillator (SNO) (b) Cadence and Matlab simulations of the STO precession frequency vs. DC current drive. The insets show the *precessional* trajectory of the STO for two different oscillation modes: in-plane and out-of-plane precession (inset). There is no perceptible difference in the end result.

Fig. 1(b) shows how the STO precession frequency f_{STO} changes with external drive signal I_{dc} . When running identical simulations in Cadence and in Matlab, we find virtually no difference in the end result. Examples of STO based circuits simulated in Cadence will also be presented.

We gratefully acknowledge financial support from The Swedish Foundation for Strategic Research (SSF), The Swedish Research Council (VR), The Göran Gustafsson Foundation and The Knut and Alice Wallenberg Foundation.

1. M. N. Baibich, J. M. Broto, A. Fert, F. N. Vandau, F. Petroff, P. Eitenne, G. Creuzet, A. Friederich, J. Chazelas, Phys. Rev. Lett. Vol. 61, pp. 2472 (1988).
2. G. Binasch, P. Grünberg, F. Saurenbach, and W. Zinn, Phys. Rev. B Vol. 39, pp. 4828 (1989).
3. J. Slonczewski, J. Magn. Magn. Mater. Vol. 159, L1 (1996).
4. L. Berger, Phys. Rev. B, vol. 54, pp. 9353 (1996).
5. W. H. Rippard, M. R. Pufall, S. Kaka, S. E. Russek, T. J. Silva, Phys. Rev. Lett. Vol. 92, pp. 027201 (2004).

Workshop

The GHz Entrepreneur

1300-1430 Thursday 6 March 2008

The workshop is about doing business from innovations and/or IP(R) in RF/Microwave. Personal reflections are given by representatives from three small enterprises, one global company and one venture company. The workshop is concluded by a discussion.

Mikael Reimers, CEO

Foodradar Systems AB
www.foodradar.com

Tomas Ornstein, CEO

Ranatec Instrument AB

www.ranatec.se

Johan Lassing, CEO

Qamcom Technology AB

www.qamcom.se

Peter Olanders, Technology Strategist

Ericsson AB
www.ericsson.com

Bengt Gustafsson, CEO
Microwave Technologies AB

Session V

1500-1600 Thursday 6 March 2008

Industrial Aspects of 100 Gbit/s Optical Communication

Bengt-Erik Olsson

Ericsson AB
Ericsson Research
431 84 Mölndal
bengt-erik.olsson@ericsson.com

10 Gigabit Ethernet (GbE) [1] is today the interface of choice for high-end servers and routers and the standard specifies implementations for up to 40 km on a dedicated optical fiber. For longer distance communication, various non-standard implementations of 10 GbE exist even though the Ethernet traffic often is encapsulated in another communication format, e.g. Optical Transport Network (OTN) [2] in order to facilitate traffic monitoring and quality assurance as well as coexistence with other traffic. There is now a need to aggregate traffic from multiple 10 GbE sources and therefore there are requests for even higher-speed communication channels and thus a next generation Ethernet is considered. Since Ethernet traditionally has taken speed increases in steps of x10, a natural next step is to consider 100 Gb/s as the next speed for Ethernet traffic. However, even in an optical fiber there are physical limitations to what bit-rate a single wavelength channel easily can accommodate and a serial bit rate of 100 Gb/s might be very difficult to transmit for more than a few hundred meters due to chromatic dispersion in the fiber. Recently, the IEEE [3] has launched a standardization effort for 100 Gb/s Ethernet for short and moderate transmission distances over dedicated optical fibers, where multiple low bit-rate optical wavelength channels in the fiber are considered. Proposed solutions include 10 channels carrying 10 Gbit/s each or 4 channels carrying 25 Gbit/s each. These solutions target primarily short distances *e.g.* up to 10 or 40 km on a dedicated fiber and often new fibers can be added at these distances to increase the total capacity. For longer distance communication, adding new fibers are usually not possible and these systems are already utilizing dense wavelength division multiplexing (DWDM) to increase the total fiber capacity. A DWDM system utilizes standardized wavelength windows for multichannel communication allowing *e.g.* 160 optical channels through the fiber. The use of a standardized frequency grid for optical communication imposes new constraints on the optical signal at ultra high bit-rates, *e.g.* 100 Gbit/s, since the bandwidth of the optical channel will severely limit the allowed bandwidth of the transmitted signal. Traditionally the available bandwidth in an optical channel has been much greater than the signal bandwidth, but transmitting 100 Gbit/s data using simple on-off keying will require more bandwidth than available on most DWDM systems. Typically commercial DWDM systems operate at either 100 GHz or 50 GHz optical channel spacing and the 3 dB bandwidth available for the data channel is often limited to 55 GHz on a 100 GHz grid and of course even lower on a 50 GHz grid. Therefore more bandwidth efficient signaling formats must be considered for 100 Gbit/s communication over DWDM channels. In this presentation the issues of standardizing 100 Gbit/s Ethernet will be discussed as well as possible implementations of bandwidth efficient 100 Gbit/s communication for use on DWDM channels using novel optical modulation formats.

[1] <http://grouper.ieee.org/groups/802/3/ae>

[2] ITU-T G.709, "Interfaces for the Optical Transport Network", March 2003.

[3] <http://grouper.ieee.org/groups/802/3/hssg/index.html>

All-Optical Waveform Sampling with Terahertz Capacity

Mathias Westlund, Peter A. Andrekson and Henrik Sunnerud

*Chalmers University of Technology, MC2, Photonics Laboratory
Authors are also with PicoSolve Inc. (www.picosolve.com)*

We present a fiber based all-optical sampling (AOS) capable of visualizing optical signals beyond 500 Gb/s. AOS provides bandwidth and precision for next generation optical communication.

The main driver behind the development of AOS techniques has been the exceptionally good temporal resolution these techniques provide ($\ll 1$ ps). Since the electronic means of measuring optical waveforms are limited in bandwidth by the use of photodiodes and electronic sampling gates to <70 GHz, the attraction to optical sampling systems providing in principle THz bandwidth is natural.

At the GigaHertz symposium we would like to focus on the following aspects of AOS:

- Principle of operation and performance of a fiber based AOS
- How software algorithms can simplify hardware design and improve performance
- Advantages compared to conventional electronic solutions
- Alternative implementations of AOS
- Experimental implementation and results

The AOS (see Fig. 1) that has been developed at Chalmers [1-3] utilize an optical pulse source that generates short intense sampling pulses together with a nonlinear phenomenon in the optical fiber to create an optical gate which is open only when the sampling pulse is present. The nonlinear phenomenon is called four-wave mixing and is an extremely fast process which enables sub-picosecond gating. At the output of the gate samples of the signal appear at a new wavelength, well separated from the sampling pulses and signal, and can be extracted using an optical filter. At this point the samples can be detected using low bandwidth electronics and fed into a computer for time-base processing and visualization.

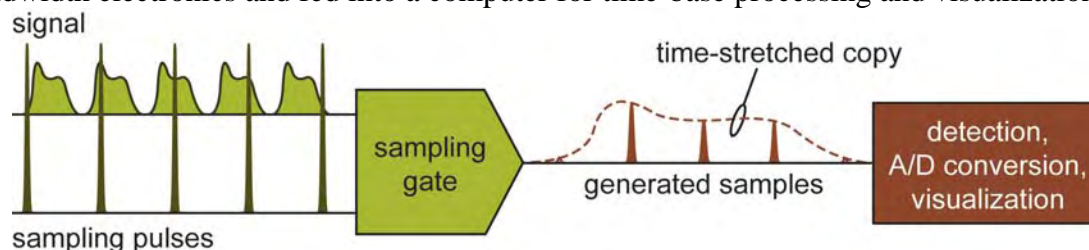


Fig. 1: Principle of optical sampling

Figure 2 shows an example of the optical sampling capacity by visualizing a 640 Gb/s data signal as a wide open eye-diagram. This AOS (which was provided by PicoSolve) has a temporal resolution of 1 ps, 40 nm optical bandwidth (full C-band), 2 mW signal sensitivity and is polarization independent, which defines the current state-of-the-art.

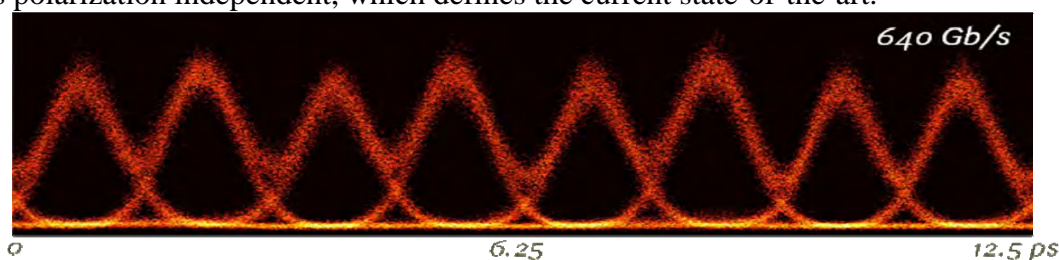


Fig 2. Optically sampled eye-diagram of a 640 Gb/s data signal.

1. M. Westlund et al., "High performance optical-fiber-nonlinearity-based optical waveform monitoring," *JLT*, **23**, pp. 2012-2022, 2005
2. M. Westlund et al. "Software-synchronized all-optical sampling for fiber communication systems," *JLT*, **23**, pp. 1088-1099, 2005.
3. M. Westlund et al., "Simple scheme for polarization-independent all-optical sampling," *PTL*, **16**, pp. 2108-2110, 2004.

High Speed 1.3 μm VCSELs for FTTH and RoF

P. Westbergh, E. Söderberg, J.S. Gustavsson, P. Modh and A. Larsson
 Photonics Laboratory, Department of Microtechnology and Nanoscience – MC2
 Chalmers University of Technology, SE-412 96 Göteborg, Sweden
 (contact e-mail: petter.westbergh@chalmers.se)

Z.Z. Zhang, J. Berggren and M. Hammar
 Department of Microelectronics and Applied Physics
 Royal Institute of Technology, SE-164 40 Kista, Sweden

With the cost/performance ratio being a critical factor for access networks such as fiber-to-the-home (FTTH) and radio-over-fiber (RoF) systems, vertical cavity surface emitting lasers (VCSELs) emitting at wavelengths compatible with single mode fibers are of interest. The VCSEL offers a combination of cost-efficient batch-level fabrication and testing/screening together with good beam quality, good high frequency modulation response at low currents and good power efficiency.

We have developed GaAs-based single mode VCSELs emitting at 1.3 μm using highly strained InGaAs quantum wells and a large detuning between the gain peak and the cavity resonance. Oxide confinement is used for current and optical confinement and a surface relief technique is used for selecting the fundamental mode and suppressing oxide modes (Fig.1).

Under large signal digital modulation, clear open eyes and error free transmission over 9 km of standard single mode fiber were demonstrated at OC-48 (2.488 Gbit/s) and 10 GbE (10.31 Gbit/s) bit rates up to 85°C (Fig.2), which proves the applicability for FTTH links.

Under large signal RF modulation, a spurious-free dynamic range (SFDR) of 100 and 95 dB·Hz^{2/3} was obtained at 2 and 5 GHz, respectively (Fig.3), which is in the range of those required for RoF links in several systems for mobile communication and wireless access.

E. Söderberg, J.S. Gustavsson, P. Modh, A. Larsson, Z.Z. Zhang, J. Berggren and M. Hammar, "High temperature dynamics, high speed modulation and transmission experiments using 1.3 μm InGaAs single mode VCSELs", IEEE J. Lightwave Techn. 25, 2791, 2007.

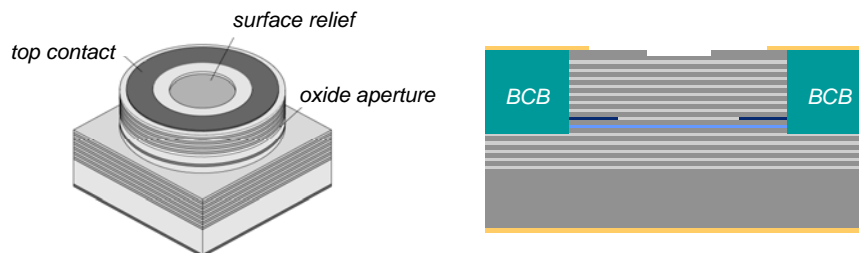


Fig. 1 Left: VCSEL design with surface relief for single mode emission. Right: Cross-sectional view showing the oxide aperture used for transverse current and optical confinement and a BCB layer used to reduce the capacitance.

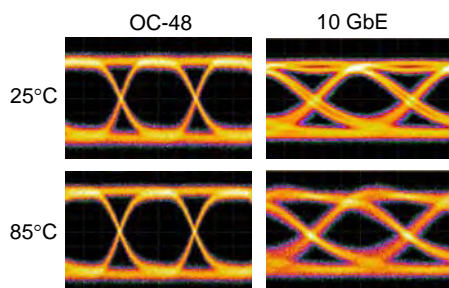


Fig. 2 Eye diagrams recorded under OC-48 and 10 GbE modulation at 25 and 85°C.

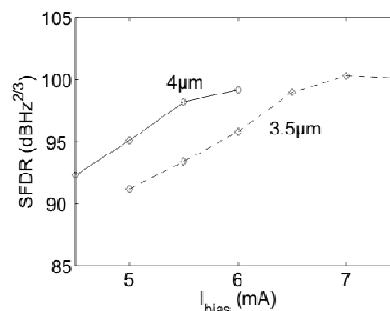


Fig. 3 SFDR at 2 GHz as a function of bias current for VCSELs with two different surface relief diameters.

